Appendix G. Alcoa SO_2 Modeling Report for Intalco 2020-02-06 and Addendum 2020-03-19

AECOM

SO_2 Modeling Report for Intalco Works

DRAFT

Intalco Aluminum LLC
Ferndale, Washington

Project Number: 60614274.100

February 2020

Quality information

Prepared by	Reviewed by	Approved by
Laura L. Warren Air Quality Scientist	Robert J. Paine Associate Vice President, Air Quality	Brian L. Stormwind Manager, Air Quality Engineering & Studies

Prepared for:

Intalco Aluminum LLC
Ferndale, Washington

Prepared by:

Laura Warren
Air Quality Scientist
T: 978.905.2422
E: Laura.Warren2@AECOM.com

AECOM
250 Apollo Drive
Chelmsford,
MA, 01824
USA
www.aecom.com

Table of Contents

List of Figures

List of Tables

1. Introduction

1.1 Background

The United States Environmental Protection Agency (EPA) promulgated a 1-hour National Ambient Air Quality Standard (NAAQS) for SO_2 in 2010. The 1-hour SO_2 NAAQS is set to 75 ppb and the form of the standard is the average of the 99th percentile of the daily maximum 1-hour average concentrations realized in each of three consecutive calendar years (the “design value,” or DV).

The EPA has implemented the 2010 1-hour SO_2 NAAQS in an approach that involves either a dispersion modeling or monitoring approach to characterize local SO_2 concentrations near isolated emission sources. EPA’s Data Requirements Rule (DRR) was finalized on August 21, 2015 and one of the sources in Washington that is subject to the DRR provisions is the Intalco Works aluminum smelter. After extensive discussions in 2015 and 2016, the Washington Department of Ecology (Ecology) agreed with Intalco that due to the unique aspects of an aluminum smelter and heat releases not normally accounted for by the AERMOD model, the appropriate approach to characterize SO_2 concentrations in the vicinity of the smelter is through monitoring.

Based upon an examination of predominant winds and line-up of the potline sources, Ecology elected to use a 2-monitor network to characterize the SO_2 concentrations in the vicinity of the smelter (at the Kickerville Road and Mountain View Road monitors), with peak concentrations expected at these locations. This monitoring network was initiated in January 2017, and the two sites are shown in **Figure 1-1**.

The monitored concentrations at the Kickerville Road site have measured 71 ppb as a 3-year average design concentration, less than the 75 ppb 1-hour SO_2 NAAQS. The design concentration is the 99th percentile, or 4th highest, daily 1-hour maximum in the 3-year period of 2017-2019. Monitoring concentrations at the Mountain View Road monitor during the last 3 years indicate the 3-year average of the 99th percentile concentrations are 106 ppb, which has exceeded the 75 ppb NAAQS[1].

With the completion of 3 years of monitoring, Ecology will undertake an evaluation of monitoring data after final validation and determine the attainment status of the area of Whatcom County in the vicinity of Intalco. As part of this evaluation, if a finding of monitored nonattainment is determined, Ecology will consider multiple factors such as meteorology, terrain, and dispersion modeling to define the geographic extent of the nonattainment area in their recommendations to EPA. This evaluation will also consider the emission sources that contribute to the nonattainment issue. Dispersion modeling for this phase is recommended by EPA to characterize a nonattainment area by modeling SO_2 emission sources using actual emissions during the relevant 3-year period (2017-2019). If EPA provides a finding of a nonattainment designation by December 2020, a future phase for Ecology, working with Intalco, would be to develop a plan to bring the area back into attainment, confirmed with modeling using a similar approach to that described in this report, which would consist of proposed changes to culpable emission sources.

This modeling report presents dispersion modeling as described in the associated modeling protocol (December 2019) in anticipation of a need to characterize SO_2 concentrations through modeling near Intalco in support of Ecology’s recommendations to EPA’s area designation. The modeling approach presented herein and in the associated modeling protocol has been developed in coordination with Ecology and EPA Region 10 and addresses feedback received from these agencies.

[1] However, peak 5-minute concentrations at both monitors are nearly always below EPA’s 200 ppb threshold for health effects, as noted in the 2010 SO_2 NAAQS rule (75 FR 35520). The Aluminum Association has filed a Petition for Reconsideration with EPA regarding the SO_2 NAAQS that requests that if the peak 5-minute value is below 200 ppb, there is no SO_2 NAAQS exceedance.

1.2 Document Organization

Section 2 provides a discussion of the SO_2 emission sources at the Intalco smelter, as well as at nearby sources. The approach for modeling the Intalco smelter as a result of the review of past procedures and extensive consultation with Ecology and EPA Region 10 is provided in Section 3. Section 4 provides a brief summary of a modeling evaluation that demonstrates good model performance at the monitoring sites (more detail in the modeling protocol and this report's **Appendix E**). Section 5 provides SO_2 characterization modeling results and provides spatial patterns of the modeled SO_2 concentrations.

Appendices in this report, which are identical to those provided in the modeling protocol, are provided in this report for reference. Appendix A describes the theory behind using urban characterization for industrial source complexes for dispersion modeling while Appendix B provides a peer-reviewed published journal article on this topic (including 3 other source characterization methods in dispersion modeling. Appendix C provides a satellite analysis of the urban heat island effect caused by the Intalco smelter. Appendix D describes the supplemental information of the Buoyant Line and Plume (BLP) model. Lastly, Appendix E presents a model evaluation regarding the development of a wind direction-dependent stack merging approach for Intalco.

Figure 1-1: SO_2 Monitors in the Vicinity of the Intalco Smelter

2. Description of SO_2 Emission Sources

2.1 Intalco Smelter

Intalco Works is an integrated primary and secondary aluminum production facility permitted to produce 307,000 short tons of primary aluminum per calendar year (full capacity). It is located in Whatcom County along the Strait of Georgia, approximately 6 km west of downtown Ferndale, WA. The area surrounding Intalco Works is rural with simple flat terrain in most directions out to approximately 50 km from the facility, but with some local areas above stack height. In addition, the Fraser River Valley to the north and northeast has been shown to influence seasonal wind conditions, especially in winter with drainage winds from the northeast. The facility has a number of sources emitting SO_2, including three side-worked prebake potlines with primary and secondary emission controls (dry alumina scrubbers and roofline wet scrubbers, which serve to minimize fluoride emissions), one anode baking furnace controlled by an alumina injection system (bake oven scrubber), and 12 natural gas-fired holding furnace stacks (casthouse stacks).

The SO_2 emission rates to modeling of Intalco facility emissions were derived from the reported monthly average SO_2 emission rates for the potline and bake oven dry scrubbing systems and for natural gas consumption. These emissions represent actual SO_2 emissions for a 3-year period of 2017-2019. Because the potline SO_2 emissions are generally steady, the monthly averaged emissions are generally representative of hourly emissions. Typical stack exhaust characteristics and typical SO_2 emission rates are shown in **Table 2-1**. The southern half of potline B (Center 4) has been curtailed during the entire 3-year monitoring period, so no emissions from Center 4 were modeled in this model application. The wet scrubber releases are only about 3% of the potline total, but were included in the modeling (added to the dry scrubber stack emissions) where wet scrubber SO_2 = dry scrubber center SO_2 + (dry scrubber center SO_2 * 0.03) * 0.03. Due to limitations in the Buoyant Line and Point (BLP) model, implemented in AERMOD in 2015, and in consultation with Ecology and EPA Region 10, the BLP model was not used in this application. The wet scrubbers were characterized by conservatively combining wet scrubber emissions through the potline dry scrubber stacks. Information on BLP model limitations is provided in **Appendix E** of this report.

Figure 2-1 shows the location of the property boundary around the facility within which Intalco controls public access. The facility buildings and SO_2 emission sources modeled are shown in **Figure 2-2**.

Table 2-1: Typical Exhaust Characteristics for SO_2 Point Emission Sources

ID / Center	No. of Stacks	Base Elevation (m)	Release Height (m)	Stack Diameter* (m)	Exit Velocity (m/s)	Exit Temperature (K)	Typical SO_2 Emission Rate (g/s)
DSA1 / Center 1	6	65.4	19.8	1.52	15.53	356.3	22.5
DSA2 / Center 2	6	63.9	19.8	1.52	15.53	356.3	22.5
DSB3 / Center 3	26	62.2	17.9	0.72	8.92	348.0	22.5
DSB4 / Center 4	26	61.4	17.9	0.72	8.92	348.0	0
DSC5 / Center 5	22	59.7	17.9	0.72	9.60	355.0	22.5
DSC6 / Center 6	22	59.0	17.9	0.72	9.60	355.0	22.5
BAKEOVEN / Center 7	1	57.5	25.5	2.13	15.64	341.3	10.2
CAST1_6	6	70.35	26.9	0.79	13.80	532.5	0.007
CAST7_8	2	70.66	23.2	0.79	13.80	532.5	0.003
CAST9_10	2	70.17	18.4	0.79	13.80	532.5	0.003
CAS11_12	2	68.81	23.2	0.79	13.80	532.5	0.003

* Stack diameters listed are for each individual stack, although the modeling considers partial merging of the dry scrubber stacks with effective diameters that are larger.

2.2 Nearby SO_2 Emission Sources

Figure 2-3 shows nearby sources and other SO_2 monitors in the general vicinity of Intalco Works. The BP Cherry Point refinery is located about 5 km north-northwest of Intalco Works, and the Phillips 66 refinery is located about 2 km south-southeast of Intalco Works. The 3-year average SO_2 emissions from these facilities were about 745 and 30 tons per year (tpy) in 2017-2019 for BP Cherry Point and Phillips 66, respectively, which are well below the 2,000 tpy threshold for characterizing SO_2 emissions according to the Data Requirements Rule. SO_2 monitoring near each of these facilities indicates design concentrations are well below 50% of the SO_2 NAAQS. For 2017-2019, it is about 11 ppb near BP Cherry Point and 23 ppb near Phillips 66, respectively. These low readings indicate that the elevated SO_2 concentrations due to Intalco's emissions are very localized. At Ecology's request, cumulative modeling was performed to include actual monthly average SO_2 emissions from sources operated at BP Cherry Point and Phillips 66 refineries with Intalco actual monthly emissions to characterize the SO_2 concentration pattern in the local area. Refinery emissions for the 2017-2019 period were provided by Ecology. Based on wind conditions and SO_2 monitoring data for the refineries, this modeling application demonstrates that the refineries do not materially influence the SO_2 concentration pattern in the area near Intalco, as discussed further in Section 5.

2.3 Regional Background

Regional background concentrations are used in modeling to represent emission sources that are not directly modeled as well as naturally occurring levels of the pollutant of interest. Once regional background levels have been identified, they are added to the modeled results at each receptor for a cumulative modeling result. As discussed above, nearby emission sources in the SO_2 characterization modeling included Phillips 66 and BP Cherry Point refineries. Although the nearby refinery emissions do not line up with Intalco's emissions for winds from the west-southwest that would impact the Mountain View Road monitor, and monitored concentrations near the refineries are low, these sources were included in the Intalco modeling as requested by Ecology and EPA Region 10. Because the monitors operated by the refineries may be impacted by Intalco and because the refineries were also included in the cumulative modeling, these monitors were not considered for characterization of regional background. In consultation with Ecology, two candidate ambient air monitors were identified to represent regional $SO_{2,}$ monitors located in Custer, WA and Anacortes, WA. Ecology considers Custer to be influenced by a waste water treatment plant to its immediate south. Therefore, Ecology expressed a preference for the Anacortes monitor (ID 53-057-0011). The Anacortes design value for 2017-2019 is 3 ppb (7.86 µg/m^3), therefore this modeling application used this concentration.

Figure 2-1: Ambient Air Boundary for Intalco Modeling

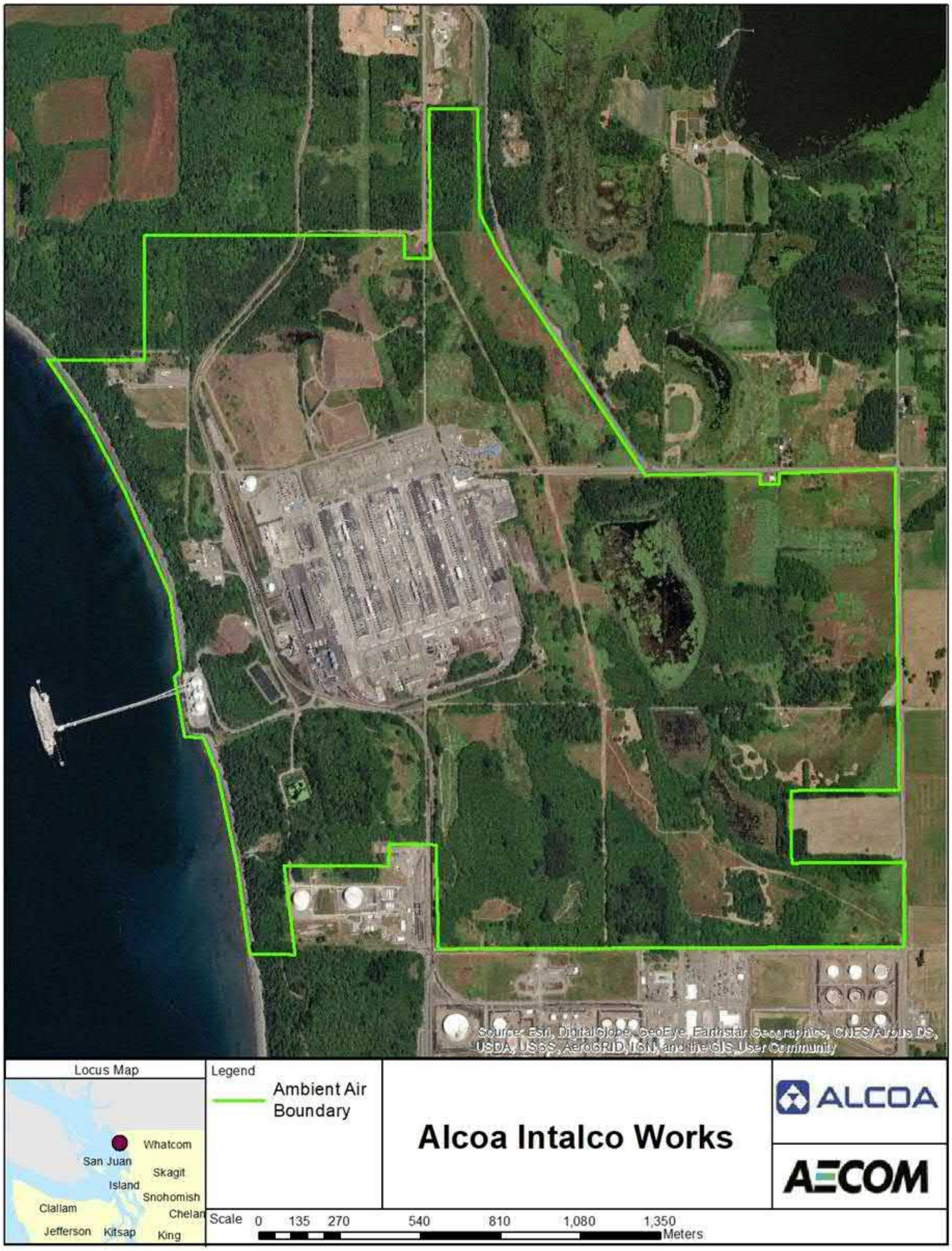

Figure 2-2: Aerial View of Intalco Buildings and SO_2 Emission Sources

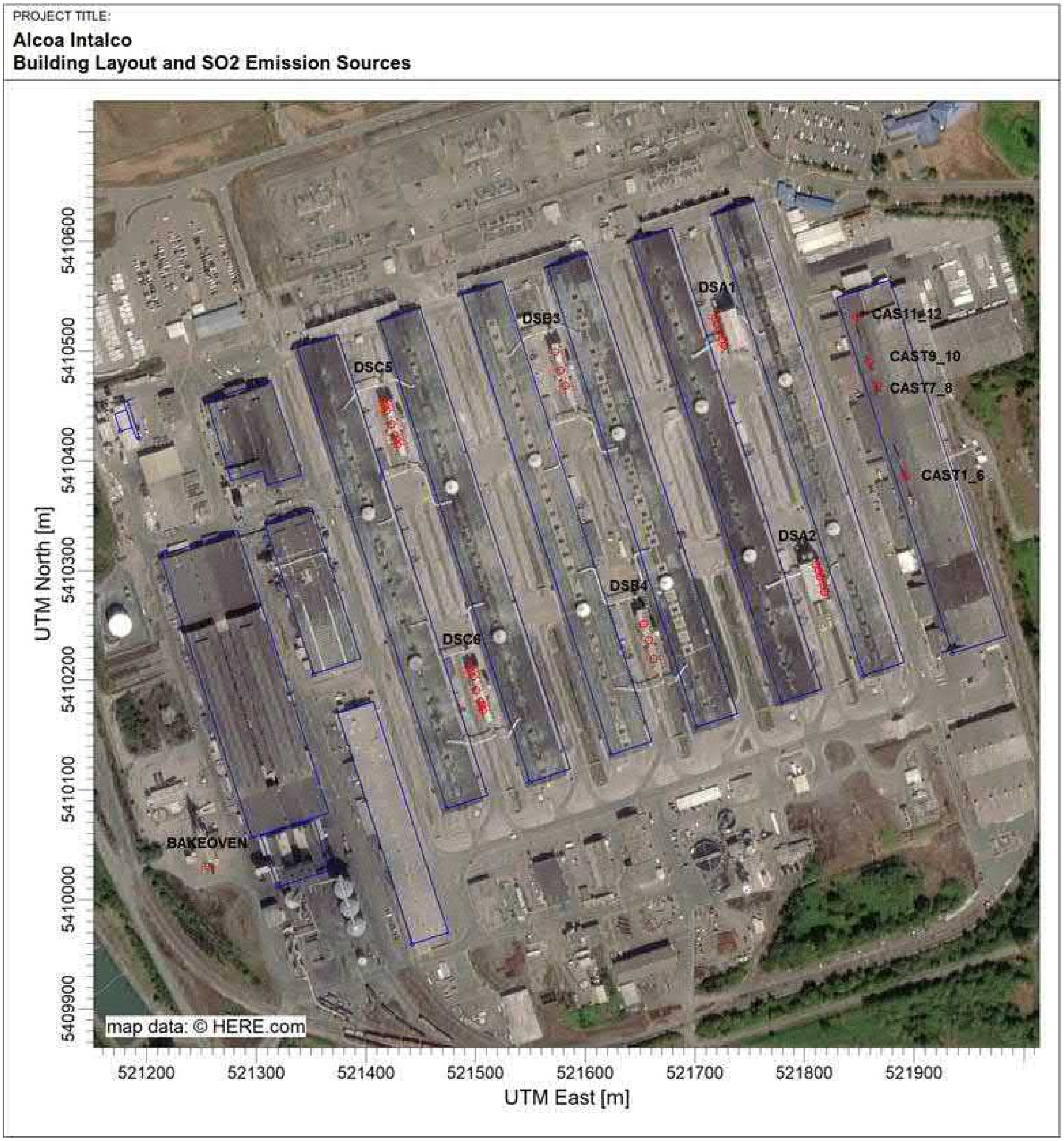

Figure 2-3: SO_2 Emission Sources and SO_2 Monitoring Sites near Intalco

3. Dispersion Modeling Approach

Modeling aluminum smelters is challenging due to issues such as partial plume merging of the many closely-spaced emission point sources and buoyant line sources as well as the presence of a localized heat signature that can be generated from the facility itself. As such, aluminum smelters cannot be accurately characterized using the guideline model, AERMOD, without consideration of site-specific features associated with this type of large industrial area. Recently, an aluminum smelter (Alcoa Warrick Operations) in Indiana has undergone approval of a modeling approach using site-specific source characterization. This case, approved by the state agency and EPA, can be used to guide the development of site-specific source characterization to model Intalco, especially with the availability of nearby monitors to test the model performance.

Alcoa Intalco is similar to the Warrick facility in the basic setup of closely-spaced, multiple dry scrubber stacks which indicates that a similar modeling approach would be reasonable. The Alcoa Warrick modeling approach, discussed in the relevant EPA Technical Support Document[2], included meteorological data refined for low wind speeds (ADJ_U*), partial merging of the smelter's dry scrubber stacks (modeled as point sources), and use of an effective urban population of 2 million to address the plant's heat island effect with 5 operating potlines. Warrick's urban population was based on engineering estimates of a 12 K temperature difference between the main heat sources and "rural" background.

For Intalco, the dispersion modeling approach used in this model application and discussed in this section also included use of ADJ_U* refined meteorology, partial merging of the smelter dry scrubber stacks, and an effective urban population guided by the satellite-detected heat signature generated by the facility. Due to the similarities of the Warrick approach and Warrick's precedent as an approved source characterization and modeling application, the modeling approach for Intalco is similar to that approved for Warrick, but there are some differences for Intalco that are associated with the placement and spacing of the emission Centers.

3.1 Use of AERMOD in Urban Mode for Smelter Sources

The model used in this application is the AERMOD version 19191 modeling system. The choice of rural or urban for dispersion conditions generally depends upon the land use characteristics within 3 kilometers of the facilities as described in Appendix W to 40 CFR Part 51[3]. Factors that affect the rural/urban choice, and thus the dispersion, include the extent of vegetated surface area, the water surface area, types of industry and commerce, and building types and heights within this area. This analysis would indicate that the land use around the Intalco smelter is rural.

Emission sources such as the Intalco aluminum smelter are unique in that they are associated with large fugitive heat releases that result in a local urban-like dispersion environment. Updates to Appendix W proposed in July 2015[4] that were promulgated in 2017 allow the consideration of the urban effects that are created by large industrial complexes, even if located in rural areas. The "highly industrialized area" effect can be addressed by a technique that accounts for the excess heat from an industrial complex and derives an effective population related to the excess heat generated by the highly industrialized area as input to AERMOD. A discussion of this approach is provided in Appendix A, which has previously been provided to EPA by the American Iron & Steel Institute (AISI). A peer-reviewed published journal article describing source characterization of the highly industrialized area heat island effect (and three other source characterization techniques) is provided in **Appendix B**. Details of satellite-derived temperature differences between Intalco and the surrounding area are presented in **Appendix C**.

[2] EPA Technical Support Document providing approval of this technique: https://www.epa.gov/sites/production/files/2017-12/documents/13-in-so2-rd3-final.pdf
[3] EPA's Guideline on Air Quality Models, available at https://www3.epa.gov/ttn/scram/guidance/guide/appw_17.pdf.
[4] 80 FR 45340, July 29, 2015

For the Intalco smelter, the urban-rural temperature difference is measured to be about 14 K, which would result in an effective urban population of about 10 million. However, model performance indicated that using an effective urban population as low as 2 million, equivalent to a 12 K temperature difference, may be used for conservatism (i.e., less dispersion of pollutants than a 10 million population would result in) and consistency with the treatment for the Warrick smelter.

A default 4-hour half-life for exponential decay of SO_2 is automatically turned on for urban sources in AERMOD. This feature was effectively turned off in this modeling application by using the “SO2” pollutant ID keyword and a user-supplied half-life of 1 billion hours because Ecology and EPA Region 10 do not believe the 4-hour half-life to be appropriate for Intalco given that the areas upwind of Intalco are generally rural. In the December 2019 modeling protocol, use of the “OTHER” pollutant ID keyword was originally proposed; however, using this pollutant ID would also turn off special processing in AERMOD that properly calculates 3-year average SO_2 design values. Use of a very high half-life value in this application was recommended by EPA Region 10 and was applied in consultation with Ecology.

3.2 Building Downwash Treatment

The effects of the large heat releases from the smelter play a role in the merging of plumes from adjacent dry scrubber stacks and in a liftoff effect that resists building downwash effects. In the case of the aluminum smelter, the potline buildings are not enclosed, but instead have openings that promote inflow from the bottom so that the natural convection will improve the dispersion (and increase the lift) of the hot effluent from the roofline wet scrubbers. The associated fugitive heat losses act to offset building downwash effects. However, downwash effects are conservatively retained in this modeling application, while the convective heating effects are accommodated with partial stack merging as described in Section 3.3. Building downwash parameters were generated using the building processor, BPIP Version 04274. The building layout for Intalco is shown in **Figure 2-3** in the previous section. Building downwash parameters were also generated for SO_2 sources at the Phillips 66 and BP Cherry Point refineries using building input information provided by Ecology.

3.3 Site-Specific Modeling Approaches

EPA Region 5 has approved an urban dispersion characterization for the Alcoa Warrick Operations aluminum smelter, as well as a partial stack merging approach for Warrick Operations based in part on technical discussions and also substantiated by AERMOD model performance.

In 2015, Ecology considered accounting for the buoyant effects within the smelter by using the BLP model for the dry scrubber stacks. There are several limitations to this approach as currently implemented in AERMOD. They are as follows:

- All lines must be identical in terms of heat effects. In the case of Intalco, the central line “B” is only activated on the northern end, thus not in compliance with this requirement.
- The distribution of emissions from the wet scrubbers is generally uniform along the lines, but not for the dry scrubber stacks. AERMOD can only accommodate one set of line sources, making it impossible to model both sets in one AERMOD run.
- BLP’s terrain treatment is not consistent with AERMOD’s and can significantly overpredict on higher terrain. Intalco has several areas well above stack top with 1-10 km of the smelter.
- BLP’s plume rise, downwash, and dispersion algorithms are not consistent with that of AERMOD and is nearly 40 years old.
- BLP lacks an urban option for use with regulatory applications.
- As noted above, EPA has already approved a partial merging approach for the Warrick smelter.

For this modeling application, it is apparent due to the orientation of the potlines and some sensitivity testing that the optimal strategy for partial stack merging is to consider a wind direction-dependent approach. This means that the number of merged modeling stacks per potline dry scrubber center varies depending on the hourly wind direction. In AERMOD, this stack merging approach is implemented by using an hourly emissions input file where all potential merged stacks are listed in the AERMOD input files, but only the desired merged stacks are activated based on the meteorological data file's hourly wind direction. Inactive stacks are assigned zero emissions. A wind direction-dependent approach was not needed for the Warrick smelter due to the presence of a large rolling mill next to the smelter that resulted in a more directionally uniform plume behavior, in addition to the location of most of the SO_2 emission sources in the same part of the smelter.

The BLP user's manual[5] states (page 2-42) that, "Observational and wind tunnel studies indicate that the line source plume rise equation should contain a wind direction dependence." The BLP manual also states (page 2-48) that, "the plume element originating from the most upwind part of the line source rises higher than plume elements released at other portions of the line" (especially from the downwind edge of the line). It is evident that for flow parallel to the line source, there is a more continuous heating potential for a plume vs. flow perpendicular to the lines. Therefore, there is less effective stack merging for flow perpendicular to the potlines in the stack merging approach utilized for Intalco. Additional information on the original testing of the BLP model is provided in **Appendix D**.

The details of the stack merging approach, which is wind direction-dependent, as well as a model evaluation of two alternate merging approaches, are provided in **Appendix E**. The wind direction-dependent approach provides more merging for flow parallel to the lines (vs. perpendicular to the lines) and more merging on the upwind emission centers (vs. the downwind emission centers). At the request of Ecology and EPA, a modeling demonstration was provided in the appendix to evaluate 2 or more modeling approaches which includes the wind direction-dependent stack merging approach and at least one fixed stack merging approach using an objective analysis determining the number of stacks to merge. A brief overview of this direction-dependent approach's performance using a full year of data is discussed in Section 4 with a detailed discussion of all modeling scenarios is provided in **Appendix E**.

The wet scrubber emissions, which constitute a small percentage of the SO_2 emissions relative to the dry scrubber stacks, are modeled with AERMOD by adding their emissions to the dry scrubber stacks as recommended by Ecology, due to the urban dispersion conditions which BLP does not handle.

3.4 Meteorological Data Processing

Hourly surface meteorological data were processed with AERMET (version 19191). This model application was performed for a 3-year period, 2017-2019. Default model options were used with the low wind speed refinement called ADJ_U*. The Mountain View SO_2 monitor, approximately 1 km east of Intalco, also measures meteorological parameters on a 10-m tower, making this site the most representative surface meteorological station for Intalco. This station's available wind direction, wind speed, and temperature data were used. The Bellingham International Airport (KBLI), an NWS ASOS station, was used for cloud cover and to substitute temperature and wind data when missing from Mountain View. Cumulative data completeness of wind and temperature data from the Mountain View monitor for the 3-year period were examined and have been confirmed to meet the acceptable criteria (data completeness of 90% or greater per quarter and per year) for modeling when substitution of Bellingham data was implemented. These criteria would not have been met with Mountain View alone due to missing temperature data in 2017. For upper air meteorological data, the closest NWS station, Quillayute Airport (KUIL), was used.

AERMET creates two output files for input to AERMOD:

[5] Buoyant Line and Point Source (BLP) Dispersion Model User's Guide, July 1980. Document P-7304B. https://www3.epa.gov/scram001/userg/regmod/blpug.pdf

- SURFACE: a file with boundary layer parameters such as sensible heat flux, surface friction velocity, convective velocity scale, vertical potential temperature gradient in the 500-meter layer above the planetary boundary layer, and convective and mechanical mixing heights. Also provided are values of Monin-Obukhov length, surface roughness, albedo, Bowen ratio, wind speed, wind direction, temperature, and heights at which measurements were taken.
- PROFILE: a file containing multi-level meteorological data with wind speed, wind direction, temperature, sigma-theta (σ_θ) and sigma-w (σ_w) when such data are available.

AERMET requires specification of the meteorological station site characteristics including surface roughness (z_o), albedo (r), and Bowen ratio (B_o). These parameters were developed according to the guidance provided by EPA in the recently revised AERMOD Implementation Guide (AIG).[6]

The revised AIG provides the following recommendations for determining the site characteristics:

1. The determination of the surface roughness length should be based on an inverse distance weighted geometric mean for a default upwind distance of 1 km relative to the measurement site. Surface roughness length may be varied by sector to account for variations in land cover near the measurement site; however, the sector widths should be no smaller than 30 degrees.

2. The determination of the Bowen ratio should be based on a simple unweighted geometric mean (i.e., no direction or distance dependency) for a representative domain, with a default domain defined by a 10-km by 10-km region centered on the measurement site.

3. The determination of the albedo should be based on a simple unweighted arithmetic mean (i.e., no direction or distance dependency) for the same representative domain as defined for Bowen ratio, with a default domain defined by a 10-km by 10-km region centered on the measurement site.

The AIG recommends that the surface characteristics be determined based on digitized land cover data. EPA has developed a tool called AERSURFACE that determines the site characteristics in accordance with the recommendations from the AIG. AERSURFACE incorporates look-up tables of representative surface characteristic values by land cover category and seasonal category. AERSURFACE was applied with the instructions provided in the AERSURFACE User's Guide.

The current version of AERSURFACE (Version 13016) supports the use of land cover data from the USGS National Land Cover Data 1992 archives (NLCD92). The NLCD92 archive provides data at a spatial resolution of 30 meters based upon a 21-category classification scheme applied over the continental U.S. The AIG recommends that the surface characteristics be determined based on the land use surrounding the site where the surface meteorological data were collected.

As recommended in the AIG for surface roughness, the 1-km radius circular area centered at the meteorological station site was created. For this analysis, the area around the Mountain View station was divided into 12 default 30° sectors. This approach was also used for the Bellingham station as it was used to substitute missing wind and temperature data.

In AERSURFACE, the various land cover categories are linked to a set of seasonal surface characteristics. As such, AERSURFACE requires specification of the seasonal category for each month of the year. The following five seasonal categories are supported by AERSURFACE. The applicable seasons associated with the 3-year 2017-2019 modeling period for this site were determined using AIG and AERSURFACE guidance, as indicated in the parentheses.

1. Midsummer with lush vegetation (June, July, August)

[6] U.S. EPA 2019. AERMOD Implementation Guide (Revised). U.S. Environmental Protection Agency, Research Triangle Park, NC. August, 2019.

2. Autumn with un-harvested cropland (September, October, November)
3. Late autumn after frost and harvest, or winter with no snow (December, January, February)
4. Winter with continuous snow on ground (Not applicable for this modeling period)
5. Transitional spring with partial green coverage or short annuals (March, April, May)

For Bowen ratio, the land use values are linked to three categories of surface moisture corresponding to average, wet, and dry conditions. The surface moisture condition for the site may vary depending on the meteorological data period for which the surface characteristics is applied. AERSURFACE applies the surface moisture condition for the entire data period. Therefore, if the surface moisture condition varies significantly across the data period, then AERSURFACE can be applied multiple times to account for those variations. As recommended in the AERSURFACE User's Guide, the surface moisture condition for each month was determined by comparing precipitation for the period of data processed to the 30-year climatological record, selecting "wet" conditions if precipitation is in the upper 30th percentile, "dry" conditions if precipitation is in the lower 30th percentile, and "average" conditions if precipitation is in the middle 40th percentile. The 30-year precipitation data set used in this modeling was taken from the NOAA Online Weather Data (NOWData)[7].

3.5 Receptor Processing

Receptor input to AERMOD was generated for areas of ambient air. According to the 1986 EPA memo, ambient air is defined as "…that portion of the atmosphere, external to buildings, to which the general public has access."[8] **Figure 2-1** (see previous section) illustrates the Intalco property where general public access is controlled, and serves as the ambient air boundary for this analysis. Ecology has prepared a receptor grid for use with this model application. This receptor grid was used with adjustments by Alcoa/AECOM for the ambient air boundary. The grid represents an approximately 47-km x 41.7-km domain with spacing similar to Ecology air toxics modeling guidance.[9] A nested receptor grid was developed where a polar grid centered on Intalco is used close to Intalco while a Cartesian (rectangular) grid is used for the outer areas. Receptor spacing is described below.

- 25 meter spacing along the ambient boundary,
- 100 m spacing out to 2,000 m from the plant,
- 300 m spacing between 2,000 m and 4,500 m from the plant,
- 600 m spacing between 4,500 m from plant out to 10,000 m, and
- 1,000 m spacing beyond 10,000.

In addition to these specifications, 100-m spaced receptors were used in the hilly areas of interest to Ecology such as Haynie Hill to the northeast, Orcas and Lummi islands, and the area south of Bellingham encompassing Larrabee State Park. **Figures 3-1 and 3-2** provide the receptor grid as viewed in the near-field and far-field. No additional 100-meter spaced receptors were necessary because the location of the maximum impact was already in an area covered by 100-meter (or denser) grid spacing. At the request of Ecology, discrete receptors were also placed at Mountain View, Kickerville, Phillips 66, and BP Cherry Point SO_2 monitoring locations.

Receptor height scales at each receptor location were developed by AERMAP (version 18081), the terrain preprocessor for AERMOD, which requires processing of terrain data files. Terrain elevations from 30-meter Shutter Radar Topography Mission data (SRTM) were used to develop the receptor terrain elevations required by AERMOD.

---

[7] https://w2.weather.gov/climate/xmacis.php?wfo=sew
[8] https://www3.epa.gov/scram001/guidance/mch/ama4.txt

Figure 3-1: Near-field View of the Receptor Grid

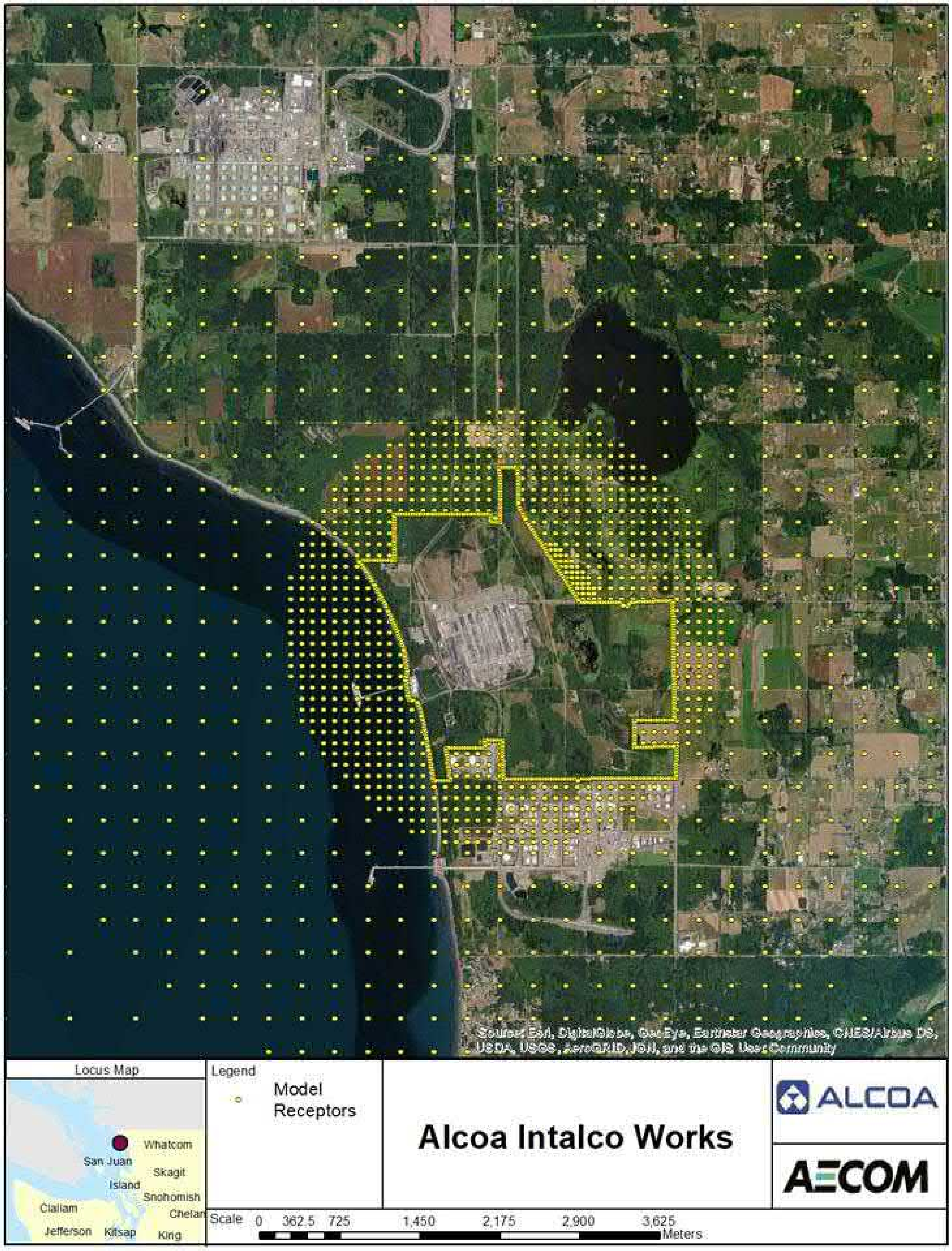

Figure 3-2: Far-field View of the Receptor Grid

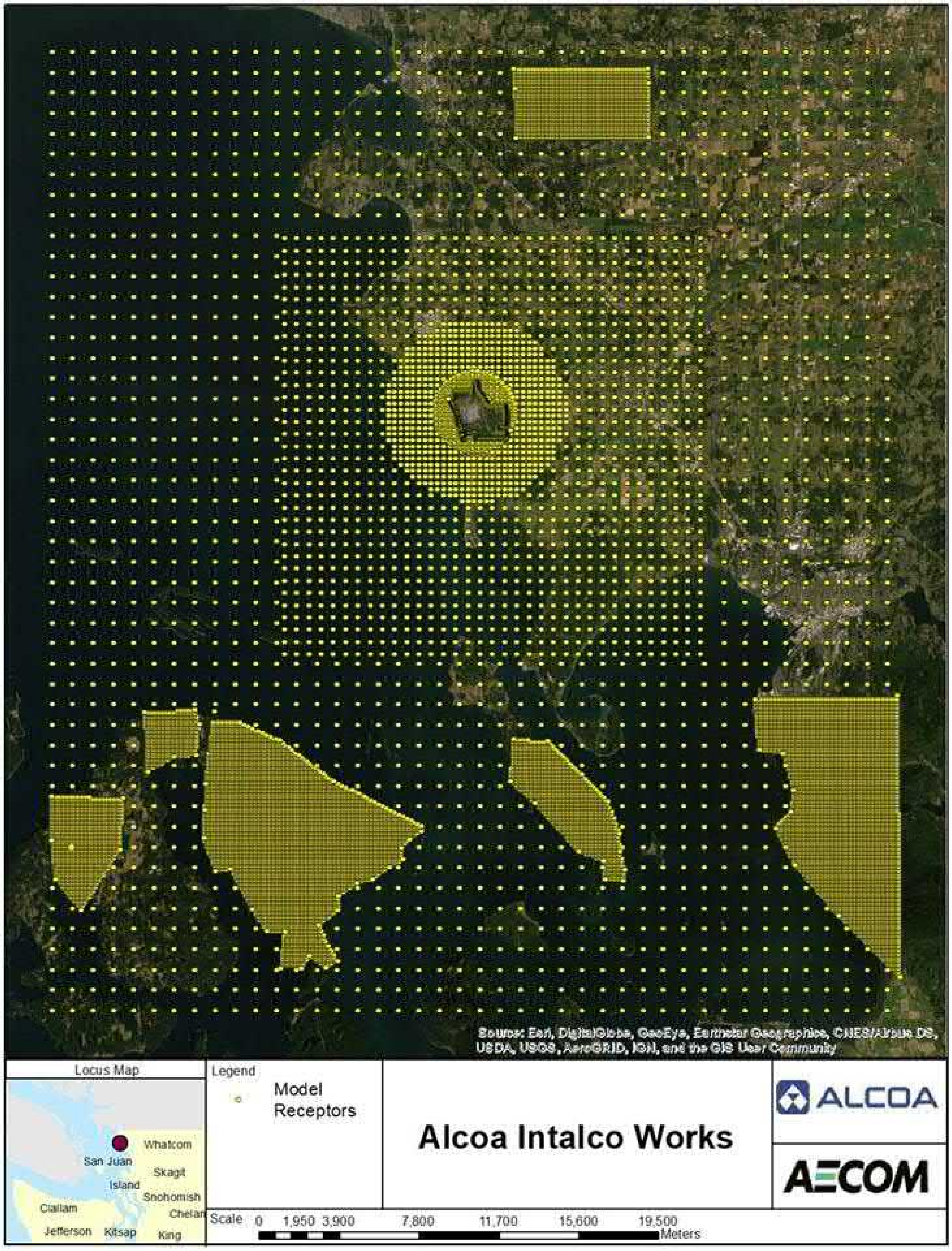

4. Model Comparison to Monitored Data

An important consideration for the selection of the AERMOD modeling approach is the performance of the model for the two local monitors (Kickerville Road and Mountain View Road) and the nearby Phillips 66 refinery monitor. A full year of data (October 1, 2017 – September 30, 2018) was used for model evaluation of this site-specific source characterization. For the model evaluation, meteorological data was processed using procedures described in Section 3.4 for the 1-year period for model evaluation and 5 site-specific land use sectors. This model evaluation is discussed briefly in the associated modeling protocol and in this report's **Appendix E** (from the modeling protocol), which notes that only Intalco actual monthly emissions were modeled, while the refinery emissions were excluded. The model evaluation and its modeling archive were provided to Ecology in October 2019 and have been reviewed and approved by Ecology.

Three candidate modeling approaches were developed and evaluated to more accurately characterize Intalco. A model evaluation was performed for two purposes: to evaluate the modeling approach described in Section 3 at nearby SO_2 monitoring sites, and also to review the modeled concentration pattern for receptors placed in all directions around the smelter. As discussed in the modeling protocol, a comparison of model to monitored concentrations was shown at the two monitoring sites, Mountain View and Kickerville, as well as the Phillips 66 monitor where testing was confined to wind directions for which the monitor was downwind of Intalco, 305-350°, because only Intalco emissions were modeled.

Table 4-1 from the modeling protocol presents the model evaluation results of the comparison of the 99th percentile peak daily 1-hour maximum ("design") concentrations for the modeling approach used in this report. Ambient SO_2 monitored observations have the potential to vary from an unbiased calibration state by up to 10% and still be considered to be acceptable within the uncertainty of the measurements. This is related to the tolerance in the EPA procedures (EPA, 2013)[10] associated with quality control checks and span checks of ambient measurements. Therefore, even ignoring uncertainties in model input parameters and other contributions that can also lead to modeling uncertainties, just the uncertainty in measurements indicates that modeled-to-monitored ratios between 0.9 and 1.1 are within the instrumentation tolerance and can be considered unbiased. The model evaluation also provided quantile-quantile (Q-Q) plots of the modeled and observed concentrations for the three modeling approaches, which further demonstrated this modeling approach as have the best model performance.

It is important to note that for modeling applications such as this application in which the purpose is to accurately predict design concentrations, evaluating modeled concentrations paired in both time and space, especially on an hourly basis, is not recommended by EPA modeling guidance.[11] For this reason, the use of quantile–quantile plots applied to data unpaired in time has been relied upon for the model evaluation provided to Ecology in October 2019.

Table 4-1: Comparison of Modeled and Observed SO_2 99th Percentile Concentrations

	Mountain View Road SO_2 (ppb)	Kickerville Road SO_2 (ppb)	Phillips 66 SO_2 (ppb)
Observed	101.4	80.5	19.0
Modeled	108.2	76.0	43.0
Ratio: Model/Obs.	1.1	0.9	2.3

[10] Quality Assurance Handbook for Air Pollution Measurement Systems, Volume II, Ambient Air Quality Monitoring Program, 2013, available at http://www.epa.gov/ttnamti1/files/ambient/pm25/qa/QA-Handbook-Vol-II.pdf. (Table 10-3 and Appendix D, page 13).
[11] EPA's Guideline on Air Quality Models, available at https://www3.epa.gov/ttn/scram/guidance/guide/appw_17.pdf.

5. Cumulative Modeling Results and Conclusions

Cumulative modeling for the 2017-2019 modeling period was performed with actual SO_2 emissions from Intalco, Phillips 66 refinery, and BP Cherry Point refinery. This modeling provides an estimate of the spatial extent of the SO_2 nonattainment area near Intalco using the modeling approach described in herein and in the associated modeling protocol, where a model evaluation was undertaken to demonstrate the approach's accuracy when compared to SO_2 monitored concentrations (see **Appendix E**).

The modeling results are presented as the 99th percentile daily maximum 1-hour concentrations averaged over the three years modeled. The concentration isopleths for the cumulative modeling are provided in **Figure 5-1** for the full receptor grid view and **Figure 5-2** for a near-field view. Concentration units are shown in micrograms per cubic meter (µg/m^3). Background concentrations of 7.86 µg/m^3 (3 ppb) have been added to this figure to account for SO_2 emission sources not modeled in this application. An SO_2 concentration of approximately 196.4 µg/m^3 corresponds to the concentration of 75 ppb as the 1-hour SO_2 NAAQS[12], as indicated by the yellow/orange shaded boundary. Modeled concentrations greater than the NAAQS are indicated in orange and red shading.

The maximum modeled design concentration occurred on the northeastern side of the ambient air boundary, not far from the Mountain View Road monitor. Also, it is apparent in these figures that the area of modeled nonattainment is limited in extent. The nonattainment area is contained within about 1.7 km of the center of Intalco. In fact, beyond 5 km, all modeled concentrations are less than 120 µg/m^3 (46 ppb), which is much less than the 75 ppb NAAQS.

Additionally, the modeled concentration spatial pattern reflects the same general trends displayed by the SO_2 monitors. Design values in the vicinity of the Mountain View monitoring location, which is the only area monitor with a design value greater than the NAAQS, has the highest modeled concentrations with concentrations greater than the NAAQS. The Kickerville monitoring location is second highest while remaining below the NAAQS. Phillips 66 and BP Cherry Point monitoring locations have much lower modeled concentrations, similar to their monitored concentrations. As such, both the monitored concentrations and modeled concentrations demonstrate that the refineries are not within the modeled nonattainment area and leads to the conclusion that they are not significantly contributing to the nonattainment issue.

The limited extent to which the refineries contribute is further illustrated in **Figures 5-3 to 5-6**, where Intalco-only modeled concentrations and refinery-only modeled concentrations are shown. Specifically, for BP Cherry Point refinery to contribute to SO_2 nonattainment, winds from the northwest would be required to bring its emissions toward Intalco, and the result of a lineup with the smelter would be seen on the south side of the smelter. However, modeled concentrations south of the Intalco ambient air boundary, where BP Cherry Point and Intalco emissions would combine, are less than the NAAQS and thus BP Cherry Point is not causing or contributing to an SO_2 nonattainment area. For Phillips 66, winds from the south-southeast would bring both Phillips 66 and Intalco emissions to the north of Intalco. However, as shown in **Figure 5-6**, the Phillips 66 design concentration is less than 5 µg/m^3 in the area north of Intalco, less than the interim significant impact level of 3 ppb[13] (7.86 µg/m^3).

In conclusion, the nonattainment area is confined to less than 2 km of Intalco center and the nearby refineries do not significantly contribute to the nonattainment area. Therefore, this modeling analysis has demonstrated that inclusion of the refineries is not necessary in future Intalco modeling.[13]

[12] EPA cites 196.4 µg/m^3 as equivalent to the 2010 SO_2 NAAQS of 75 ppb using a 2.619 µg/m^3 conversion factor; https://www.epa.gov/sites/production/files/2017-08/documents/43_wa_so2_rd3-final.pdf

[13] EPA, April 2014. Guidance for 1-Hour SO_2 Nonattainment Area SIP Submissions. https://www.epa.gov/sites/production/files/2016-06/documents/20140423guidance_nonattainment_sip.pdf, pages A-5 and A-6.

Figure 5-1: Cumulative Modeling Design SO_2 Concentrations for 2017 –2019 (Full Receptor Grid)

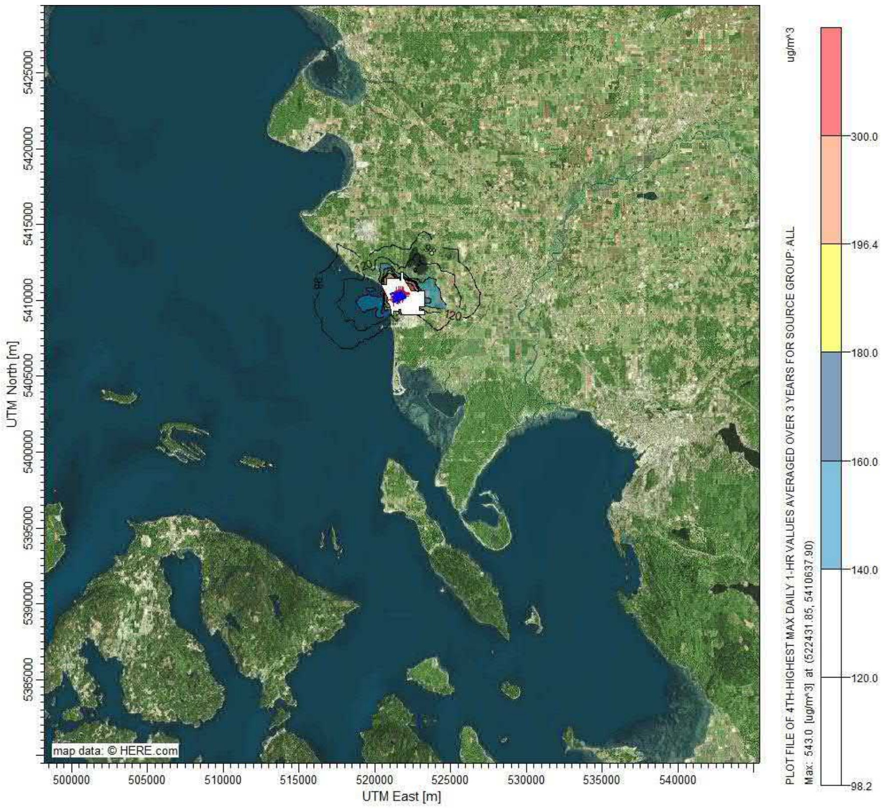

Figure 5-2: Cumulative Modeling Design SO_2 Concentrations for 2017 –2019 (Near Field View)

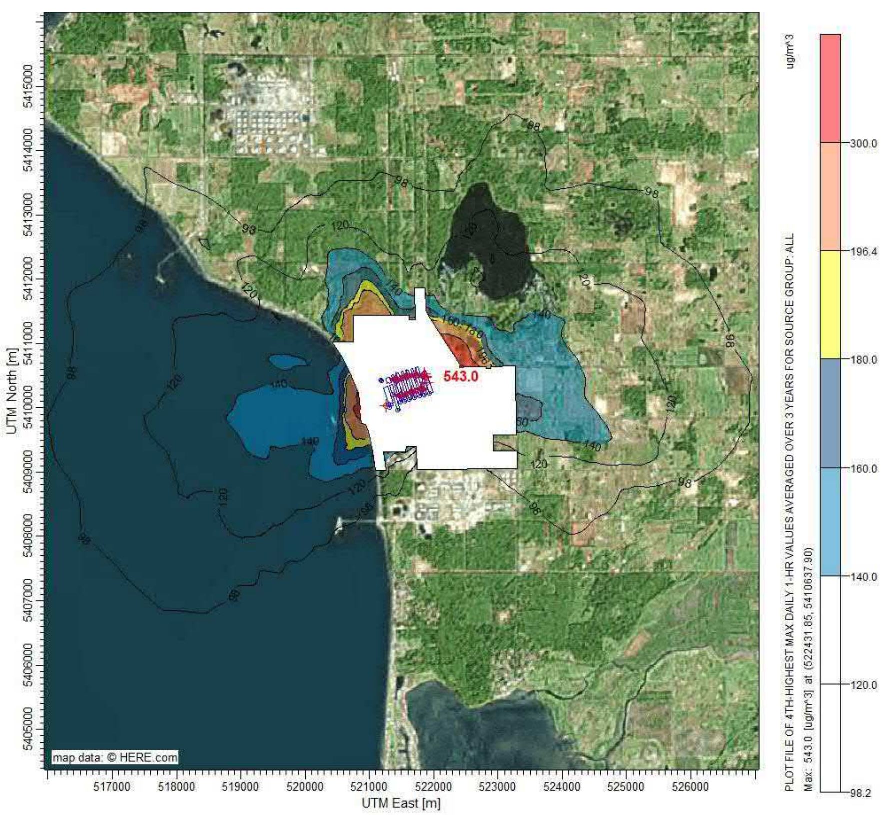

Figure 5-3: Modeled Design SO_2 Concentrations for Intalco (No Background)

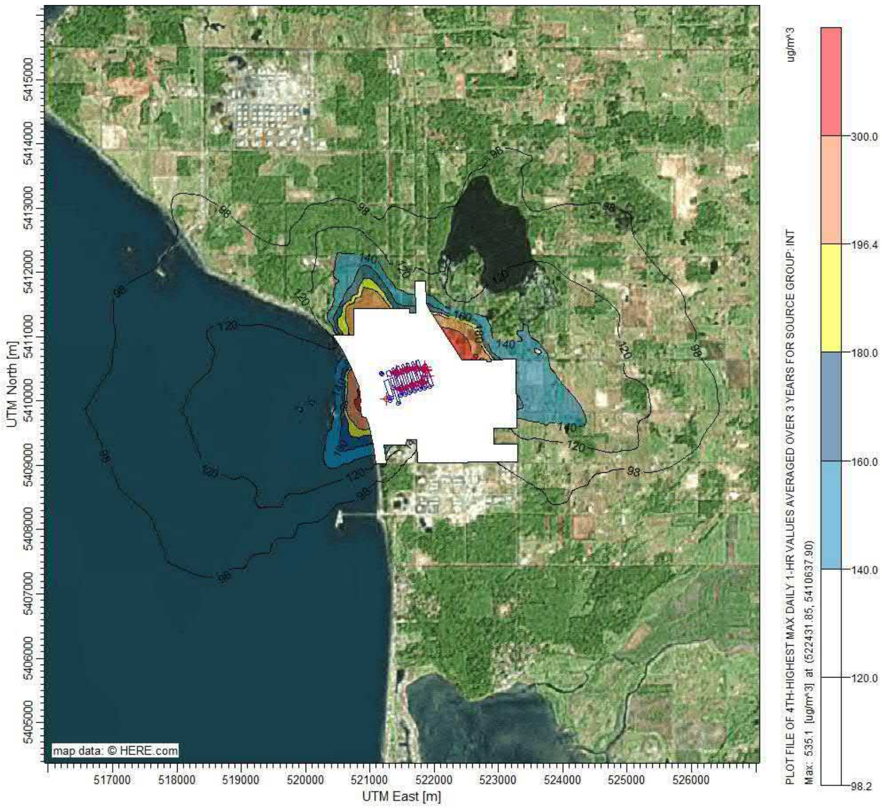

Figure 5-4: Modeled Design SO_2 Concentrations for Refineries (No Background)

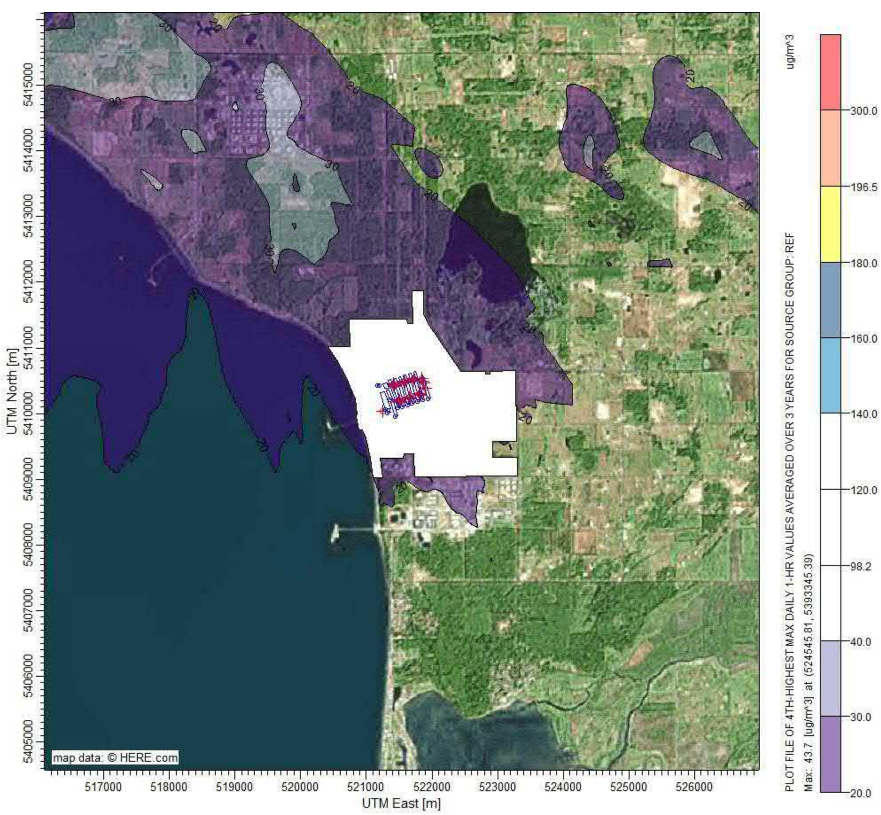

Figure 5-5: Modeled Design SO_2 Concentrations for BP Cherry Point (No Background)

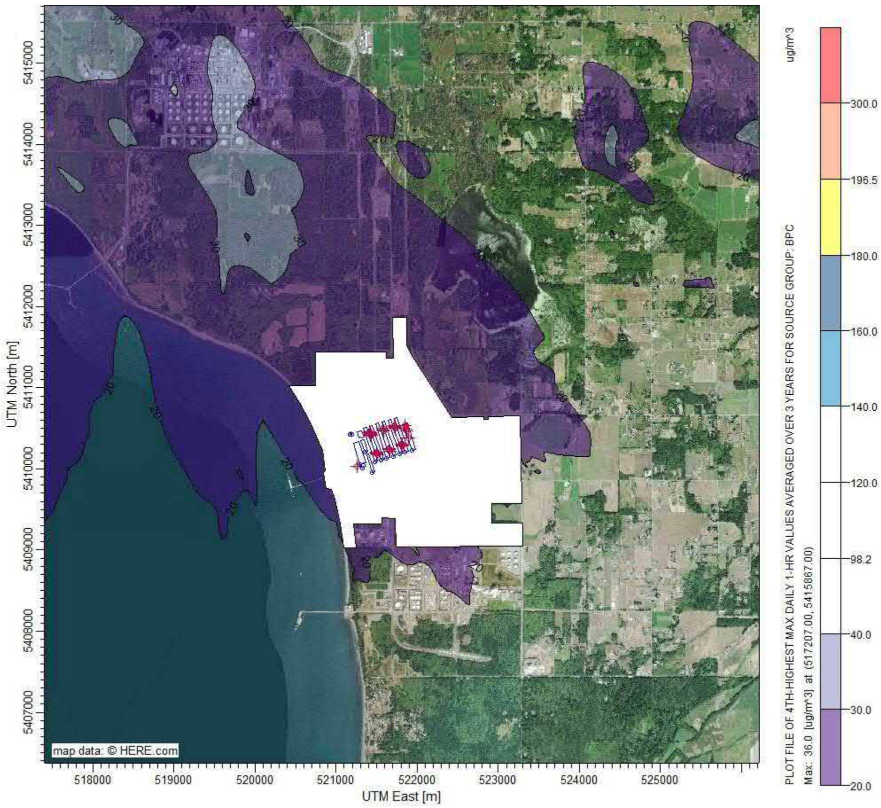

Figure 5-6: Modeled Design SO_2 Concentrations for Phillips 66 (No Background)

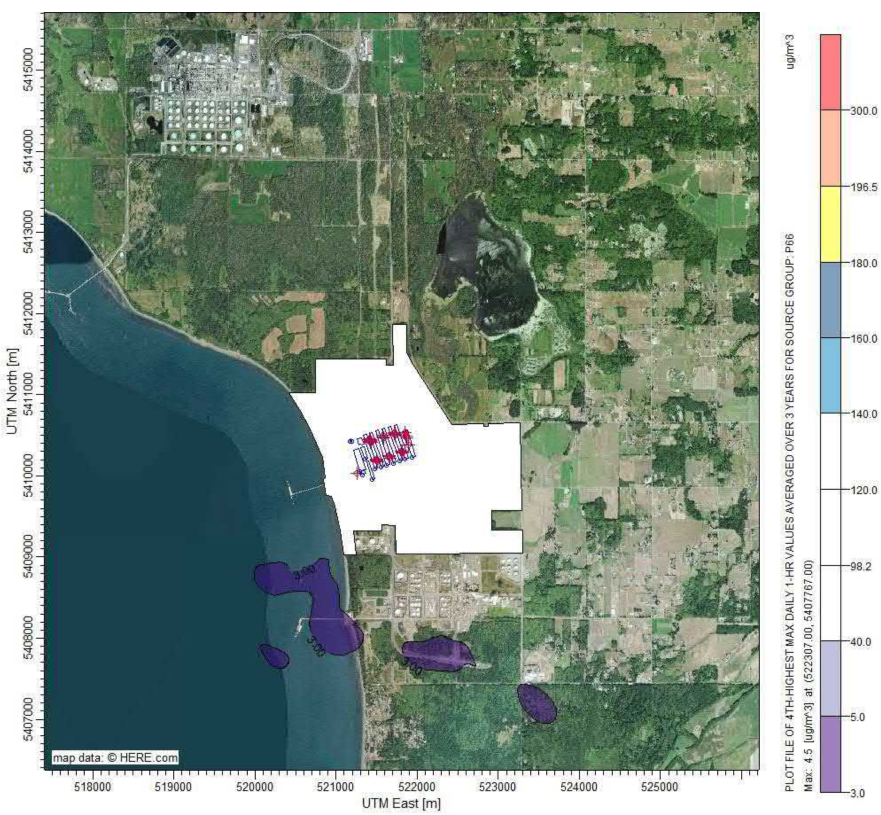

Appendix A Urban Characterization of Industrial Source Complexes for AERMOD Modeling

Urban Characterization of Industrial Source Complexes for AERMOD Modeling

Introduction

The United States Environmental Protection Agency (EPA) maintains recommendations for dispersion modeling approaches for emission sources at Appendix W, 40 CFR (Code of Federal Regulations) Part 51, available at http://www.epa.gov/ttn/scram/guidance/guide/appw_05.pdf. Supplemental AERMOD implementation guidance is available at http://www.epa.gov/ttn/scram/7thconf/aermod/aermod_implmtn_guide_19March2009.pdf.

The topic of this “white paper” is the determination as to whether a specific emission source should be characterized as being in a rural or urban area, and if urban, then the assignment of an “effective urban population”. The choice of urban vs. rural influences how the dispersion is treated, especially at night, for which an urban area is characterized by a near-neutral boundary layer with a specified height that is a function of urban-rural temperature difference (or population as a robust input metric). The current guidance addresses traditional urban areas that are characterized by large populations or urban-like surface characteristics. However, for industrial areas with large heat releases that result in large temperature excesses, the traditional classification approaches are often not appropriate. The population near such areas is often much reduced because of zoning issues, and the area beyond the immediate industrial park may be rural in nature, resulting in a misleading characterization for this type of source.

AERMOD’s Model Formulation for Urban Dispersion

In urban areas, AERMOD accounts for the dispersive nature of the “convective-like” boundary layer that forms during nighttime conditions by enhancing the turbulence over that which is expected in the adjacent rural, stable boundary layer. The enhanced turbulence is the result of the urban heat flux and associated mixed layer, which are estimated from the urban-rural temperature difference as suggested by Oke (1978; 1982)[1,2].

Although urban surface characteristics (roughness, albedo, etc.) influence the boundary layer parameters at all times, the effects of the urban sublayer on the structure of the boundary layer is largest at night and relatively absent during the day (Oke,1998)[3]. An urban “convective-like” boundary layer forms during nighttime hours when stable rural air flows onto a warmer urban surface. Following sunset, the urban surface cools at a slower rate than the rural surface because buildings in the urban area trap the outgoing thermal radiation and the urban subsurface has a larger thermal capacity. AERMOD accounts for this by enhancing the turbulence above that found in the rural stable boundary layer (i.e., a convective-like urban contribution to the total turbulence in the urban stable boundary layer). The convective contribution is a function of the convective velocity scale, which in turn, depends on the surface heat flux and the urban mixed layer height. The upward heat flux is a function of the urban-rural temperature difference, where the urban temperature is taken at the core of the urban area.

---

[1] Oke, T. R., 1978. Boundary Layer Climates. John Wiley and Sons, New York, New York, 372 pp.

[2] Oke, T. R., 1982. The energetic basis of the urban heat island. Quart.J.Roy.Meteor.Soc., 108: 1-24.

[3] Oke, T. R., 1998. An algorithmic scheme to estimate hourly heat island magnitude. Preprints, 2nd Urban Environment Symposium, American Meteorological Society, Boston, MA, 80-83.

The urban-rural temperature difference depends on a large number of factors that cannot easily be included in applied models such as AERMOD. For simplicity, the data presented in Oke (1973; 1982)[4,2] is used to construct an empirical model. Oke presents observed urban-rural temperature differences for a number of Canadian cities with populations varying from about 1000 up to 2,000,000. These data represent the maximum urban effect for each city since they were collected during ideal conditions of clear skies, low winds, and low humidities. An empirical fit to the data yields the following relationship:

$$\Delta T_{u-r} = \Delta T_{max} [0.1 \ln (P/P_o) + 1.0] \qquad (1)$$

where ΔT_{max} = 12°C, P_o = 2,000,000 (the city population associated with the maximum temperature difference in Oke's data), and P is the population of the urban area being modeled. Since the ambient nighttime temperature of an urban area is higher than its surrounding rural area, an upward surface heat flux must exist in the urban area. It is assumed that this upward surface heat flux, H_u, is related to the urban-rural temperature difference through the following relationship

$$H_u = \alpha \rho c_p \Delta T_{u-r} u_*, \qquad (2)$$

where, as noted in the AERMOD formulation document[5], α is an empirical constant (0.03), ρ is the density of air (about 1.2 kg/m^3), c_p is the specific heat at constant pressure (1 watt-sec/g-deg K), and, as noted above, u_* is on the order of 0.1 m/s. This equation can be solved for ΔT_{u-r}:

$$\Delta T_{u-r} \sim H_u/4, \qquad (3)$$

where H_u is the anthropogenic ("excess") heat release in units of watts per square meter in the "urban core" (an industrial area at least a few hundred meters on a side[6]).

For Eqn. 2, AERMOD's developers (AERMIC) chose α to ensure that the upward heat flux is consistent with maximum measured values of the order of 0.1 ms-1ºC. Because ΔT_{u-r} has a maximum value on the order of 10ºC, and u* is on the order of 0.1 ms-1, α should have a maximum value on the order of 0.1. Although AERMIC assumed that α has a maximum (city center) value of about 0.1, AERMOD uses an effective value of α that is averaged over the entire urban area. Assuming a linear variation of α from 0 at the edge of the urban area to about 0.1 at the center of the urban area results in an area average equal to one-third of that at the center (since the volume of cone is one-third of that of a right circular cylinder of the same height). Therefore, AERMIC tested an area-averaged value of α equal to 0.03 against the Indianapolis data. This choice for α is consistent with measured values of the upward heat flux in Canadian cities reported by Oke (1973; 1982)[4,2]. The results of the developmental testing indicated that this choice for α resulted in an adequate fit between observations and AERMOD-predicted concentrations.

The mixing height in the nighttime urban boundary layer, Z_{iu}, is based on empirical evidence presented in Oke (1973; 1982)[4,2] that, in turn, suggests the following relationships:

---

[4] Oke, T. R., 1973. City size and the urban heat island. Atm.Env., 7: 769-779.

[5] Available at http://www.epa.gov/ttn/scram/7thconf/aermod/aermod_mfd.pdf.

[6] In a series of personal communications, Dr. Steve Hanna indicated that the minimum size of an industrial area needed to take on "urban" characteristics has been the subject of much discussion over the years. He indicated that an "expert elicitation" would likely result in a minimum size estimate of a few hundred meters. The anthropogenic heat release per unit area of major cities such as Indianapolis (extensively studied by EPRI in the 1980s) would be on the order of 50 watts/m^2.

$Ziu \sim R^{1/2}$ and $R \sim P^{1/2}$ (4)

where R is a measure of the city size and P is the population of the city. The first relationship is based on the observed growth of the internal convective boundary layer next to shorelines (Venkatram 1978). The second relationship implicitly assumes that population densities do not vary substantially from city to city.

The equations listed above lead to the following equation for the nocturnal urban boundary layer height due to convective effects alone:

$Ziuc = Ziuo\ (P/Po)^{1/4}$, (5)

where Ziuo is the boundary layer height corresponding to Po. Based on lidar measurements taken in Indianapolis (1991), and estimates of Ziu found by Bornstein (1968) in a study conducted in New York city, Ziuo is set to 400 m in AERMOD.

<u>AERMIC Discussion Notes for the Urban Option</u>

The information provided below is excerpted from notes from the AERMIC meeting of July 17-18, 2001, during which the urban option in AERMOD was discussed when AERMOD was being developed.

At that time, there were some implementation issues with AERMOD that remained (and still remain 13 years later!), specifically the issue of an industrial source that has a large anthropogenic heat flux. In such a case, while this condition would in reality result in urban-like dispersion, the land use or population tests mentioned in Appendix W, as noted above, result in a rural assignment for input to AERMOD. Therefore, a procedure should be developed to model this source as urban in AERMOD.

The suggested approach in the AERMIC discussion was to allow the AERMOD user to specify a nontraditional type of urban source that is subject to urban dispersion due to industrial anthropogenic heat release rather than due to the presence of a traditional city. The user would specify the anthropogenic heat flux due to the source, or an urban-rural delta-T, if available; this would be used to determine a surrogate population value for input to AERMOD. The effective population could be calculated through the use of Eqn. 1 (listed above) if ΔT_{u-r} is specified, of Eqns. 1-3 if instead the anthropogenic heat flux is specified.

<u>Example Applications</u>

<u>Example 1: ΔT_{u-r} is specified</u>

In this case, suppose that the use of thermal infrared satellite[7] data provides a ΔT_{u-r} value of 10^oC. The procedures for conducting this estimate are described in a companion white paper, and are also discussed in the open literature (e.g., Fung et al., 2009[8] and Nichol, 2005[9]. This value would be averaged over some specified area, possibly the area represented by the active industrial source

[7] A companion ‘white paper” that discusses the derivation of the effective “industrial complex heat island” temperature excess is entitled, “Quantifying Urban-Rural Temperature Differences for Industrial Complexes Using Thermal Satellite Data”.

[8] Fung, W. Y., K. S. Lam, J. Nichol, and M. S. Wong, 2009. Derivation of Nighttime Urban Air Temperatures Using a Satellite Thermal Image. <u>J. Appl. Clim. and Met.</u> <u>48</u>: 863-872.

[9] Nichol, J., 2005. Remote Sensing of Urban Heat Islands by Day and Night. Photogrammetric Engineering & Remote Sensing. <u>71</u>: 613-621.

complex, but at least an area with side lengths of several hundred meters. From Eqn. 1, the surrogate population, P, is expressed as:

$$P = Po \exp[10(\Delta T_{u\text{-}r} / \Delta T_{max} - 1.0)], \quad (6)$$

where

$\Delta T_{u\text{-}r}$ is specified by the user,

$\Delta T_{max} = 12^oC$, and

Po = 2,000,000.

In this case, with $\Delta T_{u\text{-}r}$ = 10 deg C, P ~ 400,000.

<u>Example 2: anthropogenic heat flux is specified</u>

In this case, suppose that estimates of the excess heat generated yield a value averaging 40 watts per square meter of anthropogenic heat generation in an industrial area several hundred meters on a side. This value lies within the 10-100 w/m^2 range stated by Hanna et al. (2001)[10] for urban areas. In this case, the application of Eqn. 3 with typical values stated above for α, ρ, c_p, and u* results in a value of ΔTu-r of 10 deg K. Then, using Eqn. 6, the effective population is about 400,000.

Evaluation with cases for which both the ΔTu-r and the excess heat flux estimates are available is recommended for further verification of the formulations noted in this document.

[10] Hanna, S. E. Marciotto, and R. Britter. "Urban Energy Fluxes in Built-Up Downtown Areas and Variations across the Urban Area, for Use in Dispersion Models." <u>J. App. Met. and Clim.</u>, <u>50</u> : 1341-1353.

Appendix B Atmospheric Environmental Peer- Reviewed Journal Article About Source Characterization Techniques

Atmospheric Environment 129 (2016) 55–67

Contents lists available at ScienceDirect

Atmospheric Environment

journal homepage: www.elsevier.com/locate/atmosenv

Source characterization refinements for routine modeling applications

Robert Paine, Laura L. Warren*, Gary E. Moore

AECOM, 250 Apollo Drive, Chelmsford, MA 01824, USA

HIGHLIGHTS

- Dispersion modeling source characterizations for unique facilities are described.
- Highly industrialized areas causing a heat island effect can be modeled as urban.
- Stacks with waste heat countering downwash can apply weighting to these effects.
- Extra rise for moist plumes is realistically estimated for use in "dry" models.
- Stacks in a row with merged plumes can be better represented to improve modeling.

ARTICLE INFO

Article history:
Received 24 September 2015
Received in revised form
18 December 2015
Accepted 4 January 2016
Available online 8 January 2016

Keywords:
Dispersion modeling
Model evaluation
Plume rise
Downwash
Source characterization

ABSTRACT

Steady-state dispersion models recommended by various environmental agencies worldwide have generally been evaluated with traditional stack release databases, including tracer studies. The sources associated with these field data are generally those with isolated stacks or release points under relatively ideal conditions. Many modeling applications, however, involve sources that act to modify the local dispersion environment as well as the conditions associated with plume buoyancy and final plume rise. The source characterizations affecting plume rise that are introduced and discussed in this paper include: 1) sources with large fugitive heat releases that result in a local urbanized effect, 2) stacks on or near individual buildings with large fugitive heat releases that tend to result in buoyant "liftoff" effects counteracting aerodynamic downwash effects, 3) stacks with considerable moisture content, which leads to additional heat of condensation during plume rise – an effect that is not considered by most dispersion models, and 4) stacks in a line that result in at least partial plume merging and buoyancy enhancement under certain conditions. One or more of these effects are appropriate for a given modeling application. We present examples of specific applications for one or more of these procedures in the paper.

This paper describes methods to introduce the four source characterization approaches to more accurately simulate plume rise to a variety of dispersion models. The authors have focused upon applying these methods to the AERMOD modeling system, which is the United States Environmental Protection Agency's preferred model in addition to being used internationally, but the techniques are applicable to dispersion models worldwide. While the methods could be installed directly into specific models such as AERMOD, the advantage of implementing them outside the model is to allow them to be applicable to numerous models immediately and also to allow them to remain applicable when the dispersion models themselves are updated. Available evaluation experiences with these techniques, which are discussed in the paper, indicate improved model performance in a variety of application settings.

1. Introduction

The AERMOD dispersion model (Cimorelli et al., 2005), recommended by United States Environmental Protection Agency (USEPA) for general short-range modeling applications out to a distance of 50 km, is widely used in air quality permit and compliance applications on an international scale (EPA Victoria, 2015). This model has been tested and evaluated against a number of traditional stack release databases (USEPA, 2003). However, aside from traditional building downwash situations, model evaluations for AERMOD and models used in other countries generally

* Corresponding author.
E-mail address: laura.warren2@aecom.com (L.L. Warren).

http://dx.doi.org/10.1016/j.atmosenv.2016.01.003

Abbreviations

ADMS	Atmospheric Dispersion Modelling System, an air quality dispersion model used for industrial emissions developed by Cambridge Environmental Research Consultants
AERMOD	A short range, steady-state air quality dispersion modeling system developed by the American Meteorological Society/U.S. Environmental Protection Agency Regulatory Model Improvement Committee (AERMIC)
ASTER	Advanced Spaceborne Thermal Emission and Reflection Radiometer, an instrument aboard the polar orbiting satellite called Terra
CALPUFF	A non-steady state air quality dispersion modeling system used for long range transport maintained and distributed by Exponent
HIA	Highly Industrialized Areas
OML	Short range air quality dispersion model that incorporates low wind effects related to aerodynamic downwash
PRIME	Plume Rise Model Enhancements, a building downwash algorithm used in the AERMOD model
SCICHEM	SCIPUFF air quality dispersion modeling system that includes chemistry
SCIPUFF	Second-order Closure Integrated Puff, an air quality dispersion modeling system maintained and distributed by Sage Management
SO_2	Sulfur Dioxide
TAPM	The Air Pollution Model, a photochemical grid modeling system
USEPA	U.S. Environmental Protection Agency

do not include scenarios in which the emission source itself substantially alters the dispersion environment. Because model performance can be an even greater challenge for some nontraditional emission sources, accurate representation of the source and its surrounding environment that influence plume rise is important.

To address this general issue, we have implemented and tested four different source characterization procedures with AERMOD, which could also be implemented in other models. All of these approaches affect buoyant plume rise, and in the case of the urban approach for highly industrialized areas, also affects plume dispersion. These approaches are different than other dispersion modeling refinements that might affect chemical transformation of released pollutants (such as NOx) because they generally do not change meteorological processing or dispersion (except for the urban approach). These effects are also independent of (and do not duplicate or replace) the low wind AERMOD enhancements described by USEPA (2012). While AERMOD itself could be modified to incorporate these changes, applying the source characterizations outside the model is beneficial because the procedures can be applicable to other dispersion models and would be more readily available for implementation. Any model changes to AERMOD would likely take several years for formal incorporation into the USEPA regulatory version. Therefore, as designed, each of the advanced plume rise techniques can be performed now using processors outside of AERMOD. In countries where other models are recommended, the methods described in this paper can be considered for those models as well. Other models for which these approaches could be used include, among others, CALPUFF (Scire et al., 2000), The Air Pollution Model (TAPM) (Hurley, 2008), Atmospheric Dispersion Modelling System (ADMS) (CERC, 2015), SCIPUFF (Sykes et al., 1999), and OML (Olesen et al., 2007).

The first source characterization method addresses sources with large “fugitive” heat releases that result in a local urban-like dispersion environment. As used in this paper, “fugitive” refers to sources of heat that are not specifically considered as input to the dispersion model. While the stack exhaust temperature and velocity are considered for plume rise calculations, the heat releases of unrelated processes in large industrial complexes are generally ignored, although they affect the dispersion environment, as noted below. AERMOD estimates urban heat island effects using an urban/rural classification based on population or land use (USEPA, 2004a), but it does not consider the effects created by large industrial complexes located in remote, rural areas. The “highly industrialized area” (HIA) effect can be addressed by a technique that accounts for the heat from an industrial complex and derives an effective urban population equivalent to the scale of the HIA as input to AERMOD, which would model the source as urban.

A second source characterization issue unaccounted for within AERMOD is similarly related to fugitive heat releases on or near individual buildings that affect plume rise from nearby stacks. These unaccounted-for heat releases generally occur on a horizontal scale well below a kilometer and affect stack plume rise in the vicinity of individual buildings. While the areal extent of the fugitive heat releases may be too small to qualify as an urban-like HIA, they can exhibit a tendency to cause buoyant effects that counteract localized aerodynamic downwash effects that would otherwise result in plumes being caught in downdrafts behind buildings. Building aerodynamic effects are handled within AERMOD by the Plume Rise Model Enhancements (PRIME) (Schulman et al., 2000) model, which was developed with limited evaluation in low winds or with buildings associated with fugitive heat releases. To account for downwash effects for cases with fugitive heat releases from buildings, a procedure called “LIFTOFF” is described, along with a model-to-monitor field study evaluation demonstrating improved prediction of receptor impacts.

Thirdly, stacks with substantially moist plumes can lead to latent heat release of condensation after the plume exits the stack, providing additional plume rise relative to a “dry” plume scenario. Although some of the initial added buoyancy is later lost due to partial evaporation, a net gain in plume rise occurs. AERMOD (and many other steady-state plume models) have plume rise formulations that are based on the assumption of a dry plume, in that the chimney plume is considered to be far from being saturated and carries essentially no moisture. A procedure to incorporate the moist plume effect by adjusting the input exit temperature data can be performed prior to an AERMOD model analysis using a pre-processor called “AERMOIST.” This pre-processor makes use of a European validated plume rise model called “IBJpluris” that already incorporates moist plume effects and has been found to accurately predict the final rise of a moist plume (Janicke and Janicke, 2001; Janicke Consulting, 2015). The adjustments to plume rise using IBJpluris with and without moist plume effects can be transferred to AERMOD (or other models, as appropriate) by adjusting the input stack temperature of each affected source on an hourly basis, as a function of ambient temperature and relative humidity.

Finally, multiple stacks in a line can result in plume merging and buoyancy enhancement under certain conditions. The tendency of adjacent stack plumes to at least partially merge is a function of several factors which include the separation between the stacks, the angle of the wind relative to the stack alignment, and the plume rise for individual stack plumes (associated with individual stack buoyancy flux and meteorological variables such as stack-top wind speed). A procedure called "AERLIFT" has been created as a processor that works in conjunction with AERMOD for assessing and incorporating plume merging from aligned emission sources. It uses an hourly emissions file from an initial AERMOD run to refine the exhaust characteristics of the merging plumes on an hourly basis, and then AERMOD is run a second time with this new input of effective hourly exhaust parameters for each affected source.

In the sections below, we discuss the formulation and implementation of each of these source characterization effects. Note that these effects are generally independent from each other and can be run in combination, if appropriate. For example, in the case of a large industrial facility such as a steel mill, the characterization for a modeling application could include the urban characterization, liftoff effects of the plumes near buildings, moist plume effects (e.g., quench towers), and partial merging of plumes from stacks in a line.

2. Highly industrialized area heat islands

The urban heat island effect is a well-known phenomenon as it relates to urban and suburban areas that experience higher temperatures when compared to their rural surroundings. The key issue for plume dispersion in an urban area is that the urban heat island prevents the boundary layer from becoming stable at night, and results in weakly convective mixing at night within a deeper layer than that which exists in rural areas.

Urban surface characteristics such as albedo and surface roughness continuously affect boundary layer parameters (USEPA, 2004a). However, the boundary layer structure is most influenced by these urban surface characteristics at night (Oke, 1998). At night, an urban boundary layer is created when stable rural air reaches a warmer urban surface. Because buildings and urban surfaces trap heat more efficiently than rural areas, urban areas are slower to cool at night than the rural environments.

AERMOD currently accounts for urban environments by adjusting the urban area's surface heat flux and boundary layer height based on the urban-rural temperature difference of the urban core's temperature to the neighboring rural area's temperature (USEPA, 2004a). To calculate the urban-rural temperature difference, $\Delta T_{u\text{-}r}$, population information is used in the following equation:

$$\Delta T_{u-r} = \Delta T_{max}[0.1 \ln (P/P_o) + 1.0 \tag{1}$$

where $\Delta T_{max} = 12$ K, $P_o = 2{,}000{,}000$, the population related to the maximum temperature difference in Oke (1973, 1978, 1982), and P is the population of the urban area being modeled (USEPA, 2004a). AERMOD uses the population input value to simulate the height of the urban boundary layer.

The area of population considered for input into this AERMOD model formulation is defined using methods described in USEPA model guidance (USEPA, 2005). For locations considered to be isolated urban areas, published census data are used. Guidance further states that, "[f]or urban areas adjacent to or near other urban areas, or part of urban corridors, the user should attempt to identify that part of the urban area that will contribute to the urban heat island plume affecting the source(s)." (USEPA, 2015) For other situations, the user may determine the population within the area where the population density exceeds 750 people per square kilometer as described in the AERMOD Implementation Guide (USEPA, 2015).

To determine upward surface heat flux, H_u, resulting from the urban-rural temperature difference at night, the following relationship can be derived:

$$H_u = \alpha \, \rho \, c_p \, \Delta T_{u-r} u_* \tag{2}$$

where α is an empirical constant (0.03) described in the AERMOD model formulation document, ρ is the density of air (about 1.2 kg/m^3), c_p is the specific heat at constant pressure (1 W-s/g-K), and u_* is on the order of 0.1 m/s (USEPA, 2004a). This equation can be solved for $\Delta T_{u\text{-}r}$ (in units of K):

$$\Delta T_{u-r} \approx H_u/4 \tag{3}$$

where H_u is the anthropogenic heat release in units of watts per square meter in the "urban core."

A lesser known cause of urban heat island effects, and unaccounted for in AERMOD, but described by Hanna and Britter (2002) is an industrial complex that mimics a heat signature similar to cities. Fugitive heat releases at industrial facilities can be equivalent to the level of heat trapped by urban surfaces and buildings, and contribute to the effects seen in highly industrialized areas on a more compact scale, but more centered at the location of the emissions. These HIAs are not considered in the traditional urban classification approaches used for AERMOD, even though Irwin (1978) suggested this approach in an internal USEPA memo. The population near such areas is often much reduced because of zoning issues, and the area beyond the immediate industrial park may be rural in nature, resulting in a misleading characterization for this type of source. This mischaracterization was recognized in an independent study by Schewe and Colebrook (2013), who recognized the appropriateness of the urban approach for a large industrialized area.

2.1. Surrogate population for highly industrialized area characterization

Based upon Irwin's suggestions and with some adaptations to the AERMOD formulation, we are providing an approach here to specify a nontraditional type of urban source that is subject to urban dispersion due to industrial anthropogenic heat release rather than due to the presence of a traditional city. The user would specify the anthropogenic heat flux resulting from the source, or an urban-rural temperature difference, if available. This would be used to determine a surrogate "effective" population value for input to AERMOD. The effective population could be calculated through the use of eq (1) if $\Delta T_{u\text{-}r}$ is specified or eqs (1)–(3) if the anthropogenic heat flux is specified. A value of $\Delta T_{u\text{-}r}$ less than 3–4 K is likely insufficient to support an urban designation with a large effective population because, according to eqs (1)–(3), the resulting effective population would be too small (e.g., only 2,500 for a 4 K temperature difference). A more practical temperature difference threshold is about 8 K, which corresponds to an effective population of 70,000.

In eqs (2) and (3), it is important to note that the "urban core" of a HIA heat release (H_u) depicts an area with a horizontal extent of at least a few hundred meters on a side. In a follow-up to Hanna and Britter (2002), Dr. Hanna indicated that the minimum size of an industrial area needed to take on urban characteristics has been the subject of much discussion (Hanna et al., 2011; Hanna, 2014 – personal communication to authors). In his personal communication, Hanna referred to his 2011 reference (noted below) and indicated that an "expert elicitation" would likely result in a minimum size estimate of a few hundred meters. The anthropogenic heat release per unit area of major cities such as Indianapolis (extensively studied by the Electric Power Research Institute (EPRI) in the 1980s) would be on the order of 50 W/m^2. This value lies within the 10–100 W/m^2 range stated by Hanna et al. (2011) for urban areas.

2.2. Satellite analysis and model evaluation

A modeling study was undertaken using an evaluation database in Lake County in northwestern Indiana USA to test the performance of the AERMOD model for a HIA. Several AERMOD options were tested to determine the most representative scenario of 1-h average ground-level SO_2 modeled concentrations due to emissions from industrial complexes such as steel mills with respect to ambient monitoring stations in Gary and Hammond, Indiana (Fig. 1). The Gary monitor was located about 300 m from the nearest source, and generally within 2 km of the cluster of sources in close proximity to the monitor. The Hammond monitor was generally between 1 and 4 km away from nearby sources. Downwash effects, if present, would have affected the Gary monitor more than the Hammond monitor.

USEPA guidance for land use characterization indicated that this area should be modeled as rural, but the heat releases from the numerous iron and steel industry sources in this area create a dispersion environment that is effectively representative of an urban area with a large population.

For this model evaluation, the thermal imagery method was selected to determine the temperature difference between the populated areas and the industrial facilities. The procedures for conducting this estimate, discussed in more detail in open literature (e.g., Fung et al., 2009; Nichol, 2005; Voogt and Oke, 2003), are to obtain thermal infrared radiation (TIR) data for multiple time periods from polar-orbiting satellite instruments such as Advanced Spaceborne Thermal Emission and Reflection Radiometer (ASTER) and Landsat 8 (NASA, 2004; USGS, 2015). These data are then processed to account for surface emissivity, based on additional land use-related satellite data coinciding with the same time periods of interest, to derive a form of land surface temperature called brightness temperature. The satellite data used in these analyses must have relatively cloud-free skies so that the resulting temperature is representative of the ground rather than a cloud layer. The ASTER and Landsat 8 instruments have the ability to reliably detect land surface temperature perturbations as small as 1–2 K (Fung et al., 2009).

Whenever possible, multiple satellite images should be selected representing $\Delta T_{u\text{-}r}$ to examine diurnal trends as well as seasonal temperature variations of the HIA's surroundings. Ultimately, satellite data availability and the need for a nearly cloud-free image often limit a comparison of this nature. The $\Delta T_{u\text{-}r}$ uncertainty is reduced when the HIA emits heat at a constant rate such as steel, iron, or aluminum processing plants which generally operate 24 h per day, 7 days per week.

Brightness temperature in northwest Indiana was reviewed to estimate the temperature difference for the area of interest, derived from measurements by the ASTER instrument. On a summer day, maximum temperatures associated with industrial facilities were approximately 310–315 K which led to a temperature difference of about 11–12 K (Fig. 2). Although the satellite-measured temperature difference between the HIAs and the populated areas would often be greater at night, the temperature difference in this case was based upon a summer day due to satellite data availability. Note that this temperature difference measured by the satellite automatically accounts for the “urbanized” temperature excess of the HIA caused by the overall industrial heat releases not otherwise accounted for in the model. Using eq (1), this temperature difference was consistent with heavily populated areas with typical populations on the order of 1,000,000 instead of the region's U.S. Census Bureau population data of 10,000.

Three scenarios for the northwest Indiana application were run with building downwash and actual emissions for the year 2008 using AERMOD with default options: 1) rural land use, 2) urban land use with a small (actual) population of 10,000, and 3) urban land use with a large population of 1,000,000. Two model receptors were used to coincide with the SO_2 monitoring locations nearest to the facilities. In all three scenarios, the highest concentrations most frequently occurred during the night or early morning hours. The rural and small urban population modeling approaches led to AERMOD overpredictions of 1-h SO_2 as high as a factor of 10 at two monitors ranging from 1 to 10 km from the sources being modeled. The urban, large population scenario resulted in improved model performance by reducing the atmospheric stability at night, leading to higher plume rise and a deeper mixing layer for plume dispersion. The results still indicate that AERMOD overpredicted the 99th percentile daily maximum 1-h SO_2 ground-level concentration

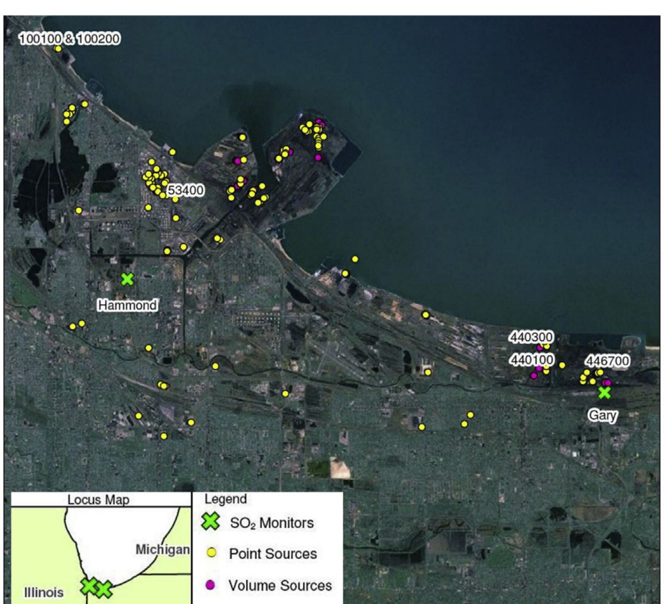

Fig. 1. Location of various emission sources in the Gary and Hammond, IN area in relation to the SO_2 ambient air monitors.

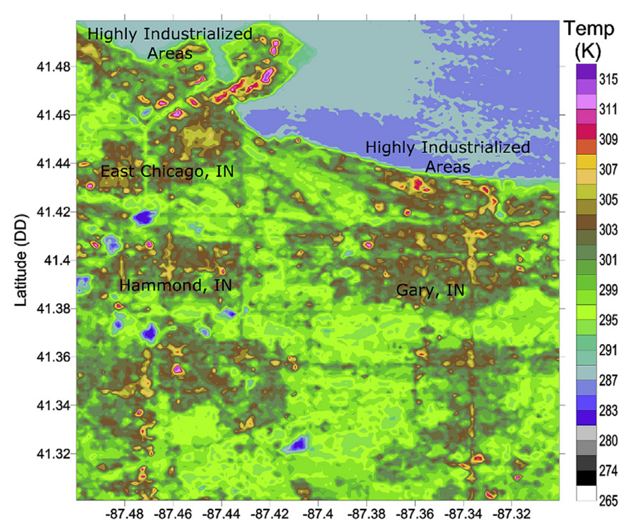

Fig. 2. Brightness temperature from ASTER band 14 on June 10, 2008 at 11 a.m. local time.

Table 1
AERMOD modeling results for rural and urban land use scenarios.

Monitor	Land use	Population	99th percentile of the daily maximum 1-h SO_2 (μg/m^3)
Hammond (96 μg/m^3)	Rural	NA	290.4
	Urban	10,000	935.5
	Urban	1,000,000	179.0
Gary (175 μg/m^3)	Rural	NA	1298.2
	Urban	10,000	1855.9
	Urban	1,000,000	392.2

Note: 1-h SO_2 99th percentile (4th highest) monitored values are listed in by monitor in parenthesis.

(which is the basis for the ambient standard in the United States) by a factor of about 2 at the Hammond and Gary monitors (Table 1). Additional refinements such as the use of liftoff effects as noted below might have further reduced this overprediction, but that analysis was not performed in this evaluation. In general, these results in comparison to the other scenarios indicate that improved model performance could be obtained by using an urban dispersion approach with an effective large population (e.g., on the order of 1,000,000).

Since actual rather than potential emissions were used in this evaluation, it is not likely that emission input uncertainty would cause the large overpredictions noted. It is possible that downwash effects are part of the overprediction problem, but such predictions are a function of the nocturnal temperature lapse rate, which is significantly different in urban vs. rural dispersion conditions in AERMOD. We strongly believe that the use of the urban characterization, as well as implementation of low wind speed improvements, are the enhancements leading to improved model performance. This northwest Indiana study involved the two monitors for which results have been reported. Additional case studies are needed to further verify these findings and approaches of which we present to encourage independent researchers to conduct such studies.

3. Plume liftoff in industrial complex environments with fugitive heat and low wind conditions

AERMOD estimates building downwash effects by applying its downwash model, PRIME, concentration estimates in the near-field where building wakes are predicted, while transitioning to the AERMOD estimates without building wake considerations in the far field (USEPA, 2004a). This transition is performed without consideration of low wind speed conditions, which can lead to poor model performance, particularly when building aerodynamic effects are estimated by the model under nearly calm conditions. Downwash conditions in near calm winds are likely to be subject to the effects of wind meander, leading to an intermittent downwash effect in any given direction. Such low wind effects have not been adequately evaluated.

In the current AERMOD implementation using default model options on a facility with short stacks close to the heights of nearby buildings, very high 1-h ground-level concentrations due to building downwash have been found by the authors to be predicted even with nearly calm winds in stable conditions. The top three predicted concentrations occurred with wind speeds less than 1.5 m/s. This is a condition for which persistent downwash effects might not be expected due to strongly buoyant plumes and weak building aerodynamic effects. For example, the CALPUFF model (Scire et al., 2000) does not consider building downwash to occur for wind speeds less than 0.5 m/s. In discussions among co-designers of the PRIME downwash algorithm in AERMOD, Dr. Lloyd Schulman and Mr. Robert Paine, Dr. Schulman confirmed that the PRIME downwash algorithm was never tested for such light wind, stable conditions, and there is no mechanism in the model for addressing the lack of or intermittent nature of the wake behind a building in very light wind conditions (Schulman, personal communication to the author, November 4, 2011). The model is assuming a plume is caught in a building wake, even in such light wind conditions, and then impacting ground-level receptors at the fenceline under very low dilution conditions. Note that when the PRIME algorithm was developed, modeling and evaluating downwash under very light winds was not a major concern when airport wind speeds in the United States were not reported below 3 knots (about 1.5 m/s). In recent years, the further use of sonic anemometers at airports and the processing of 1-min data have made the need to accommodate very low wind speeds a significant challenge. It is also noteworthy that for airport databases (including that for the northwest Indiana study), there are no turbulence measurements, and so the simulation of turbulence is affected by the boundary layer parameterization. This is one reason why the use of urban dispersion and possibly the low wind improvements to AERMOD will lead to better performance for the plume liftoff field study and its associate model evaluation presented in more detail in a subsequent section. To the extent that building downwash may be a factor, it should be noted that the depth of the enhanced turbulence region in PRIME may be overstated, as indicated by Petersen (2015).

In light winds with significant wind meander, building wake effects are unsteady, as noted by Robins (1994). However, AERMOD's basic meander treatment for low winds only applies to non-downwash dispersion, and was never implemented in the PRIME model within AERMOD. Therefore, the building downwash impacts due to PRIME predictions do not account for the intermittency of downwash effects that would tend to reduce hourly-averaged ground-level concentrations in one location. A downwash approach that accounts for low wind speeds and the inherent intermittency of steady wake effects under such conditions is already incorporated into regulatory models similar to AERMOD such as the Danish OML model (Olesen and Genikhovich, 2000) and the United Kingdom ADMS model (Robins et al., 2013).

In addition to the mistreatment of low wind conditions, a plume is able to gain buoyancy within an environment where the source's buildings provide fugitive heat on a smaller scale in comparison to a highly industrialized area. AERMOD and other steady-state plume models do not consider the additional buoyancy plume uplift due to these waste heat releases (in addition to stack releases of the pollutants of interest) in the area of an emission source, especially on or around the controlling building. An example of this is a cooler vent from taconite production furnaces; the vents do not release pollutants, but they duct very hot air to the building roof environment that will affect the aerodynamics around the building. For these cases with significant additional heat releases in the same vicinity, but not related to the pollutant stacks, plumes will resist downwash effects, especially in light wind cases. This resistance allows the plume to avoid downdrafts behind the building, which are nullified by “liftoff” conditions due to the excess heating (Hanna et al., 1998).

3.1. The LIFTOFF approach

The heat flux associated with thermal releases triggering plume liftoff can be estimated and used in an alternative approach with the use of a buoyancy flux term, F_b. Hanna et al. (1998) suggest a combined dimensionless buoyancy flux:

$$F \quad = F_b / \quad W U^3 \tag{4}$$

where F_b is the buoyancy flux, U is a reference wind speed, and W is the initial plume width. An approach that can be used as a post-processor to any dispersion model such as AERMOD, called “LIFTOFF”, accounts for conditions with no downdraft effects using a weighting factor between one extreme (liftoff conditions, no downwash) and non-liftoff conditions (normal downwash) modeled in separate AERMOD runs. This weighting factor, γ, ranges from 0 to 1 on an hourly basis (Hanna et al., 1998):

$$\gamma = \exp \qquad 6F^{**0.4} \tag{5}$$

where with large buoyancy, the downwash weight approaches 0 and with minimal buoyancy, it approaches 1. To perform these calculations, an estimate of the heating is needed for the buoyancy flux term, F_b. To quantify the combined effects of the heat release, wind, and plume width, it is necessary to estimate these values. Once these values are obtained, the final calculation can be performed using the hourly weighting factor between modeled concentrations with and without downwash ($C_{Downwash}$ and $C_{No\ Downwash}$, respectively) to determine the final LIFTOFF concentrations, $C_{LIFTOFF}$:

$$C_{LIFTOFF} = \gamma\, C_{Downwash} + (1 \quad \gamma)\, C_{No\ Downwash} \tag{6}$$

To account for low wind effects, LIFTOFF reads the 10-m reference wind speed information from the AERMET SURFACE file for each hour. In combination with the heat release and plume width information, LIFTOFF applies a weighting scheme as shown in eq (6), which is similar to the dependence on the wind intermittency for the approach used in the OML model (Olesen and Genikhovich, 2000). In general, during low wind events, it is expected that the no-downwash solution will be weighted more heavily than the downwash solution. The degree of weighting is also dependent upon the magnitude of the heat release and the initial plume width which is conservatively taken to be as large as the building width. Although the USEPA's Building Profile Input Program (USEPA, 2004b) is generally used to determine the building width, these input values can be manually edited in the event that this preprocessor overestimates the effective building width which can occur when the wind direction coincides with a long and narrow building.

For modeling applications without source-related fugitive heat releases, LIFTOFF should not be used because the calculated effect will be zero with no heat release rate. It is likely that the current PRIME model overpredicts in low winds due to its lack of considering wind meander and the related intermittent wake effects. However, with fugitive heat releases, there is a dependency of the liftoff potential on wind speed because a high wind speed would tend to dilute the effects of the heating. Therefore, the dependence of the LIFTOFF approach on all three components: heat release rate, wind speed, and initial source width is warranted. It is important, however, that any current evaluations of LIFTOFF with a substantially modified PRIME model would be useful to determine whether the weighting factor between the downwash and no downwash solutions should be adjusted.

For buoyancy effects due to source-related heat release scenarios, LIFTOFF calculates F^{**} and applies the resulting weighting factor between the downwash and no downwash model runs. These calculations are performed for each hour using the wind direction and require building width information which serves as a conservatively large estimate of the initial plume width. Additionally, an estimation of the heating is needed for the buoyancy flux term. External heating measurements can be obtained from an engineering evaluation or by estimating the temperature excess in satellite thermal imagery data using the same procedure described to estimate $\Delta T_{u\text{-}r}$ for a highly industrialized area. The temperature difference is used to solve for H_u in eq (3), where the buoyancy flux, F_b, is proportional to the heat release rate, H_u (USEPA, 1995; Briggs, 1969).

3.2. Model evaluation case study of the LIFTOFF approach

Model performance of the LIFTOFF procedure at an industrial facility featuring process areas with considerable fugitive heat releases was assessed using data from a three-month field study with four SO_2 monitors located on-site. These SO_2 monitors were oriented around the facility's three point sources in areas where the highest modeled impacts occurred based on AERMOD using default options and downwash without consideration of liftoff conditions. Monitors were approximately 400–1200 m away from the point sources (Fig. 3). The buildings affecting the point sources are shown in Fig. 4. The aspect ratio of the horizontal to vertical building dimensions was approximately 2.5:1.

Using the facility's continuous emission monitor data, several model scenarios were tested including AERMOD with default options and building downwash, AERMOD with default options and no building downwash, and the LIFTOFF technique. Although the facility was located in an isolated, rural area, it had a significant source-to-ambient temperature difference of approximately 8 K as measured by satellite imagery (Fig. 5). The area of fugitive heat was approximately 300   600 m, leading to a heat release of approximately 6 MW.

Modeled and monitored 1-h ground-level concentrations were

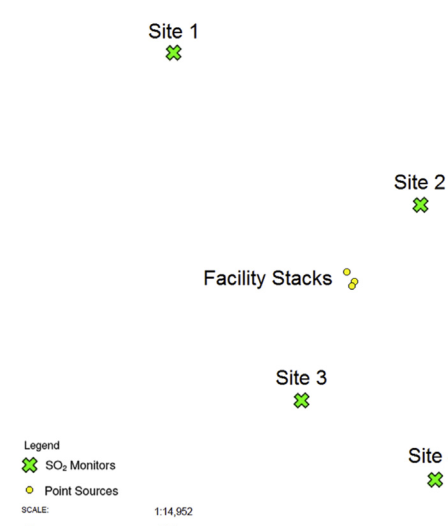

Fig. 3. At left, the industrial facility point source emissions in relation to SO_2 ambient air monitor locations.

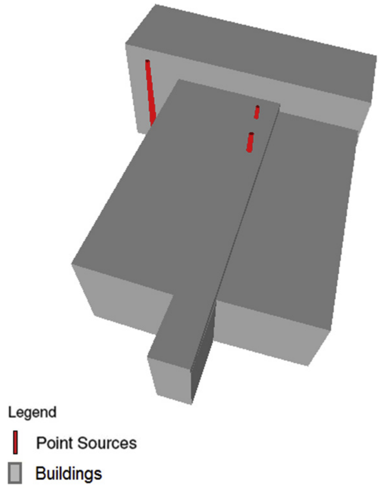

Fig. 4. At right, a 3D view, looking toward the northeast, of the industrial facility's building dimensions and point source locations.

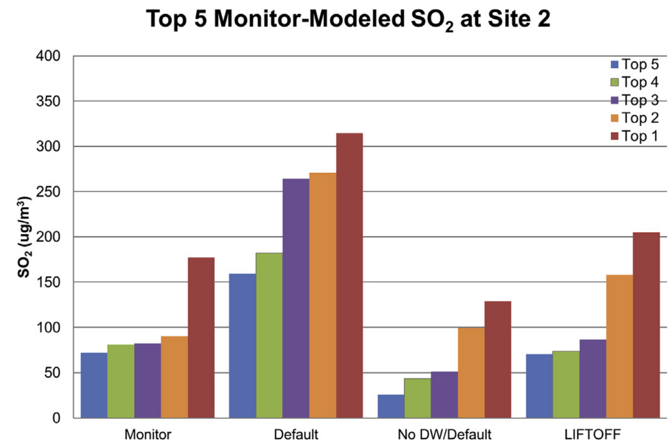

Fig. 6. Top 5 ranked daily maximum 1-h SO_2 at site 2. "Default" uses default options and downwash. "No DW" uses default options without downwash effects. "LIFTOFF" refers to the approach weighs the downwash and no downwash effects on an hourly basis.

ranked from highest to lowest and compared. In general, for the top five ranked concentrations, AERMOD with downwash indicated large overpredictions, while AERMOD without downwash exhibited a modest underprediction tendency. However, the LIFTOFF scenario (which is a weighted average of the downwash and no downwash cases computed from hourly wind and building dimension data) was relatively unbiased, and generally exhibited a modest overprediction tendency as shown by Fig. 6 for Site 2. Site 2 is the location that measured the highest SO_2 concentration during the field study. At all monitors, the top five ranked LIFTOFF concentrations were generally higher than the top five ranked observations, which is most evident in quantile-quantile comparisons of monitored to modeled concentrations as shown in Fig. 7 for each site. The LIFTOFF results have a modest overprediction and avoid the large overpredictions that are evident if no consideration is made for the fugitive heat release. More information on this model evaluation is provided in the corresponding supplemental material.

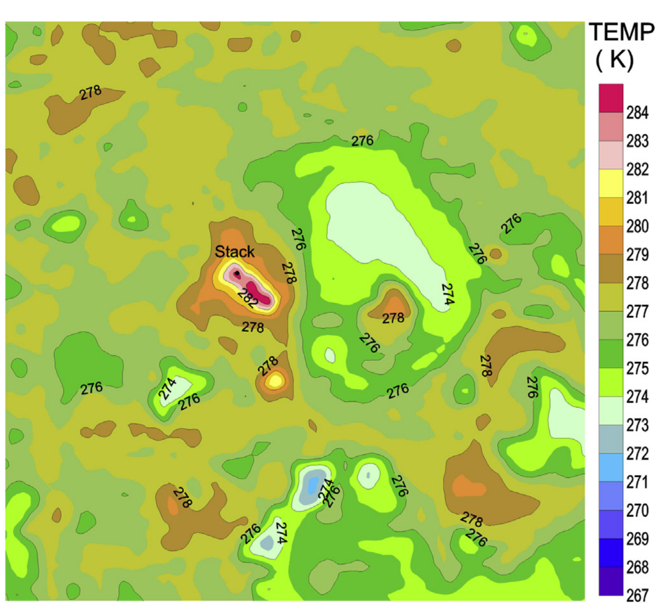

Fig. 5. Brightness temperature from Landsat 8 TIR band 11 April 21, 2013 10 p.m. local time.

4. Effects of a moist plume on plume rise calculations

The final plume rise formula in AERMOD and most other dispersion models is based on the assumption of a dry plume, where the stack plume is far from being saturated and carries essentially no liquid water load. However, in many cases for moist plumes, the effect on plume rise can be significant due to heat of condensation and should be accounted for, particularly for emission sources that operate flue gas desulphurization equipment, or scrubbers, designed to remove several pollutants from combustion plumes. The scrubbing process acts to partially or fully saturate exhaust gases while minimizing any liquid "drift" emerging from the scrubber to minimize chemically erosive processes. This process acts to cool the plume relative to the unscrubbed exhaust, resulting in a reduction of plume rise. However, the moist plume exits the stack and the heat of condensation released by the liquid water particles acts to make the plume gases warmer, giving the plume additional buoyancy. Some of this buoyancy is lost as the droplets evaporate on mixing, but a net gain in plume rise is realized from the heating/cooling process. The largest net rise is realized for the situation where the ambient air itself is near saturation.

A validated, moist plume rise model called "IBJpluris" has been found to accurately predict the final rise of a moist plume (Janicke and Janicke, 2001) and can be used to complement the dispersion modeling process when moisture content can be a significant factor. The IBJpluris model formulation includes a general solution for bent-over moist (initially saturated) chimney plumes (Janicke and Janicke, 2001). The model was reviewed by Presotto et al. (2005), which indicated that despite a number of entrainment formulas available, IBJpluris possessed the physical capability of representing the impacts of heat of condensation on symmetric chimney plume rise. The Presotto et al. (2005) paper also reported field evaluation results for the IBJpluris model involving aircraft measurements through moist plumes emitted by stacks and cooling towers. Therefore, IBJpluris was selected as the core model for developing and applying a simple adjustment method to the standard Briggs (1975) plume rise formula used by AERMOD to account for thermodynamic modification of plume rise.

4.1. The moist plume pre-processor

A method has been developed and incorporated into a pre-processor called "AERMOIST", whereby adjustments can be made

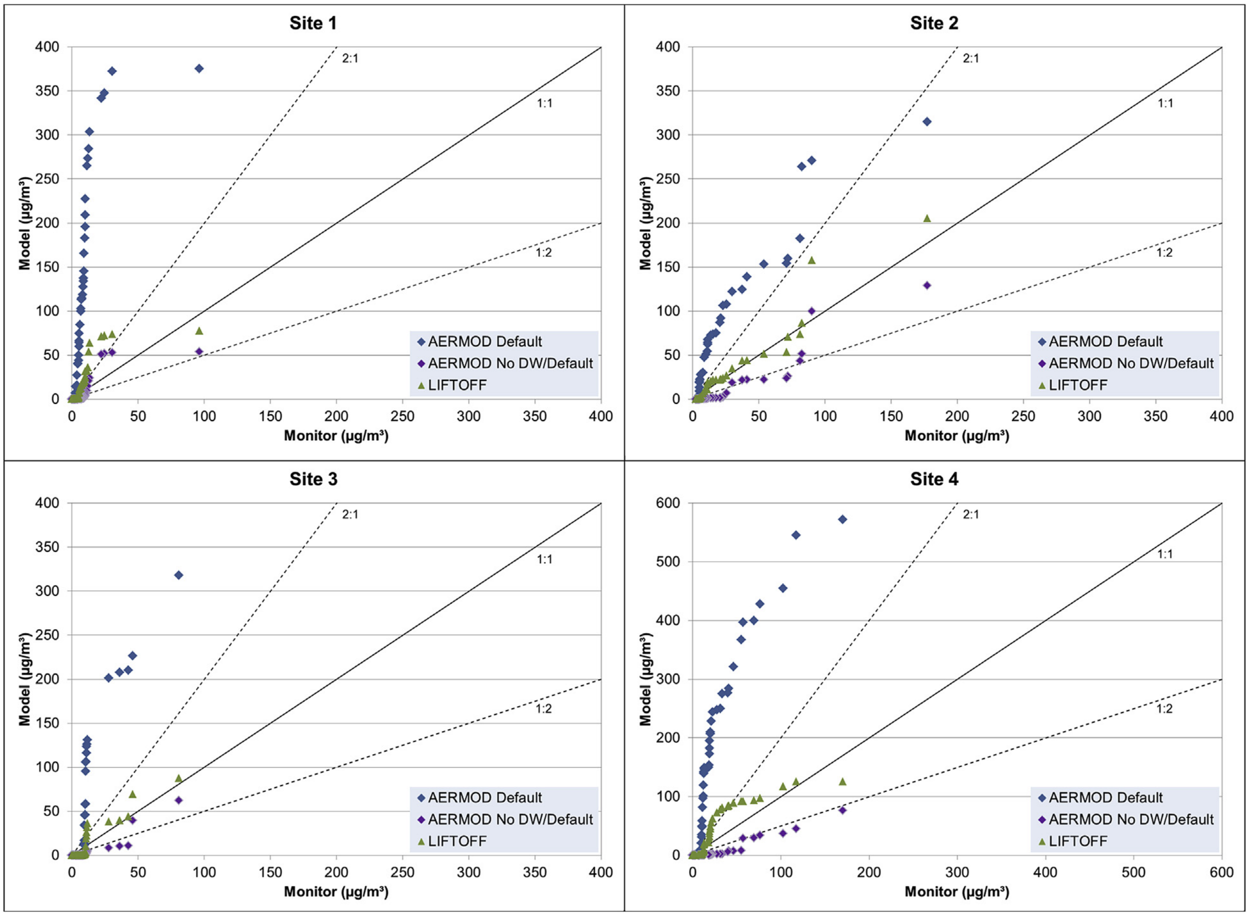

Fig. 7. Quantile-quantile comparisons between monitored and modeled daily maximum 1-h SO_2 concentrations at sites 1–4. "AERMOD Default" uses default options and downwash while "AERMOD No DW/Default" uses default options without downwash. "LIFTOFF" refers to the approach that weighs the downwash and no downwash effects on an hourly basis.

to better simulate the rise of a moist plume using a dry plume model like AERMOD. This is done by performing IBJpluris model runs for both the actual moist plume and a dry plume so that the adjustments for the difference can be made and transferred to hourly plume input data for models such as AERMOD. By assuming the ambient environment that the plume rises through is identical for both a dry and wet plume, a reasonable assumption is that the ratio of the wet to dry plume rise for IBJpluris can be used to adjust the dry dispersion model plume rise to a moist plume rise prediction:

$$[\Delta h_w(\text{model})]/[\Delta h_d(\text{model})] \multimap [\Delta h_w(\text{IBJpluris})]/[\Delta h_d(\text{IBJpluris})]\circ \quad (7)$$

where Δh is the change in final plume rise, and subscripts "w" and "d" correspond to moist and dry plumes, respectively. The approach assumes that this scaling ratio is independent from changes in wind speed and stability, although the variations in rise may be rather large. This assumption is reasonable since the rise is functionally related to the sum of exiting buoyancy and vertical momentum fluxes and the difference between dry and moist rise depends mainly on buoyancy, which is primarily temperature- and relative humidity-dependent.

The rising plume, by analogy, can be treated as if it were a rising moist thermal and cloud dynamic process. Concepts such as the buoyancy factor (Jacobson, 2005) can be applied since this same buoyancy factor appears in the Briggs (1975) dry plume rise. The major difference is that the cloud buoyancy depends on the virtual temperature, which depends on temperature, pressure, and relative humidity of both the plume and the environment. The buoyancy factor, F_b, for both plume and cloud water as normalized density can be expressed by the difference between plume temperature and ambient temperature, divided by the plume temperature, when virtual temperature is equal to dry bulb temperature. The approximate term appears in Briggs (1975) final plume rise formula for the dry buoyancy flux term. The final rise Δh_f is a power law function of F_b, where the power is '1/3' as derived by Briggs (1975). Following Jacobson (2005), the moist buoyancy can be expressed in terms of the virtual temperatures and water vapor partial pressures of the plume and the ambient environment as T_{va}, T_{vp}, and P_a, P_{wa}, P_{wp}, where P_{wp} is assumed to be saturated, P_s. The virtual temperature, T_v, can be expressed in terms of dry bulb temperature, T (Arya, 2001):

$$\begin{aligned} T_v &= T(1 \quad 0.608\, q_v)\circ \\ &= T\{1 \quad 0.608[0.622\,(RH)\,P_s/(P_{da} \quad 0.622\,(RH)\,P_s)]\}\circ \end{aligned} \quad (8)$$

where q_v is the mixing ratio in kg of moisture per kg of dry air, P_{da} is the dry atmosphere pressure, and RH is relative humidity as a fraction. For a plume exit temperature of 325 K, the virtual temperature of a saturated plume is 390 K. As the saturated plume temperature increases, so do the effects of virtual temperature, especially for higher stack temperature and relative humidity.

Using a relationship for estimating the saturation vapor pressure of water derived from the Clausius-Clapeyron equation (Arya, 2001), the relative humidity of a plume can be estimated from the moisture content (%) at the plume exit temperature:

$$P_s = 6.112\exp\{6816[(1/273.15) - (1/T)] \circ\ 5.1309\ln(273.15/T)\} \tag{9}$$

where all pressures are in hectopascals (millibars). The IBJpluris model has the ability to treat sub-saturated plumes as long as the plume emission temperature is held constant. Using eq (9) and the moisture content of the exiting plume, the relative humidity of the plume can be estimated. As the ambient air retains more moisture, the plume travels higher before reaching equilibrium with the ambient air.

4.1.1. Equivalent dry plume temperature approach

An effective approach for representing moisture in plumes is to adjust only the plume temperature rather than changing both plume and ambient temperatures, which would be required if virtual temperature were to be used directly. This revised plume temperature is generated by AERMOIST and can be referred to as an "equivalent dry plume temperature", and it is always greater than the original plume temperature and does not equal the virtual temperature. This hourly equivalent plume temperature is input to a dispersion model such as AERMOD in an hourly emissions input file so that the moist plume rise is more accurately modeled. The scaling relationship based on the right hand side of eq (7) forms the first part of the adjustment model. The plume height scaling parameter is given by the moist over the dry buoyancy flux:

$$\beta = \circ\ \Delta h_w^3 \big/ \Delta h_d^3 \tag{10}$$

where subscripts w and d refer to moist and dry buoyancy fluxes, respectively.

Two equations relating final rise to equivalent plume and ambient temperature are:

$$\Delta h_d^3 = \partial\lambda F_{bdry} = \partial\lambda\left[\ T_p \quad T_a\ /T_p\right] \tag{11}$$

$$\Delta h_w^3 = \partial\lambda F_{bwet} = \partial\lambda\left[\ T_p^{eq} \quad T_a\ /T_p^{eq}\right] \tag{12}$$

The exponent of 3 in eq (10) is due to the Briggs (1975) plume rise dependence on the buoyant flux, F_b, to the '1/3' power. As the vertical momentum flux becomes a larger fraction of the total flux, the effective exponent for the buoyant rise becomes smaller because the momentum plume rise is proportional to the momentum flux, F_m, to the 1.5 power. In AERMOIST, the exponent is treated as a user input to be conservative (<3) when the total plume rise may have appreciable momentum at release. A smaller buoyant rise exponent, such as 2.5, helps to insure that the model is conservative and the plume rise is not overstated.

From the equations stated above, the equivalent plume temperature, T_p^{eq}, can be solved for directly as:

Table 2
Moist plume characteristics used in the test case.

Stack height (m)	Exit diameter (m)	Exit temperature (K)	Exit velocity (m/s)
171.45	14.23	325.37	15.16

$$T_p^{eq} = \partial T_p\ T_a/\left[(1 \quad \beta)T_p \quad \beta T_a\right] \tag{13}$$

The ratio, β, is a function of both humidity and temperature and is found by the dry and moist IBJpluris simulations. As β goes to 1, the equivalent plume temperature approaches the dry plume temperature, T_p.

To provide the hourly equivalent plume temperature to AERMOD, a simple interpolation bilinear model is constructed using a series of βs across a range of temperature and relative humidity. At the end points of each range, β is calculated using IBJpluris and applied in a Taylor first-order expansion to create a bilinear model for the wet to dry ratio of plume rise within each range, $\beta(T_a,RH_a)$. The model assumes that ambient air at stack exit will be in the range from 253 to 313 K. Ambient temperatures outside of this range are clipped. The ambient relative humidity is assumed to lie between 0% and 95%. Values above 95% are clipped because these lie in a range of extreme sensitivity to conditional instability.

In AERMOIST, the IBJpluris model is exercised in both dry and wet mode for each range and an array of temperatures and humidity over the range of possible values, $\beta(T_i,RH_j)$ ratios, is saved for each stack that is modeled and are used to estimate the model adjustment coefficients, $C_{i,j}$ and $D_{i,j}$. The continuous model for the moist to dry plume rise ratio becomes:

$$\beta(T_a, RH_a) = \beta\ T_i, RH_j\ \ + (\ T_a \quad T_i)\ C_{i,j} \quad RH_a \quad RH_j\ \ D_{i,j} \tag{14}$$

The $\beta(T_a,RH_a)$ are used to estimate the equivalent hourly plume temperatures for input to the dispersion model for each hour of emissions. By modifying only the plume temperature, multiple sources can be included in the model run, each with their own series of equivalent hourly plume temperatures. Dry plumes can also be modeled with standard, constant input data.

4.1.2. Moist plume rise testing

The IBJpluris model was exercised for a typical saturated, scrubbed power plant, with characteristics as listed in Table 2. The exiting plume moisture content for this test stack is 13.4%, and for a surface pressure of 1000 hPa, P_s =∂134 hPa which, according to eq (8), translates into a saturated plume (RH_p = 100%) for an observed stack temperature of 325 K. The source's plume characteristics suggest that such an observed temperature (dry bulb) is actually near 340 K in terms of the virtual temperature for the saturated plume.

The profile used by AERMOIST assumes neutral conditions with a height constant humidity and turbulence profile. For a given environmental humidity value, the plume was modeled with dry humidity (0%) and a moist humidity based on the actual moisture content of the plume. The resulting plume rises as a function of downwind distance are illustrated for the dry (0% RH_p) and the moist (100% RH_p) plume cases with a dry ambient humidity (0% RH_a), and for a saturated plume emitted into a nearly saturated environment in Fig. 8. The rise at 2000 m downwind is 189.8 m for the dry plume and dry environment, 209.3 m for a saturated plume in a dry ambient environment, and 219 m for the saturated plume rise in a 90% constant RH environment. At an ambient temperature of 293 K, the percent increase over the dry case is 10.3% and when a moist environment is considered, it is 15.4%.

AERMOIST systematically exercises IBJpluris for each of the temperatures and relative humidity ranges (bins). Assuming final rise estimates at 2000 m downwind for a select set of temperature and relative humidity ranges, it is apparent that the largest rise of the saturated plume occurs at 90% humidity environmental conditions for the cooler ambient temperatures. The dependency on ambient humidity of final rise at any ambient temperature is rather

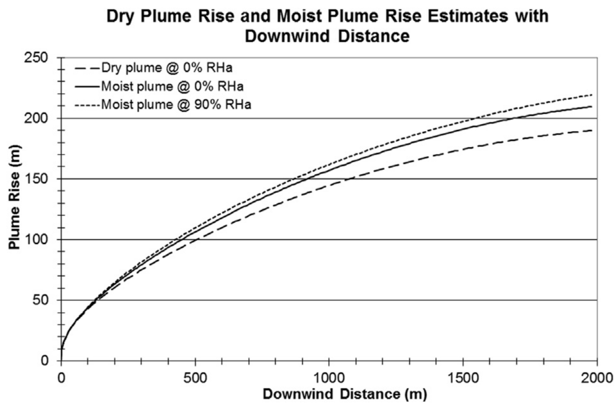

Fig. 8. Plume rise as a function of downwind distance for dry rise and an initially saturated plume by the test source for two constant relative humidity environmental conditions.

small for a dry plume, allowing for ambient RH to be ignored for dry plumes. However, moist plume rise will increase substantially as the ambient humidity approaches saturation with an increase of over 10% from dry, cool air to moist cool air. Using virtual temperature by itself does not explain this effect. As the ambient temperature increases and the buoyancy factor decreases, the change in plume rise with humidity is reduced. The resulting equivalent plume temperatures for use in dispersion modeling generated by AERMOIST, which actually runs the validated IBJpluris plume rise model, produce improved plume rise estimates for moist plumes. As evaluated by Presotto et al. (2005), the IBJpluris model predicts a more realistic plume rise for moist plumes than a model that represents a moist plume as a dry plume. Therefore, using the AERMOIST technique in conjunction with a dry plume model such as AERMOD will result in improved model performance by reduction its inherent model overprediction.

5. Plume merging of stacks in a line

When adjacent stacks are positioned in a line, the individual plumes have shown to have a tendency to merge causing a buoyancy enhancement under certain conditions. This plume merging tendency is influenced by the stacks' proximity, the wind direction relative to the stack configuration, and individual stack plume rises. Briggs (1984), refers to the results of wind tunnel studies for a row of identical stacks that indicate the usefulness of a merger parameter, S′, to determine the effect of the angle of the wind relative to the stack alignment:

$$S' = (\Delta s \sin\theta) \Big/ \left[L_b^{1/3} (\Delta s \cos\theta)^{2/3}\right] \quad (15)$$

where Δs is the average spacing between the aligned stacks, θ is the wind angle relative to the alignment angle of the adjacent, inline stacks, L_b is the buoyancy length scale where:

$L_b = F_b/U^3$,
F_b is the buoyancy flux where $F_b = g\, V_s^2 D_s^2/4\, [(T_p - T_a)/T_p]$,
U is the wind speed at plume height,
V_s is the stack gas exit velocity,
T_p is the stack gas temperature,
T_a is the ambient temperature, and
D_s is the stack diameter.

By definition, S′ is undefined when the wind is exactly normal to the alignment angle, so in practice for that case, an angle not exceeding 89.99° is used in the approach described in the next section.

Wind tunnel studies using neutral conditions showed that S′ less than 2.3 results in buoyancy enhancement while values above 3.3 indicate no enhancement (Briggs, 1984). Intermediate values would indicate partial enhancement. For those wind angles that allow plume merging, a formulation for the buoyancy enhancement accounting for other factors noted above due to the merging of adjacent plumes can be taken from the Manins implementation (Manins et al., 1992) of the Briggs formulation:

$$E = (N - S)/(1 - S) \quad (16)$$

$$S = 6 \left\{ \left[(N - 1)\, \Delta s \,/\, \left(N^{1/3}\, \Delta h\right)\right] \right\}^{3/2} \quad (17)$$

where E is the buoyancy enhancement factor, N is the number of stack in the row, S is a separation factor, and Δh is the plume rise for one stack. While the buoyancy flux would be enhanced, the momentum flux should be unchanged. The formula for the momentum flux in AERMOD and many other dispersion models is:

$$F_m = T_a / T_p \; V_s^2 D_s^2/4 \quad (18)$$

Therefore, the buoyancy enhancement would increase T_p and V_s in a manner to provide the appropriate multiplier to F_b while retaining F_m by retaining the ratio of V_s^2/T_p.

Several investigators noted in Briggs (1984) have studied and reported buoyancy enhancement for only two stacks. Briggs noted that "all of the authors referenced in this section compared the predictions of their models, at least for N = 2, with the semi-empirical results of Briggs (1974) and concluded that, as different as these approaches seem, their predictions were very similar." Additionally, the plume rise enhancements plotted in neutral conditions by Anfossi (1985) indicated that even for stacks separated by 77 m, some enhancement was observed in conditions of substantial buoyancy.

Additional supporting evidence for plume merging from two stacks is available from more recent journal articles. These articles are consistent in reporting an angular dependence on the extent of the merging. Macdonald et al. (2002) indicated that there is a definite enhancement for flow parallel to the line of stacks. For larger angles, due to dual rotors from plumes (clockwise looking downwind on the right side and counterclockwise on the left side), there can sometimes be some plume rise suppression between two closely spaced stacks for wind angles approaching a perpendicular to the line of stacks. These authors also noted plume rise enhancement for power plant stacks separated by a distance of more than 1 km, providing support for no arbitrary distance cutoff for this algorithm. The Briggs algorithm will automatically reduce the plume rise enhancement as the distance between the stacks increases.

Furthermore, Overcamp and Ku (1988) conclude that "tests with azimuthal angles of 0° and 30° showed enhanced rise". Tests with azimuthal angles of 60° and 90° did not appear to exhibit enhanced rise (Overcamp and Ku, 1988), information that was incorporated into the Briggs formulation. Similar confirmation of plume merging effects from two identical, separated stacks is documented by Contini et al. (2006). The dependence of the enhanced buoyancy on the approach angle to the stacks is similar to findings by the other investigators.

5.1. The AERLIFT technique

The AERLIFT technique has been developed to account for potential merging of plumes from aligned emission sources and the resulting partial to full enhanced plume buoyancy. This intermediate processor, run outside of the AERMOD modeling system for this implementation, creates an enhanced hourly emissions file using information from an initial model run with information for effective stack exhaust characteristics of the partially merged plumes. The model is then run a second time using the adjusted source parameters.

To define the parameters necessary for calculating the buoyancy enhancement on an hourly basis, the initial dispersion model run for the stacks involved is set up to run with a 10-km ring of 360 receptors set 1 apart in flat terrain. Next, the AERLIFT processor takes the meteorology and the model output data (i.e., the hourly and source specific final plume rise and effective wind speed) to determine first whether plume merging occurs, and if so, by how much.

The maximum enhancement factor applied to the buoyancy flux is the number of stacks in the line. The AERLIFT processor applies the enhancement factor to the original stack velocity and temperature, and derives an altered set of parameters that increases the buoyancy flux by the appropriate factor while preserving the momentum flux. This is done to conservatively apply the enhancement to only the buoyancy component. During stable hours, AERLIFT uses the plume rise directly in eq (17). For added degree of conservativeness, during unstable hours for when the stack top is less than the mixing height, AERLIFT selects the minimum between the final plume rise and the mixing height, which is defined as the maximum of the mechanical and convective mixing heights, for use in eq (17).

Finally, a second dispersion model run is performed using the appropriate terrain options and modeling receptors for the emission source as well as the enhanced hourly emission file from AERLIFT.

5.2. Evaluation of AERLIFT

AERMOD has been tested with the AERLIFT approach with a model evaluation field study conducted by Eastman Chemical Company in Kingsport, Tennessee, USA (described by Paine et al., 2013; Szembek et al., 2013). This study featured a 1-year monitoring period with 4 monitors featuring a line of 5 coal-fired boiler stacks. The inclusion of the AERLIFT approach significantly reduced AERMOD overpredictions, as noted by Szembek et al. (2013). The need for this feature was particularly evident when plumes from a row of 5 stacks indicated overprediction for impacts at a monitor located in elevated terrain, in spite of other model improvements from the low wind options (adjusted u* and LOWWIND options in AERMOD). When this single feature was tested in isolation, it resulted in a higher plume rise and a better model evaluation result in both flat and elevated terrain. This improvement was due to the effect of AERLIFT on plume rise and the attendant effect on predicted concentrations.

6. Examples of source characterization applications

Examples of the use of both the highly industrialized area (urban) application and the LIFTOFF approach would be a large aluminum smelter or large steel mill. These sources typically feature extensive areas of excess heat releases and stacks in the midst of the heated building areas. The heat release can be quantified with either a satellite thermal imagery analysis or through engineering estimates of the heat loss.

An example of a facility with only the LIFTOFF effect would be a smaller heated industrial area such as a taconite ore processing facility. This type of facility might typically have the heat release area encompassing only a few hundred meters. If the facility's point sources have considerable plume moisture, then the AERMOIST approach may also be used.

Stack releases from processes involving flue gas desulfurization controls would be good candidates for the AERMOIST approach. Flue gas desulfurization controls treat the plume by injecting an alkaline reagent into the flue gas to remove SO_2 from the gas. This treatment results in higher plume moisture content than those without the treatment, thus making it viable for the AERMOIST approach.

For any of these applications, a situation with a row of stacks (even if only 2) would qualify for the AERLIFT approach, especially if they are within a few stack diameters of each other. As noted above, the stack separation distance affects the plume rise change due to stack merging.

At the time this paper was submitted in revised form, there were a few modeling applications in the United States for which these methods have been proposed and are either being applied based upon the past evaluations reported in this paper, or are going to be evaluated in the near future based upon new field data. In the case of the Eastman Chemical evaluation study (Paine et al., 2013; Szembek et al., 2013), the urban characterization as well as LIFTOFF have been used in the same application as approved USEPA techniques.

7. Summary

Steady-state plume models such as AERMOD have not been extensively tested or designed for scenarios where an emission source modifies the dispersion environment. Model performance for these conditions has become increasingly important in light of short-term pollutant standards, e.g., for 1-h SO_2 and 1-h NO_2 United States ambient standards. Four independent source characterization techniques described in this paper have been adapted and evaluated to better represent plume rise effects for nontraditional sources and their surrounding environment. These techniques are implemented as universally applicable to many dispersion models and are thus designed to be used as external processors that interact with the main dispersion model.

Two of these source characterization methods address fugitive heat releases at industrial complexes. The first occurs on a large scale resulting in a local urban-like dispersion environment called a “highly industrialized area”. To account for this excess heat, an effective population equivalent to the scale of the HIA can be calculated using an already existing relationship between population to urban-rural temperature difference and used as input to the dispersion model. We recommend that this approach is applied to areas with a scale of at least several hundred meters and an excess temperature between the HIA and the surrounding area of at least 8 K. The second, smaller scale excess heat release issue relates to building downwash effects, and can be addressed by using the LIFTOFF procedure and a weighting relationship using procedures developed by Hanna et al. (1998). Both the HIA's effective population and LIFTOFF technique can be applied in the same modeling application. Both have been evaluated and shown to provide modest overpredictions.

Stacks with moist plumes can lead to latent heat release of condensation after the plume exits the stack, providing additional plume rise relative to a dry plume case. This effect has been neglected in many dispersion models, but with the increasing use of flue gas desulfurization controls that inject considerable water vapor into the plume exhaust, accommodating this effect is very important. The AERMOIST procedure incorporates this moist plume effect by refining the hourly input exit temperature data based on a scaling ratio developed using a previously validated European model (the IBJpluris model) which incorporates moist plume effects. Stack sources for which this approach is particularly relevant is for processes involving wet and dry flue gas desulfurization controls.

Lastly, multiple stacks in a line can result in plume merging and buoyancy enhancement under certain conditions. The AERLIFT processor assesses and incorporates plume merging from aligned emission sources using an hourly emissions file from an initial model run. The exhaust characteristics of the merging plumes are refined by AERLIFT on an hourly basis, and then the dispersion model is run a second time with a new input of effective hourly exhaust parameters for each affected source.

These advanced plume rise procedures have been designed for use with dispersion models without the need to change the modeling system code, and are shown to improve model performance. They can be used individually, or in combination. By including these procedures outside of the modeling code as source characterization techniques, these procedures are available to a large suite of modeling approaches. In addition, their use as more accurately portraying the source plume behavior is inherently a refinement outside the model's treatment of plume transport and dispersion. Although we have provided available model performance results, we encourage much wider testing and evaluation of these approaches in a variety of settings.

Acknowledgements

The authors would like to gratefully acknowledge the American Iron and Steel Institute for providing funding for this research.

Appendix A. Supplementary data

Supplementary data related to this article can be found at http://dx.doi.org/10.1016/j.atmosenv.2016.01.003.

References

Anfossi, D., 1985. Analysis of plume rise data from five TVA steam plants. J. Appl. Meteorol. Clim. 24, 1225–1236. http://dx.doi.org/10.1175/1520-0450(1985)024<1225:AOPRDF>2.0.CO;2.

Arya, S., 2001. Chapter 5: air temperature and humidity in the PBL. In: Introduction to Micrometeorology. Academic Press, Oxford, UK.

Briggs, G.A., 1969. Plume Rise. USAEC Critical Review Series, National Technical Information Service, Springfield, VA.

Briggs, G.A., 1974. Cooling Tower Environment – 1974: Plume Rise from Multiple Sources (CONF-740302). ERDA Symposium Series, National Technical Information Services, U.S. Dept. of Commerce, Springhill, VA.

Briggs, G.A., 1975. Plume rise predictions. In: Lectures on Air Pollution and Environmental Impact Analyses. American Meteorological Society, Boston, MA.

Briggs, G.A., 1984. Chapter 8: plume rise and buoyancy effects. In: Atmospheric Science and Power Production. Technical Information Center, Office of Scientific and Technical Information, U.S. Dept. of Energy, Oak Ridge, TN; Springfield, VA.

Cambridge Environmental Research Consultants Ltd, 2015. ADMS 5 Atmospheric Dispersion Modelling System User Guide. http://www.cerc.co.uk/environmental-software/assets/data/doc_userguides/CERC_ADMS_5_1_User_Guide.pdf (accessed 30.11.15).

Cimorelli, A.J., Perry, S.G., Venkatram, A., Weil, J.C., Paine, R.J., Wilson, R.B., Lee, R.F., Peters, W.D., Brode, R.W., 2005. AERMOD: a dispersion model for industrial source applications. Part I: general model formulation and boundary layer characterization. J. Appl. Meteorol. 44, 682–693. http://dx.doi.org/10.1175/JAM2227.1.

Contini, D., Hayden, P., Robins, A., 2006. Concentration field and turbulent fluxes during the mixing of two buoyant plumes. Atmos. Environ. 40 (40), 7842–7857. http://dx.doi.org/10.1016/j.atmosenv.2006.07.024.

Environmental Protection Authority Victoria, Australia. Monitoring the Environment: AERMOD Air Pollution Modelling. http://www.epa.vic.gov.au/our-work/monitoring-the-environment/monitoring-victorias-air/aermod-air-pollution-modelling (accessed 22.09.15).

Fung, W.Y., Lam, K.S., Nichol, J., Wong, M.S., 2009. Derivation of nighttime urban air temperatures using a satellite thermal image. J. Appl. Meteorol. Clim. 48, 863–872. http://dx.doi.org/10.1175/2008JAMC2001.1.

Hanna, S.R., Briggs, G.A., Chang, J.C., 1998. Lift-off of ground-based buoyant plumes. J. Hazard. Mater. 59, 123–130.

Hanna, S.R., Britter, R.E., 2002. Chapter 2: overview of meteorology and atmospheric dispersion. In: Wind Flow and Vapor Cloud Dispersion at Industrial and Urban Sites. John Wiley & Sons, Inc., Hoboken, NJ http://dx.doi.org/10.1002/9780470935613.refs.

Hanna, S., Marciotto, E., Britter, R., 2011. Urban energy fluxes in built-up downtown areas and variations across the urban area, for use in dispersion models. J. Appl. Meteorol. Clim. 50, 1341–1353.

Hurley, P., 2008. TAPM V4. Part 1: Technical Description. In: https://publications.csiro.au/rpr/download?pid=procite:0cff4149-4feb-4b86-abcb-c707168ecb0b&dsid=DS1 (accessed 30.11.15).

Irwin, J.S., 1978. Proposed Criteria for Selection of Urban versus Rural Dispersion Coefficients. Draft Staff Report (Docket No. A-80–46, II-B-8). Meteorology and Assessment Division, U.S. Environmental Protection Agency.

Jacobson, M.Z., 2005. Fundamentals of Atmospheric Modeling. Cambridge University Press, New York, NY.

Janicke, U., Janicke, L., 2001. A three-dimensional plume rise model for dry and wet plumes. Atmos. Environ. 35, 877–890.

Janicke Consulting, Environmental Physics, 2015. Plume Rise Model IBJpluris. http://www.janicke.de/en/download-programs.html (accessed 11.03.15).

Macdonald, R.W., Strom, R.K., Slawson, P.R., 2002. Water flume study of the enhancement of buoyant rise in pairs of merging plumes. Atmos. Environ. 36 (29), 4603–4615. http://dx.doi.org/10.1016/S1352-2310(02)00464-8.

Manins, P., Carras, J., Williams, D., 1992. Plume rise from multiple stacks. Clean. Air – Aust. 26 (2), 65–68.

National Aeronautics and Space Administration Jet Propulsion Laboratory, 2004. Advanced Spaceborne Thermal Emission and Reflection Radiometer. http://asterweb.jpl.nasa.gov (accessed 14.12.15).

Nichol, J., 2005. Remote sensing of urban heat islands by day and night. Photogramm. Eng. Remote Sens. 71, 613–621.

Olesen, H.R., Genikhovich, E., Ministry of Environment and Energy, 2000. Building Downwash Algorithm for OML Atmospheric Dispersion Model. http://www2.dmu.dk/1_viden/2_Publikationer/3_arbrapporter/rapporter/AR123.pdf (accessed 09.03.15).

Olesen, H.R., Berkowicz, R.B., Lofstrom, P., 2007. OML: Review of Model Formulation. National Environmental Research Institute, Denmark, p. 130. NERI Technical Report No. 609. www.dmu.dk/Pub/FR609.pdf (accessed 30.11.15).

Oke, T.R., 1973. City size and the urban heat island. Atmos. Environ. 7 (8), 769–779.

Oke, T.R., 1978. Boundary Layer Climates. John Wiley and Sons, New York, NY, p. 372.

Oke, T.R., 1982. The energetic basis of the urban heat island. Quart. J. Roy. Meteor. Soc. 108, 1–24.

Oke, T.R., November 2–4, 1998. An algorithmic scheme to estimate hourly heat island magnitude. In: Paper presented at the Second Symposium on Urban Environment. Am. Meteorol. Soc., Boston, MA.

Overcamp, T.J., Ku, T., 1988. Plume rise from two or more adjacent stacks. Atmos. Environ. 22 (4), 625–637.

Paine, R., Tringale, F., Gossett, S., 2013. Resolution of 1-hour SO_2 non-attainment area in Kingsport, TN: advanced meteorological and monitoring study. In: Control #7, Air & Waste Management Association Specialty Conference, Guideline on Air Quality Models: the Path Forward, Raleigh, NC. March.

Petersen, R., 2015. Building downwash – problems, solutions and next generation. In: 11th USEPA Modeling Conference, August 13. http://www3.epa.gov/ttn/scram/11thmodconf/presentations/3-6_Building_Downwash-CPP-11thMC.pdf (accessed 30.11.15).

Presotto, L., Bellasia, R., Bianconi, R., 2005. Assessment of the visibility impact of a plume emitted by a desulphuration plant. Atmos. Environ. 39 (4), 719–737.

Robins, A., 1994. Flow and dispersion around buildings in light wind conditions. In: Castro, Rockliff (Eds.), Stably Stratified Flows. Clarendon Press, Oxford UK, p. 372.

Robins, A., Apsley, D., Cambridge Environmental Research Consultants, 2013. Modelling of Building Effects in ADMS. http://www.cerc.co.uk/environmental-software/assets/data/doc_techspec/CERC_ADMS5_P16_01.pdf (accessed 22.09.15).

Schewe, G., Colebrook, J., 2013. Use of the urban option in AERMOD for a large industrial facility. In: Control #21, Air & Waste Management Association Specialty Conference, Guideline on Air Quality Models: the Path Forward, Raleigh, NC. March.

Scire, J.S., Strimaitis, D.G., Yamartino, R.J., 2000. A User's Guide for the CALPUFF Dispersion Model (Version 5). Tech. Rep. Earth Tech, Inc., Concord, MA, p. 521. http://www.src.com/calpuff/download/CALPUFF_UsersGuide.pdf (accessed 01.12.15).

Schulman, L.L., Strimaitis, D.G., Scire, J.S., 2000. Development and evaluation of the PRIME plume rise and building downwash model. J. Air Waste Manag. Assoc. 50, 378–390.

Sykes, R.I., Cerasoli, C.P., Henn, D.S., 1999. The representation of dynamic flow effects in a Lagrangian puff dispersion model. J. Hazard. Mater. 64, 223–247.

Szembek, C., Paine, R., Gossett, S., 2013. Resolution of 1-hour SO_2 non-attainment area in Kingsport, TN: model evaluation analysis results to date. In: Control #8, Air & Waste Management Association Specialty Conference, Guideline on Air Quality Models: the Path Forward, Raleigh, NC. March.

U.S. Environmental Protection Agency, 1995. SCREEN3 Model User's Guide. http://www.epa.gov/scram001/userg/screen/screen3d.pdf (accessed 09.03.15).

U.S. Environmental Protection Agency, 2003. AERMOD: Latest Features and Evaluation Results. http://www.epa.gov/ttn/scram/7thconf/aermod/aermod_mep.pdf (accessed 05.03.15).

U.S. Environmental Protection Agency, 2004a. AERMOD: Description of Model

Formulation. http://www.epa.gov/scram001/7thconf/aermod/aermod_mfd.pdf (accessed 13.03.15).
U.S. Environmental Protection Agency, 2004b. User's Guide to the Building Profile Input Program. http://www3.epa.gov/scram001/userg/relat/bpipdup.pdf (accessed 22.11.15).
U.S. Environmental Protection Agency, 2005. Guideline on Air Quality Models (Appendix W); 40 FR 68218. http://www.epa.gov/ttn/scram/guidance/guide/appw_05.pdf (accessed 14.12.15).
U.S. Environmental Protection Agency, 2012. AERMIC Update. http://www3.epa.gov/ttn/scram/10thmodconf/presentations/1-9-Brode_10thMC_AERMIC_Update_03-13-2012.pdf (accessed 14.12.15).
U.S. Environmental Protection Agency, 2015. AERMOD Implementation Guide. http://www.epa.gov/ttn/scram/7thconf/aermod/aermod_implmtn_guide_3August2015.pdf (accessed 27.08.15).
U. S. Geological Survey, 2015. Landsat Missions: Landsat 8. http://landsat.usgs.gov/landsat8.php (accessed 14.12.15).
Voogt, J.A., Oke, T.R., 2003. Thermal remote sensing of urban climates. Remote Sens. Environ. 86, 370–384.

Appendix C Satellite Images Used for Urban Characterization of the Intalco Smelter

Satellite-derived land surface temperatures were generated for the Alcoa Intalco area in order to evaluate and quantify the industrial complex heat signature. According to satellite data, the highly industrialized area at the facility is extensive. Satellite imagery indicates that the heat signature for the smelter area is approximately 14 K.

Landsat 8 Thermal Infrared (TIR) satellite data were downloaded from U.S. Earth Explorer and selected for further processing using a 50% or less cloud cover criteria (to avoid scene contamination and obscuration) for the period of January 2013 – June 2018. Using this criterion, a total of 13 scenes were available and obtained. These scenes were processed using a computer program to derive land surface temperature data from the TIR data. They were then visually evaluated for cloud contamination and other obstructions. Scenes in which views of the smelter were obstructed were not considered for the analysis. The final analysis was based upon 9 scenes with unobstructed views of the smelter.

The final scenes for this analysis represent all 4 seasons with 1 for winter, 3 for spring, 4 for summer, and 1 for autumn. **Table C-1** provides the results of this analysis. The "urban" temperature (Tu) was determined as the maximum temperature over the smelter area while the background rural temperature (Tr) represented the average temperature over several areas surrounding the smelter, outside of the urban heat signature, as shown in **Figure C-1**. **Figures C-2 to C-10** illustrate each of the scenes from this analysis.

Table C-1: List of Selected Satellite Images for Urban – Rural Temperature Analysis

Date / Scene	Season	Maximum Temp. (K); Tu	Background Temp. (K); Tr	∆Tu-r
29-May-15	Spring	311.3	296.2	15.0
14-Jun-15	Summer	313.1	297.7	15.4
30-Jun-15	Summer	315.1	299.8	15.3
4-Oct-15	Autumn	303.8	292.9	10.9
9-Feb-16	Winter	295.0	286.1	8.8
31-May-16	Spring	303.0	288.8	14.3
5-Jul-17	Summer	315.6	298.5	17.1
22-Aug-17	Summer	313.3	299.3	14.0
5-May-18	Spring	305.8	291.6	14.2
			Average ∆Tu-r	13.9

Figure C-1: Location of Points Selected to Represent the Background "Rural" Temperature

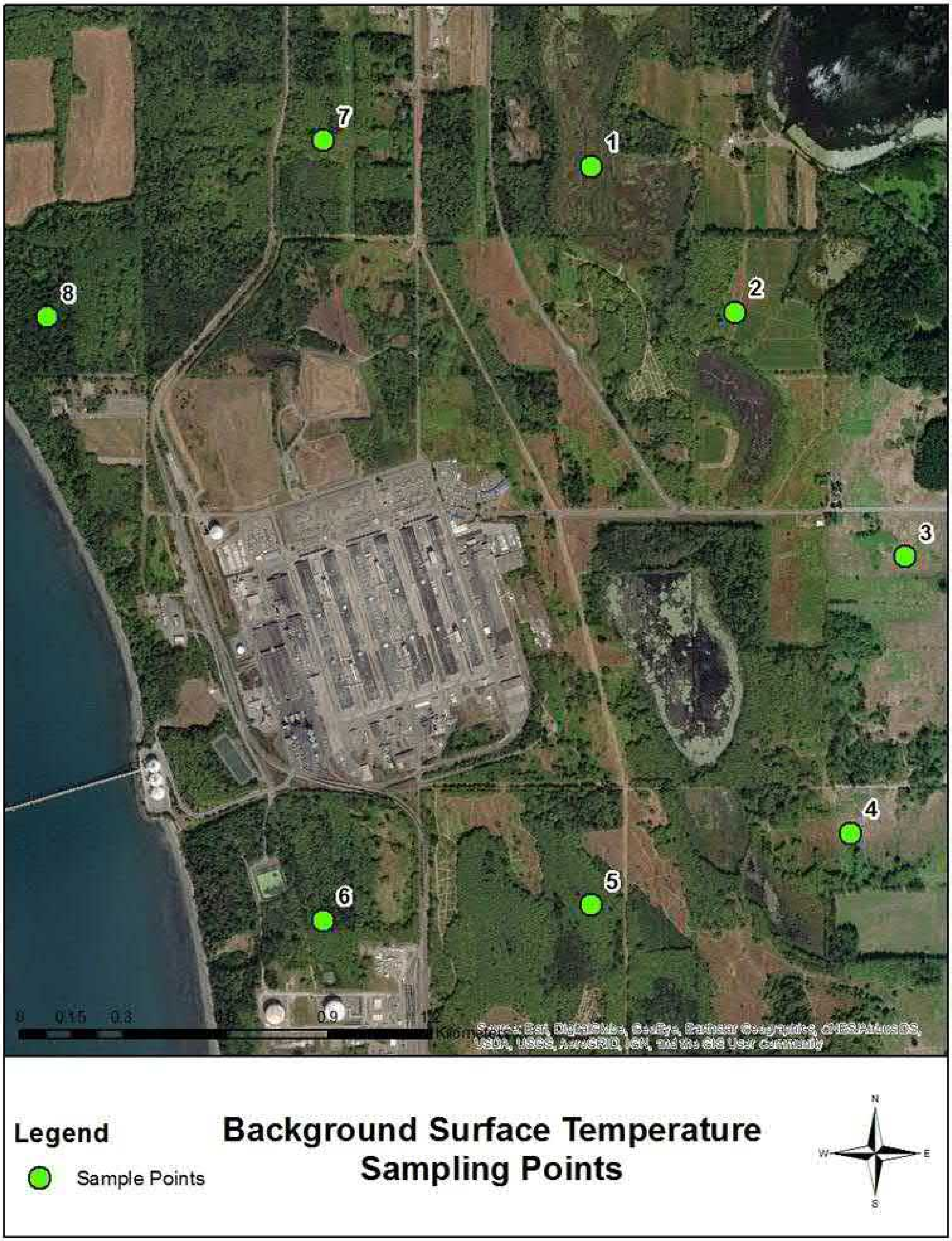

Figure C-2: Surface Temperature Pattern on May 29, 2015

Figure C-3: Surface Temperature Pattern on June 14, 2015

Figure C-4: Surface Temperature Pattern on June 30, 2015

Figure C-5: Surface Temperature Pattern on October 4, 2015

Figure C-6: Surface Temperature Pattern on February 9, 2016

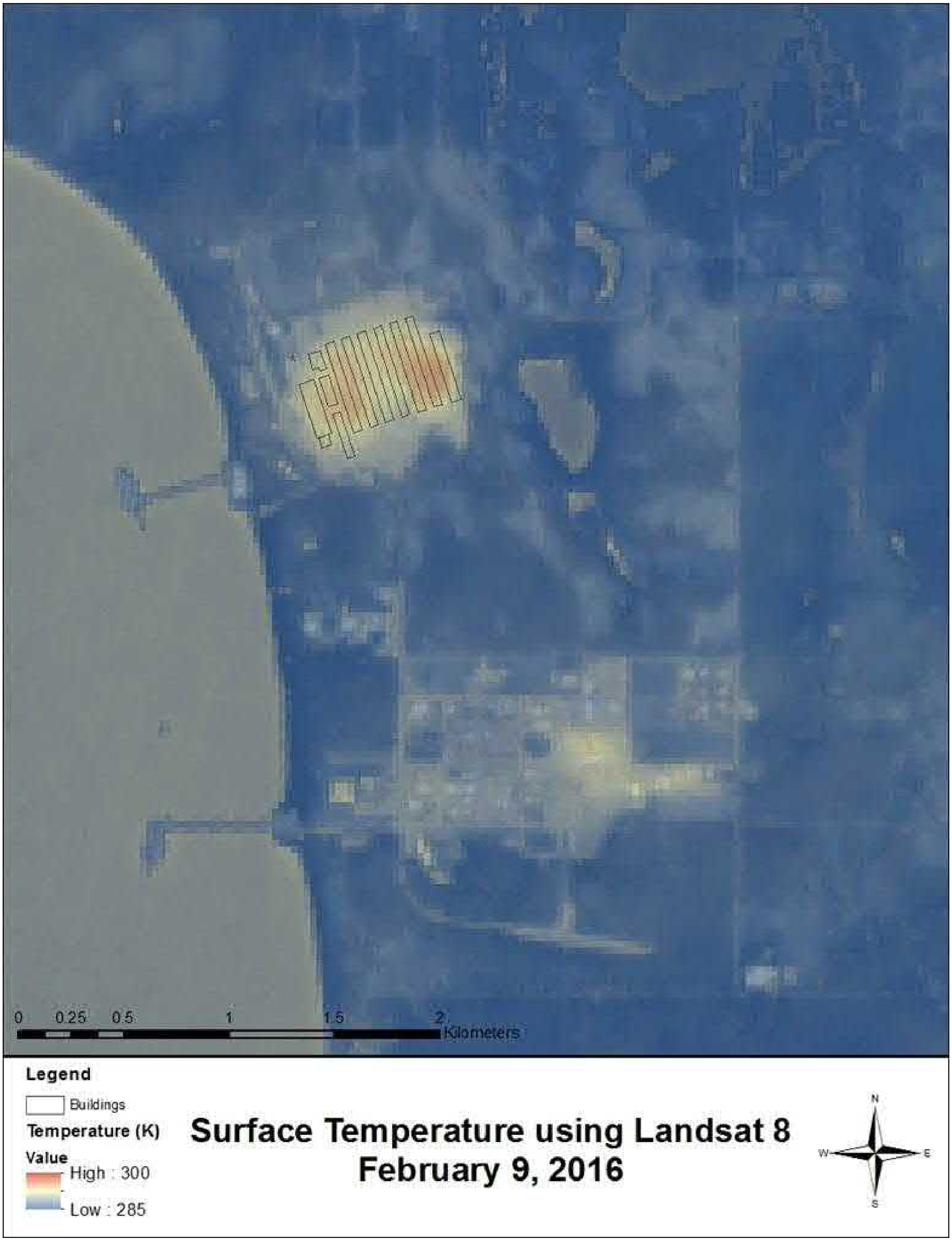

Figure C-7: Surface Temperature Pattern on May 31, 2016

Figure C-8: Surface Temperature Pattern on July 5, 2017

Figure C-9: Surface Temperature Pattern on August 22, 2017

Figure C-10: Surface Temperature Pattern on May 5, 2018

Appendix D Supplemental Information on BLP Evaluation Testing

This appendix provides additional information regarding the initial evaluations and sensitivity testing of the Buoyant and Line Point (BLP) model[14]. This model was developed by the Aluminum Association and involved a tracer study featuring SF_6 releases from an aluminum smelter with tracer gas emissions coming from roof vents.

As documented by Scire and Schulman[15], The tracer study occurred at the Reynolds Metals Patterson Reduction Plant located in Arkadelphia, Arkansas (see **Figures D-1 and D-2**). The tracer gas was injected into the potroom at three points along the line source and the hourly-averaged concentrations were measured at a network of 19 bag samplers. The bag samplers were located on lines at distances of about 750, 1500, and 2250 meters downwind from the buoyant line source (see **Figure D-3**).

Figures D-4 and D-5 show predicted and observed concentration patterns near the Arkadelphia smelter. The key aspects of the concentration patterns are that they have a relatively tight gradient, with the concentrations rapidly approaching background levels within 2 km of the smelter. The observed concentrations are seen to fall off linearly with distance.

The Scire and Schulman paper also indicates the dependence of the line source plume rise with alignment of the wind either along the lines (0°) or perpendicular (90°); see **Figure D-6**. This information indicates that with all other factors being equal, there would be higher plume rise along the lines due to the alignment of the buoyancy from the underlying heat coming from the line source. This concept was incorporated into the formulation of the Intalco modeling approach.

[14] Available at https://www.epa.gov/scram/air-quality-dispersion-modeling-alternative-models#blp; also installed into AERMOD.

[15] Scire, J.S. and L.L. Schulman, 1981. Evaluation of the BLP and ISC models with SF_6 tracer data and SO_2 measurements at aluminum reduction plants. Paper presented at a specialty conference on Dispersion Modeling from Complex Sources. Edited by the Air Pollution Control Association, co-sponsored by APCA's TS-4.2 Non-Ferrous Smelting & Refining Committee, the Aluminum Association, the American Meteorological Society, and the U.S. Environmental Protection Agency. St. Louis, MO. April 7-9, 1981.

Figure D-1: Map Showing Location of the Arkadelphia Smelter

Figure D-2: Aerial Photo of Arkadelphia, AR Aluminum Smelter

Figure D-3: Layout of SF_6 Samplers Near the Reynolds Smelter

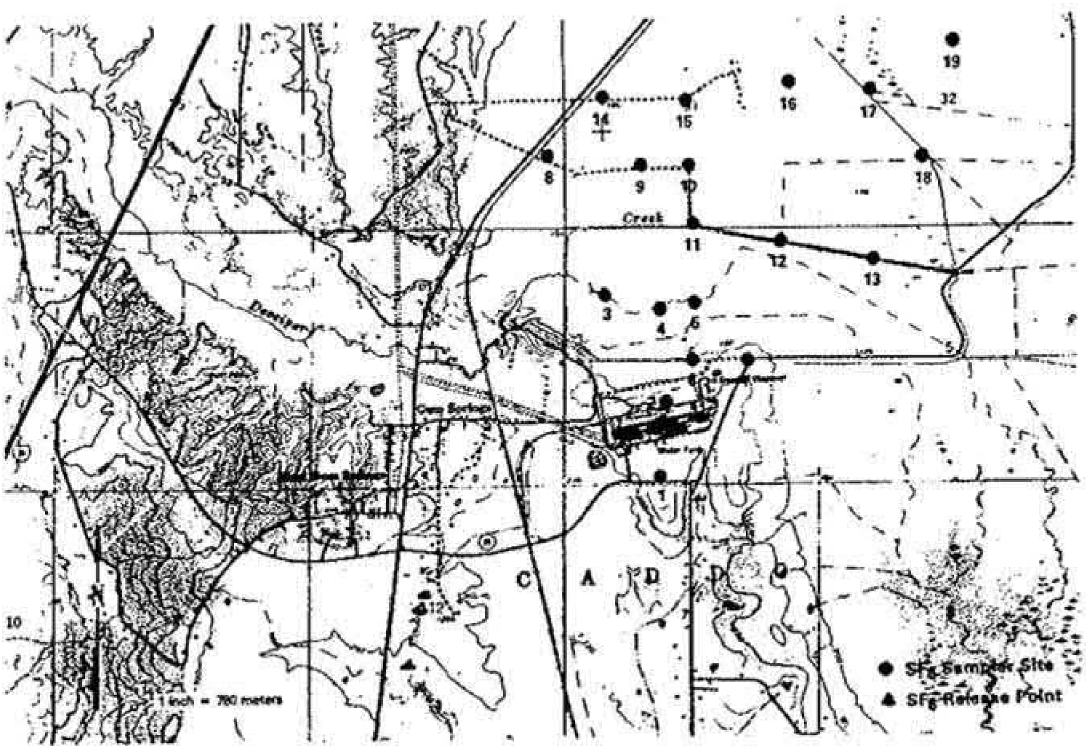

Figure D-4: Observed and BLP-Predicted Concentration Patterns for One of the Sampler Hours at the Arkadelphia Smelter

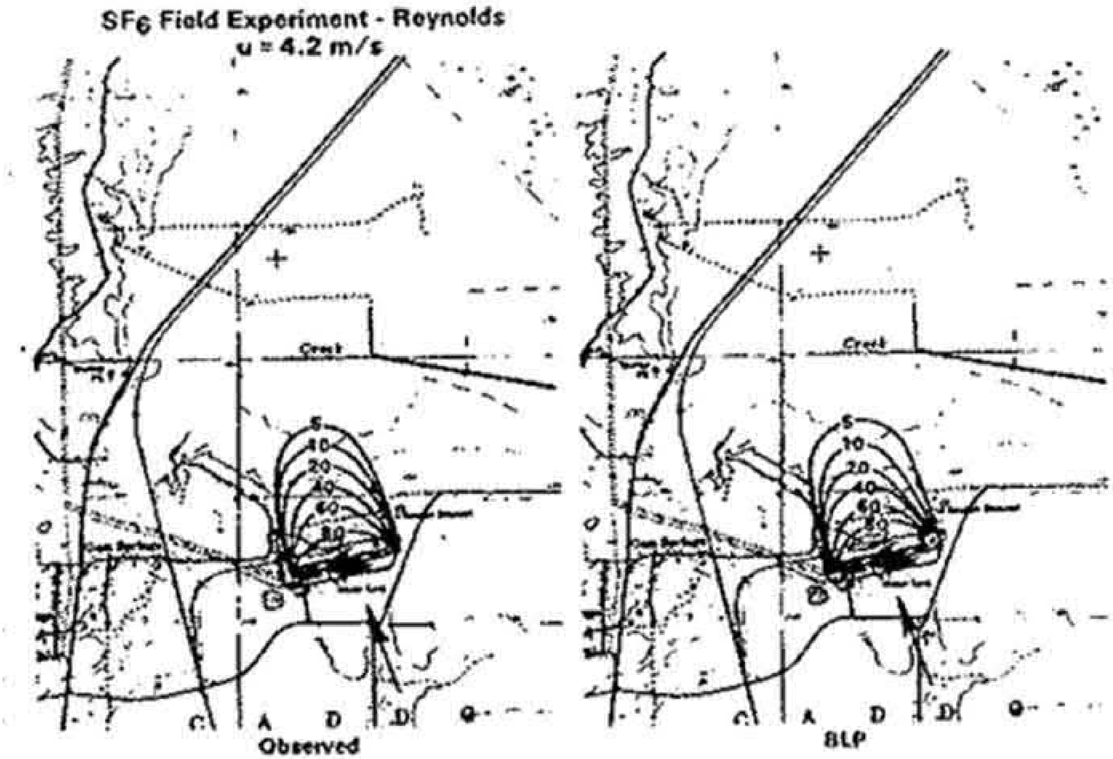

Figure D-5: Observed and BLP-Predicted Concentration Patterns for Another of the Sampler Hours at the Arkadelphia Smelter

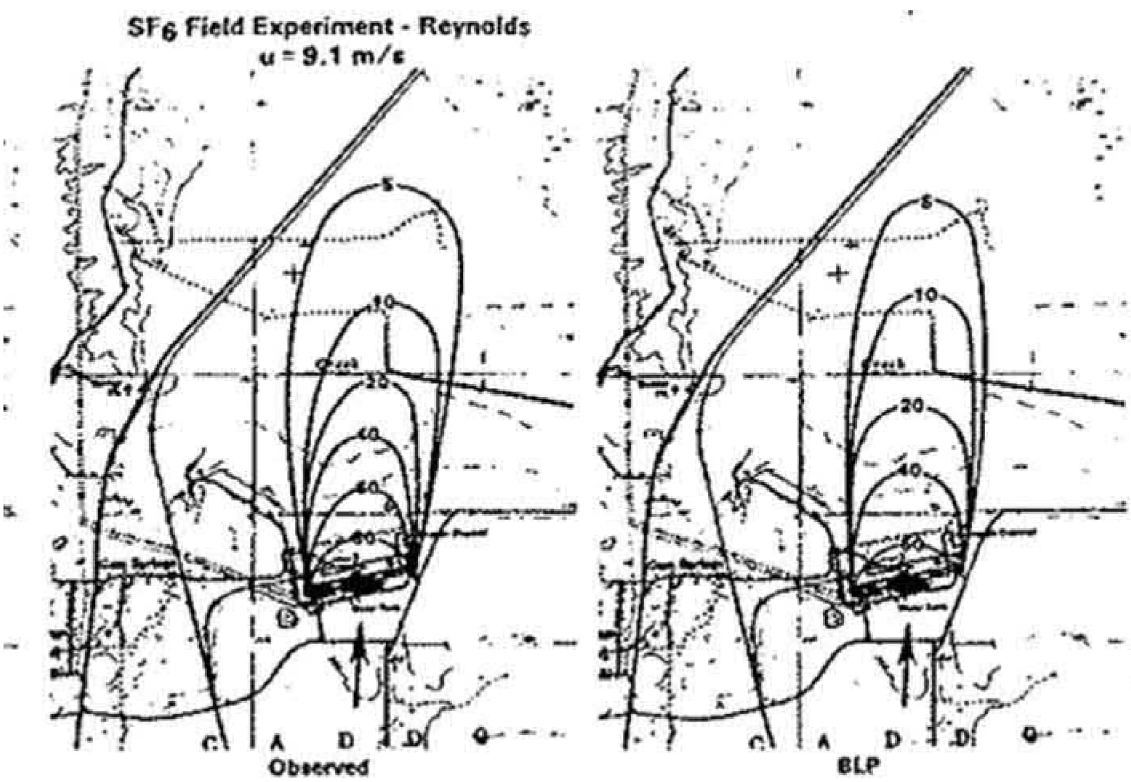

Figure D-6: Line Source Plume Rise as a Function of Alignment Angle

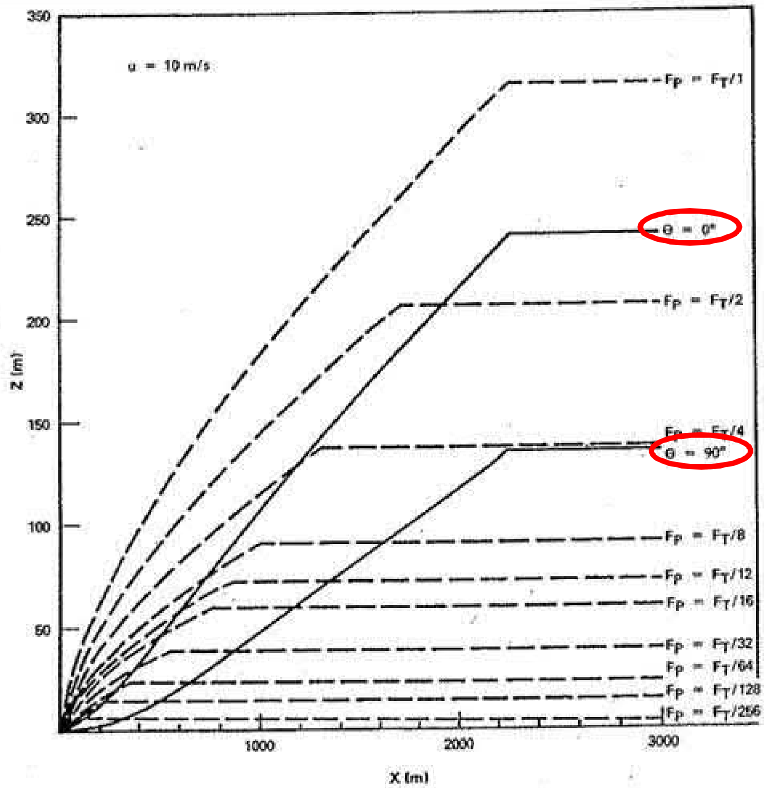

Appendix E Direction-Dependent Stack Merging Approach for Intalco Modeling

This appendix presents the technical approach for modeling dry scrubber stacks at the Intalco Aluminum LLC (Intalco) aluminum smelter, which requires partial merging of stacks as a function of wind direction to accommodate smelter fugitive heat effects in order to optimize AERMOD model performance at the three SO_2 monitors near the smelter. As noted in a number of applications, modeling aluminum smelters with AERMOD using default options has been shown to produce large overestimates in modeled concentrations compared to monitored concentrations.[16,17]

At aluminum smelters, the area in the vicinity of the numerous dry scrubber stacks features considerable amounts of fugitive heat releases that are not directly accounted for in dispersion modeling, as shown in **Figure E-1**, which illustrates visual and infrared photos of a bank of dry scrubber stacks at an Alcoa aluminum smelter. This additional heat acts to enhance or boost the plume buoyancy in comparison to environments without this fugitive heat release. The path of the emissions over other parts of the hot smelter area will dictate the amount of buoyancy enhancement that needs to be simulated with a direction-specific stack merging approach.

Figure E-7: Visual and Infrared Photos of Aluminum Smelter Dry Scrubber Stack Area

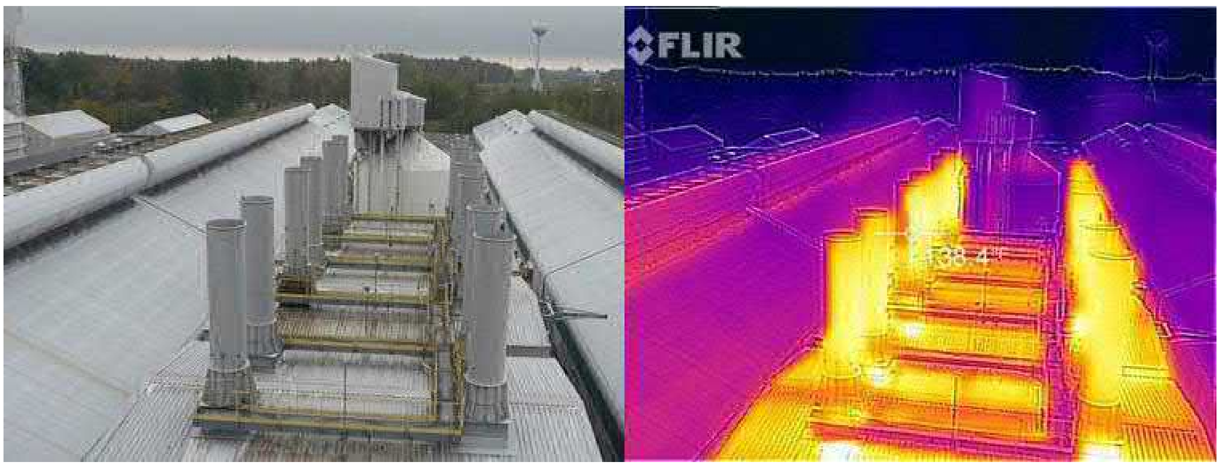

One approach to account for this enhanced plume buoyancy uses partial dry scrubber stack merging in combination with the urban model option. Recently, this type of source characterization technique was developed and successfully applied to another aluminum smelter (Alcoa's Warrick Operations in southern Indiana). That source characterization did not require a formal EPA Model Clearinghouse approval for a nonguideline modeling technique under Section 3.2.2 of 40 CFR Part 51. Good model performance was demonstrated for that facility in its model-to-monitor evaluation and was accepted by the state agency (Indiana Department of Environmental Management, IDEM) and by EPA Region 5. The Warrick characterization used the following model configuration:

- Urban model option to represent the industrialized heat island complex; population of 2,000,000 representing a 12 K urban-rural temperature difference derived by engineering estimates, later confirmed by satellite data.
- Partial merging of dry scrubber stacks (modeled as point sources), where the actual stacks were grouped into merged stacks based on spatial configuration.

[16] https://www.epa.gov/sites/production/files/2017-12/documents/13-in-so2-rd3-final.pdf
[17] http://lar.wsu.edu/nw-airquest/docs/20160615_meeting/F-Dhammapala_on_Modeling_dry_scrubber_stacks_as_buoyant_line_sources_in_AERMOD-20160616.pdf

A similar approach is proposed for Intalco. The Intalco characterization uses the following model configuration:

- Urban model option to represent the industrialized heat island complex; population of 2,000,000 representing a 12 K urban-rural temperature difference derived by satellite data.
- Partial merging of dry scrubber stacks (modeled as point sources), where stack merging varies as a function of hourly wind direction.
- Conservatively combining through modeling the wet scrubber emissions (3% of the potline SO_2 emissions) through the dry scrubber stacks.

For Intalco, sensitivity modeling runs for the model-to-monitor evaluations indicated that partial merging that varies as a function of wind direction is necessary for this facility. Using a direction-dependent stack merging approach is a concept that is supported by field studies at aluminum smelters and formulations that were used in the development of the Buoyant Point and Line (BLP) model, as discussed below.

Direction-dependent stack merging was not necessary for Alcoa Warrick, likely because of the significant supplemental heat source located north of the smelter's dry scrubber stacks, the Warrick rolling mill. The rolling mill expanded the urban heat island and resulted in a stack merging approach for critical receptors on the northern and eastern fenceline that did not need a direction-specific approach. A comparison of Intalco and Warrick satellite-detected surface temperatures is shown in **Figure E-2**.

Another approach that has been suggested in the past to account for a smelter's dry scrubber stack heat releases is to use the Buoyant Line and Point (BLP) model to model the dry scrubber stacks.[17] Unfortunately, BLP has several limitations that make it difficult to apply to the dry scrubber stacks specifically. However, BLP model formulation and theory explains why a partial stack merging approach (as point sources) in AERMOD results in a more accurate representation of Intalco.

Figure E-8: Satellite-derived Surface Temperatures for Intalco on May 31, 2016 (left) and Warrick on April 24, 2014 (right)

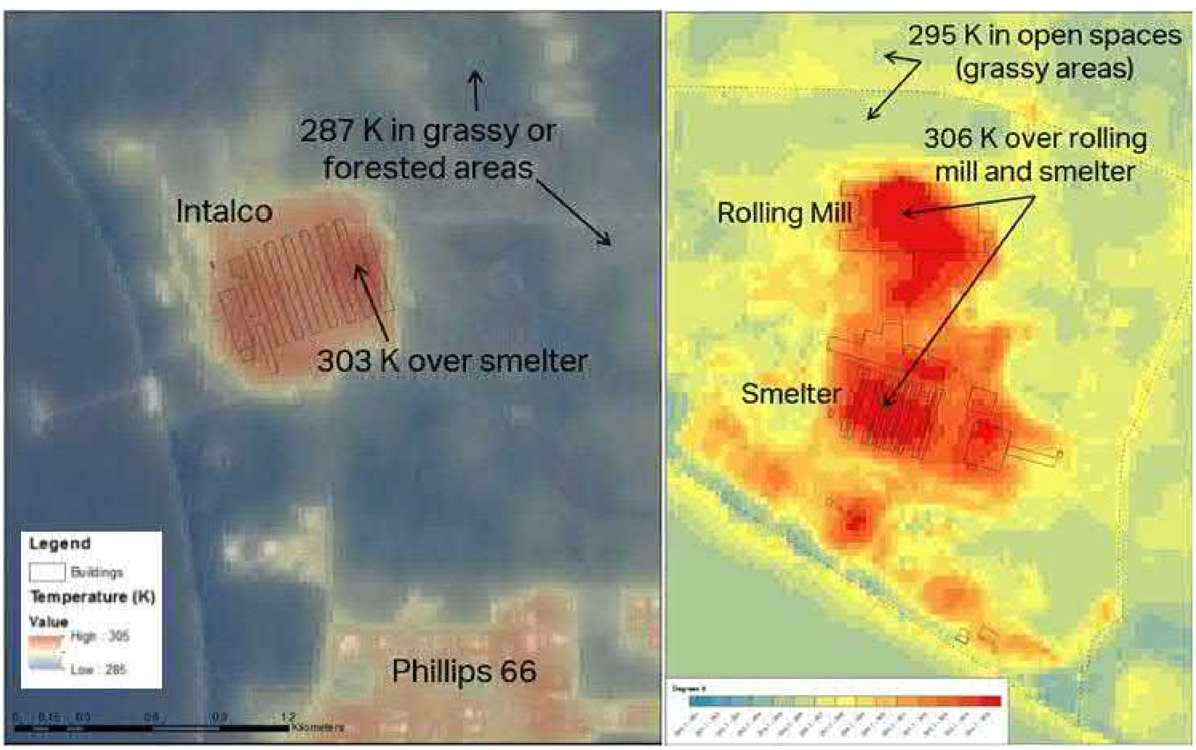

Limitations of BLP

The BLP model was designed for simulating plume rise and dispersion from buoyant line sources, but in the case of the Intalco smelter, most of the emissions are from point sources in between the line sources. As such, BLP is not equipped to handle plume meandering behavior for point sources such as the dry scrubber stacks. Additionally, the best characterization of the smelter's dispersion is the use of an urban treatment, but BLP is currently only able to model rural conditions using default model options. On that point alone, BLP is disqualified from use for modeling the dry scrubber stack emissions except through a nonguideline model approval.

BLP also requires a series of parallel line sources that are all the same length, have the same buoyancy, and have equal spacing between each line. Intalco's potline configuration is shown in **Figure E-3**, where Center 4 has been curtailed. The existence of only half a potline in operation is not consistent with the BLP requirements stated above, and the formulation is therefore not applicable to this situation. On that point as well, BLP cannot be used for the dry scrubber stacks at Intalco.

Another issue with BLP is that it assumes that the emissions are continuous along the buoyant line. However, for this application, the dry scrubber stack emission sources are clustered in groups in between the potlines. This is another reason why BLP is not applicable for the dry scrubber stacks at Intalco.

BLP is also not applicable to complex terrain situations. In the vicinity of the Intalco smelter, with stacks only about 15 m high, there are numerous areas (the closest within 1 km to the northeast) that are higher than stack top. This consideration also disqualifies BLP for use in any area other than simple terrain areas.

EPA has implemented a new alpha model option in AERMOD version 19191 that updates BLP to model emission sources in urban environments following discussions with AECOM on this topic. However, alpha options are intended for experimental use only, and are not yet recommended for regulatory modeling. Due to this limitation and in consultation with Washington Department of Ecology and EPA Region 10, dry scrubber stack emissions and wet scrubber emissions will be combined in the modeling and emitted from the dry scrubber stack point sources, avoiding direct use of the BLP model for any Intalco emission sources.

Figure E-9: Layout of Intalco's Dry Scrubber Centers (1-6) and Bake Oven Center (7)

Considerations for Point Source Merging for Dry Scrubber Stacks

Although BLP is not directly applicable to the modeling of the dry scrubber stacks, there are aspects of its formulation that are relevant for formulating a modeling approach using point sources for the potline centers. The following discussion in Section 2.4 of the BLP User's Guide[18] (page 2-42) is applicable.

"Observational and wind tunnel studies indicate that the line source plume rise equation should contain a wind direction dependence. For winds aligned parallel to the long axis of a line source, consider the path of a plume element originating from the upwind end of the line source. As the plume element rises and travels along the length of the line, it merges with other buoyant elements. At the downwind edge of the line source, the input of buoyant plume elements stops. Figure 2-9 [*reproduced as* **Figure E-4** *below*] is a cross section of the plume at the downwind edge of the line source. The plume elements originating from the most upwind section of the line source have risen substantially more than the plume elements near the downwind edge of the line source. The integration of the Gaussian plume equation over the length of the line source consists of breaking the line source into a number of points or line segments; this approach allows different plume elements to have different effective stack heights."

This approach is implemented in the Intalco site-specific source characterization approach using point sources by merging the upwind emission dry scrubber stack centers more than those that are downwind. The plume rise for flow perpendicular to the lines is expected to be less than that for flow parallel to the lines. This issue is noted in the Scire and Schulman 1981 paper[19] that discusses how modeling of point sources with the appropriate number (involving merging, as we are proposing here) can affect the comparison of the point and line modeling results. In general, the plume rise with the flow along the potline (ϴ = 0 degrees) is higher than that for flow perpendicular to the potline (ϴ = 90 degrees). Fewer total numbers of stacks from merging sources would be appropriate for the alongwind direction versus the perpendicular direction. Figure 4, shown as **Figure E-5**, from the 1981 paper illustrates this concept.

As discussed previously, the wind direction-varying approach was not used for Warrick due to the presence of a large heat source adjacent to the smelter that more evenly distributes the heat influences at that site in various directions.

Figure E-10: BLP User's Guide Figure 2-9

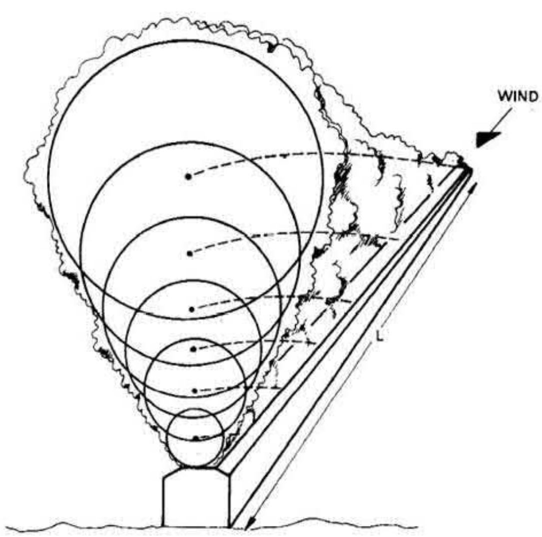

Figure 2-9 Cross Section of Line Source at $X = X_{FB}$ with Parallel Winds

[18] https://www3.epa.gov/ttn/scram/userg/regmod/blpug.pdf

[19] Scire, J. and L. Schulman, 1981. Evaluation of the BLP and ISC Models with SF_6 Tracer Data and SO_2 Measurements at Aluminum Reduction Plants. Air Pollution Control Association Specialty Conference on Dispersion Modeling from Complex Sources.

Figure E-11: Plume Rise for Flow Along and Perpendicular to Buoyant Line Sources

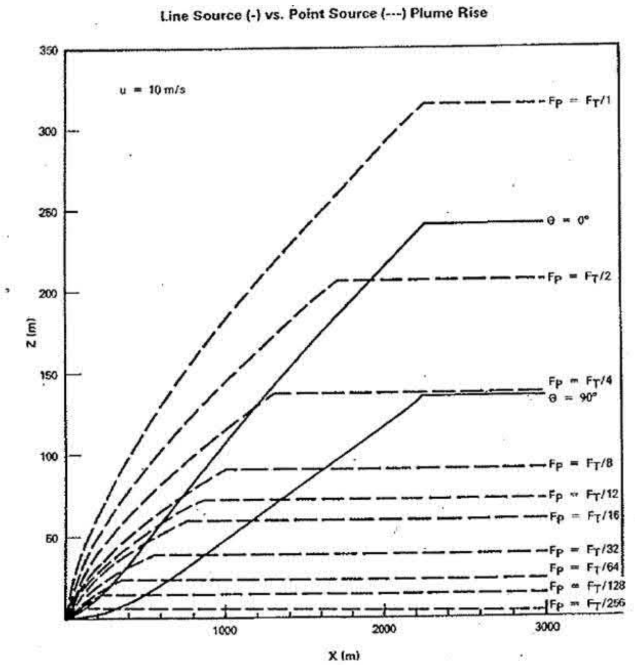

Figure 4. Comparisons of point source plume rise (dashed lines) and line source plume rise (solid lines).

Development of Stack Merging Approach for Intalco

Model evaluations were performed to determine model performance compared with monitored concentrations at three nearby monitors: Mountain View Road, Kickerville Road, and Phillips 66 refinery monitoring sites (**Figure E-6**). For the Phillips 66 monitor, model performance testing was confined to wind directions for which the monitor was downwind of Intalco, 305-350°, because only Intalco emissions were modeled. A full year of monitoring data, Mountain View Road meteorological data, and Intalco SO_2 emissions data were used in this evaluation. Monthly Intalco SO_2 emissions for the modeling period are listed in **Table E-1** for the dry scrubber stack centers and the bake oven. The wet scrubbers were also included with emissions modeled at 3% of the potline total where potline total = dry scrubber center SO_2 + (dry scrubber center SO_2 / 0.97) * 0.03. The “other” pollutant keyword was used to avoid the use of a default 4-hour half-life for exponential decay of SO_2 for urban sources that Ecology and EPA Region 10 do not believe to be appropriate for Intalco.

Model evaluation results for three stack merging modeling scenarios are presented here, each demonstrating the steps taken in identifying the need for a wind-direction dependent stack merging approach. Scenario A provided an initial model configuration tested using an objective approach to determine the number of merged modeling stacks per center to address modeled impacts at the monitor with the highest observations (Mountain View Road). The stack merging was based in part on the physical stack configurations. This scenario demonstrated good model performance at the Mountain View Road monitor, but poorer performance (model overprediction) at the Kickerville Road monitor.

Given the experience gained by scenario A, it was discovered that scenario A performed well for Mountain View Road due in large measure to plume rise behavior and downwash characteristics for WSW winds from Intalco toward the monitor were consistent with BLP model theory for wind flow perpendicular to the potlines. Stack merging for upwind centers would result in higher plume rise (fewer merged stacks, and more buoyancy per stack) than downwind centers. In contrast, stack merging for flow along the potlines would be expected to result in higher plume rise (fewer stacks over all centers) than flow perpendicular to the potlines. While each center has a different set of stacks, the total volume flow for each center and potential SO_2 emissions are generally the same at each center. Therefore, the centers can be viewed as equivalent in terms of the total buoyancy of each of these stack groups.

Based on this new understanding, merged stacks for scenario B were developed to optimize model results at the Kickerville Road monitor for southerly winds (flow along the potlines) toward the monitor, where more merging occurs for upwind centers than for downwind centers. However, while the scenario B case performed well at Kickerville Road, it underpredicted for Mountain View Road if the scenario B stack merging was used in all directions. After reviewing model results for both scenarios, scenario C implemented a wind direction-dependent stack merging approach that preserved scenario A and B merged stack approaches for wind directions toward Mountain View and Kickerville, respectively, and interpolated the stack merging approach for directions in between. In addition, for directions opposite to the two Intalco monitors, the stack merging approach was simply shifted 180 degrees because the upwind and downwind emission centers were also shifted 180 degrees. This approach led to a direction-dependent stack merging method established for 16 22.5-degree sectors around the compass.

A constant, regional background concentration of 11.0 ppb, the BP Cherry Point monitor's 2016-2018 design value, was added to all modeled concentrations. The Phillips 66 monitor was considered for background, but was determined to be unsuitable for two reasons. First, the monitor is intended to measure a maximum concentration gradient related to Phillips 66 refinery sources rather than providing a regional signature. Second, although the BP Cherry Point refinery monitor, like Phillips 66, was intended to measure a maximum concentration gradient related to the BP Cherry Point refinery, it has much less impact on the Intalco and Phillips 66 monitors being used in this model comparison, and therefore use of the BP Cherry Point monitor for background concentration is conservative for this application. Note that when either the Phillips 66 or BP Cherry Point emission sources are modeled, as will be proposed in the modeling protocol for determining the extent of the SO_2 nonattainment area, these monitors are not appropriate to use for background concentrations.

Each model evaluation run used two metrics to demonstrate model performance:

1) A comparison of the 99th percentile (4th highest) peak daily 1-hour maximum concentration between the modeled and observed values, and

2) A quantile-quantile (Q-Q) plot of predicted and observed concentrations based upon pairing of the ranked values at each monitor.

The comparison of the 99th percentile peak daily 1-hour maximum ("design") concentration should take into account the fact that ambient SO_2 monitored observations have the potential to vary from an unbiased calibration state by up to 10% and still be considered to be acceptable within the uncertainty of the measurements. This is related to the tolerance in the EPA procedures (EPA, 2013)[20] associated with quality control checks and span checks of ambient measurements. Therefore, even ignoring uncertainties in model input parameters and other contributions that can also lead to modeling uncertainties, just the uncertainty in measurements indicates that modeled-to-monitored ratios between 0.9 and 1.1 are within the instrumentation tolerance and can be considered "unbiased".

Q-Q plots of the predicted and observed concentrations at the three monitors have a diagonal line from lower left to upper right representing the "perfect model" line, and lines at 0.9 and 1.1 ratios of modeled-to-observed ratios representing the instrumentation tolerance unbiased window.

[20] Quality Assurance Handbook for Air Pollution Measurement Systems, Volume II, Ambient Air Quality Monitoring Program, 2013, available at http://www.epa.gov/ttnamti1/files/ambient/pm25/qa/QA-Handbook-Vol-II.pdf. (Table 10-3 and Appendix D, page 13).

Table E-1: Monthly Intalco SO_2 Emission Rates for the 12-month Period Modeled

Source	SO_2 Emission Rates in 2017-2018 (g/s)											
	Oct	Nov	Dec	Jan	Feb	Mar	Apr	May	Jun	Jul	Aug	Sep
Each Center *	19.65	20.08	20.70	21.57	21.23	22.05	21.90	22.36	21.99	22.67	22.44	21.26
Bake Oven	7.09	7.52	7.82	9.31	8.98	9.96	10.04	10.19	10.16	9.01	9.75	9.47

* Emissions for Center 4 are zero due to its curtailment.

Figure E-12: Monitor Locations

Stack Merging Scenario A

The first stack merging scenario, scenario A, was designed so that the dry scrubber stacks were merged using an objective analysis based on a relationship between to the number stacks within each center and their configuration for flow toward the Mountain View Road monitor. The number of dry scrubber stacks and their associated diameters per center are shown in **Table E-2**. Each center has a different configuration, as shown in the table. Stacks in centers 3, 4, 5, and 6 have similar configurations in which they each have over 20 stacks with identical stack diameters of 0.72 m and are grouped into two sections (**Figure E-7**).

For centers 5 and 6, due to the 2-section stack configuration, it was determined that plumes from 22 stacks would merge together in a way best represented by 2 modeled stacks. Because centers 3 and 4 have additional stacks in comparison to centers 5 and 6, 26 stacks were merged into 3 modeled stacks. Centers 1 and 2 have the fewest number of stacks (6) with diameters that are more than twice the size of the other centers (**Figure E-7**). Stacks for these centers are also at a greater distance from each other than the other centers. As a result, the initial reasoning was that these stacks may merge less and were therefore merged into 5 modeled stacks for this scenario. This merged modeling approach is depicted in **Figure E-22**.

Table E-2: Dry Scrubber Stack Configuration

ID	Number of Stacks	Stack Diameter (m)	Release Height (m)
DSA1	6	1.52	19.8
DSA2	6	1.52	19.8
DSB3	26	0.72	17.9
DSB4	26	0.72	17.9
DSC5	22	0.72	17.9
DSC6	22	0.72	17.9

Figure E-13: Dry Scrubber Stack Configuration for Centers 5 (left) and 1 (right)

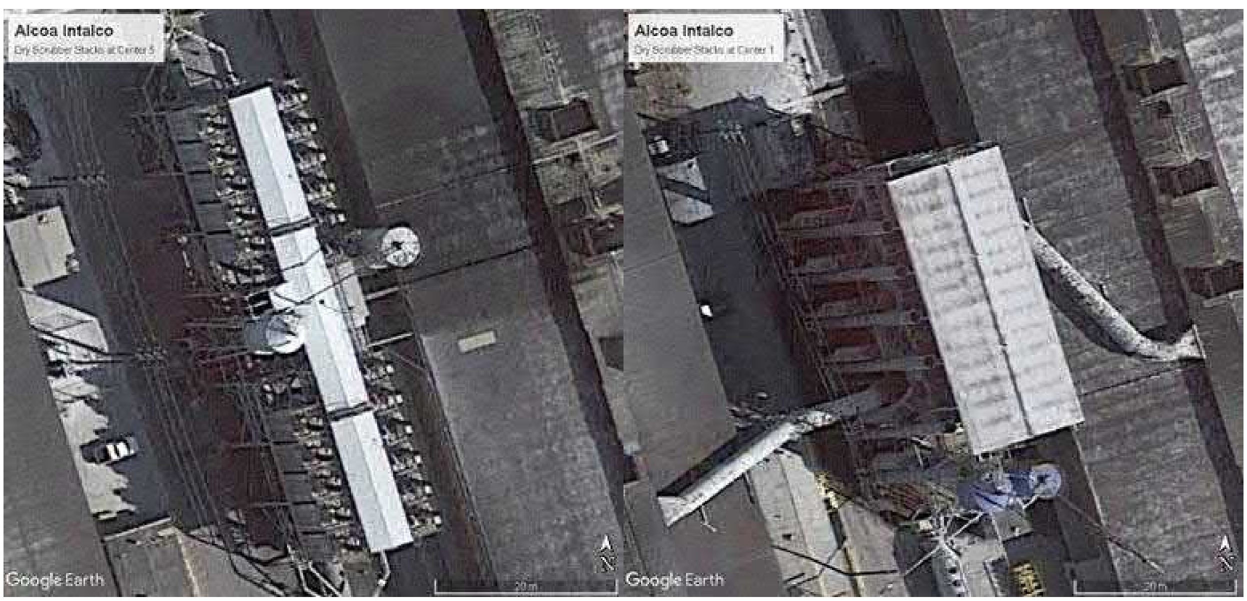

Stack Merging Scenario B

Modeling results from scenario A indicated good performance for Mountain View, the monitor measuring the highest SO_2 concentrations, with poorer (overpredicting) performance for Kickerville. In spite of the similar distances from the smelter to the Kickerville and Mountain View monitors and the more frequent winds toward Kickerville, the monitored impacts at Kickerville have been significantly lower (by about 1/3). The logical explanation for the differential outcome of monitored design concentrations, which is borne out by the BLP formulation discussion provided above, is that the effective plume rise for flow along the potlines is higher than that across the potlines. Upon closer examination, scenario A's merged stacks were consistent with this theory in that, for winds toward Mountain View Road (involving flow across three sets of lines from the WSW), the merging that would likely result in the best model performance would be fewer merged stacks for the upwind-most center and more merged stacks for the downwind center. For flow along the potlines as Kickerville would experience, plumes would have higher plume rise (fewer stacks over all centers) than flow perpendicular to the potlines. Therefore, a second stack merging scenario, scenario B, was developed to improve model performance for the Kickerville monitor.

For scenario B, BLP formulation concepts noted previously were used to guide the selection of how stacks were merged for the various centers at Intalco. When the Kickerville monitor is downwind of Intalco, winds generally transport plumes from the dry scrubber stacks toward the monitor, parallel to the potlines. Therefore, more merging than that done for scenario A was incorporated into scenario B to reflect this along-potline flow. For scenario B, centers farthest from Kickerville and thus on the upwind side of the buildings were merged into 1 modeled stack while centers closest to Kickerville were merged into 2 modeled stacks, as shown in **Figure E-19**.

Stack Merging Scenario C

Scenarios A and B were each designed in a manner that resulted in nearly unbiased model performance at the Mountain View and Kickerville monitors, respectively. Despite the initial methodology behind scenario A's merging based on stack configuration, it was later determined that this merging was logical from the standpoint of BLP formulation for the Mountain View monitor. Scenarios A and B were then evaluated without any change in merging by wind direction for all three monitors. Following an examination of scenarios A and B model results which indicated they would not perform well at monitors in directions that they were not designed for, scenario C was developed. Scenario C, a wind direction-varying approach for stack merging, was made equivalent to scenario A for winds blowing toward the Kickerville monitor and to scenario B for winds blowing toward the Mountain View monitor. For wind directions in between the SSE (toward Kickerville) and from the WSW (toward Mountain View), the stack merging approach was interpolated between the scenario A and B solutions within scenario C. For directions opposite to these monitors (and to the interpolated solutions), the stack merging was shifted 180 degrees among the identical centers.

The stack merging was organized across 16 sectors with widths of 22.5 degrees. This afforded a reasonable resolution in the wind direction variation without having an excessive number of sectors. The basic approach for intermediate wind sectors was to transition from the flow along the potlines to from across the potlines in a smooth sequence. Therefore, the transition as a function of sector was as listed in **Table E-3.** In the table, scenario A is for the sector toward the NNW, and scenario B is for the sector toward the ENE. In AERMOD, the merging was implemented by using an hourly emissions input file for AERMOD where all potential merged stacks were listed in the AERMOD input files, but only the desired merged stacks were activated based on the meteorological data file's hourly wind direction. Inactive stacks were assigned zero emissions.

With the orientation of the smelter potlines along the 345°-165° line, two of the sectors are aligned to be centered along that axis, as shown in **Figure E-12**. **Figures E-13 to E-24** indicate the stack merging approach for each of the 6 major dry scrubber centers at the Intalco smelter. Each center has approximately the same total exhaust flow and temperature characteristics. Depending upon the number of stacks for each center specified, they are distributed evenly along the axis of the space occupied by the actual stacks. The modeled stack exhaust parameters such as exit velocity and exit temperature were not changed from those shown in the modeling protocol Table 2-1. However, stack diameters were adjusted for the various stack merging options using a diameter of a circle with an area equivalent to that of the sum of the areas being combined. For example, if 6 actual stacks are merged into 3 stacks for modeling purposes, then the diameter of each of the 3 stacks is SQRT(2) times the diameter of each individual stack in order to conserve the sum of the stack areas.

Table E-3: Scenario C - Number of Stacks Per Center for Various Wind Sectors

Sector Toward	Center 1	Center 2	Center 3	Center 4	Center 5	Center 6
NNW	2 (downwind)	1 (upwind)	2 (downwind)	1 (upwind)	2 (downwind)	1 (upwind)
N	2 (downwind)	1 (upwind)	2 (downwind)	1 (upwind)	2 (downwind)	1 (upwind)
NNE	3 (downwind)	3 (middle)	3 (middle)	2 (middle)	2 (middle)	1 (upwind)
NE	4 (downwind)	4 (downwind)	3 (middle)	3 (middle)	2 (upwind)	2 (upwind)
ENE	5 (downwind)	5 (downwind)	3 (middle)	3 (middle)	2 (upwind)	2 (upwind)
E	4 (downwind)	4 (downwind)	3 (middle)	3 (middle)	2 (upwind)	2 (upwind)
ESE	3 (middle)	3 (downwind)	2 (upwind)	3 (downwind)	1 (upwind)	2 (middle)
SE	1 (upwind)	2 (downwind)	1 (upwind)	2 (downwind)	1 (upwind)	2 (downwind)
SSE	1 (upwind)	2 (downwind)	1 (upwind)	2 (downwind)	1 (upwind)	2 (downwind)
S	1 (upwind)	2 (downwind)	1 (upwind)	2 (downwind)	1 (upwind)	2 (downwind)
SSW	1 (upwind)	2 (middle)	2 (upwind)	3 (middle)	3 (middle)	3 (downwind)
SW	2 (upwind)	2 (upwind)	3 (middle)	3 (middle)	4 (downwind)	4 (downwind)
WSW	2 (upwind)	2 (upwind)	3 (middle)	3 (middle)	5 (downwind)	5 (downwind)
W	2 (upwind)	2 (upwind)	3 (middle)	3 (middle)	4 (downwind)	4 (downwind)
WNW	2 (middle)	1 (upwind)	3 (middle)	2 (upwind)	3 (downwind)	3 (middle)
NW	2 (downwind)	1 (upwind)	2 (downwind)	1 (upwind)	2 (downwind)	1 (upwind)

Model Evaluation Results

Modeled concentrations for scenario A resulted in good model performance at the Mountain View Road monitoring site. However, this merging approach overestimated for the other monitors because the upwind-downwind pattern for centers would be expected to change with wind direction. Results are presented in **Table E-4** where a model/observed ratio = 1 is a perfect model. Modeled concentrations using the scenario B approach resulted in good model performance with the Kickerville Road monitoring site. However, this approach underestimated significantly at the Mountain View Road monitor (**Table E-5**). Lastly, scenario C modeling results, shown in **Table E-6**, indicate good model performance at both Intalco monitors and the best model performance (among the scenarios tested) for the Phillips 66 monitor. Q-Q plots for all three modeling scenarios are shown in **Figures E-8 to E-10**, where "MV" signifies Mountain View Road and "KV" signifies Kickerville Road. Design values for each scenario are compared with the monitored concentrations demonstrate scenario C's improved performance to the other scenarios (**Figure E-11**).

Table E-4: Scenario A Comparison of Modeled and Observed SO_2 Design Concentrations

Scenario A	Mountain View Road SO_2 (ppb)	Kickerville Road SO_2 (ppb)	Phillips 66 SO_2 (ppb)
Observed	101.4	80.5	19.0
Modeled	108.2	103.9	65.9
Ratio: Model/Obs.	1.1	1.3	3.5

Table E-5: Scenario B Comparison of Modeled and Observed SO_2 Design Concentrations

Scenario B	Mountain View Road SO_2 (ppb)	Kickerville Road SO_2 (ppb)	Phillips 66 SO_2 (ppb)
Observed	101.4	80.5	19.0
Modeled	60.5	76.0	46.6
Ratio: Model/Obs.	0.6	0.9	2.5

Table E-6: Scenario C Comparison of Modeled and Observed SO_2 Design Concentrations

Scenario C	Mountain View Road SO_2 (ppb)	Kickerville Road SO_2 (ppb)	Phillips 66 SO_2 (ppb)
Observed	101.4	80.5	19.0
Modeled	108.2	76.0	43.0
Ratio: Model/Obs.	1.1	0.9	2.3

Conclusions

For Intalco, the wind direction-dependent approach for stack merging results in having good model performance at both Intalco SO_2 monitors as well as the best model performance among the scenarios tested for the nearby Phillips 66 refinery monitor, as shown by the Q-Q plots. The figures show three model scenarios for each monitor comparison, one with wind direction-dependent merging while the other two used fixed stack merging approaches that optimized model performance for only one of the monitors at a time.

The Q-Q plots show that the directionally-varying approach can optimize model performance at both of the Intalco monitors, but using a fixed merging approach can only provide good performance at one of the Intalco monitors. At the other monitor, the model performance either overpredicts substantially (at Kickerville Road using the Mountain View Road stack merging approach), or underpredicts substantially (at Mountain View Road using the Kickerville Road-oriented stack merging approach). For the Phillips 66 monitor, the directionally-varying approach has the best performance.

The design value comparison for each modeling scenario illustrates scenario C's improved performance compared with the other scenarios. In conclusion, the site-specific source characterization direction-dependent modeling approach, scenario C, out-performed any modeling scenario tested without a wind direction dependency.

Figure E-14: Q-Q Plot of the Mountain View Road Monitor

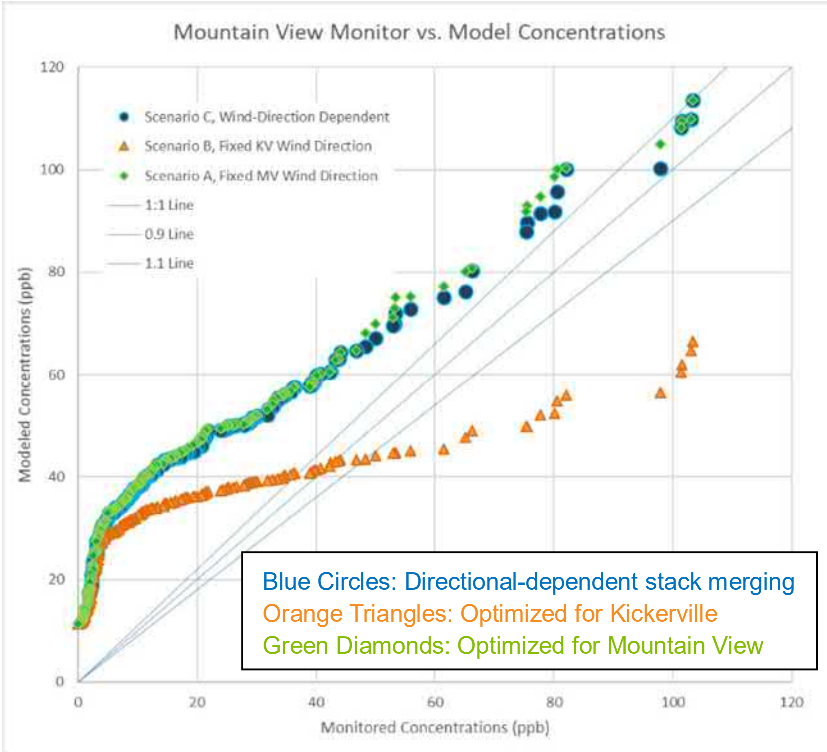

Figure E-15: Q-Q Plot for the Kickerville Road Monitor

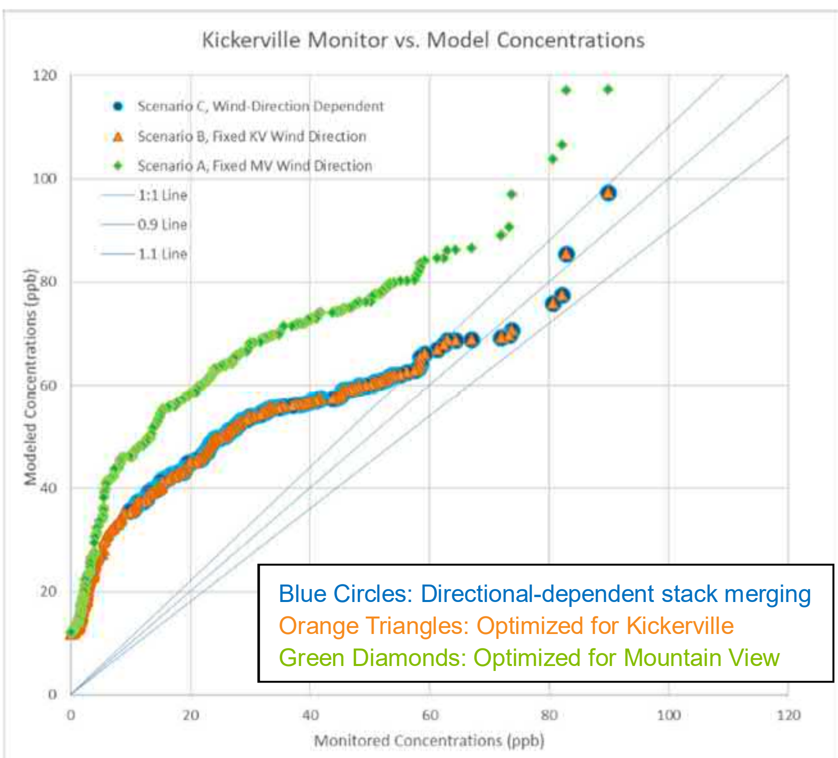

Figure E-16: Q-Q Plot for the Phillips 66 Monitor

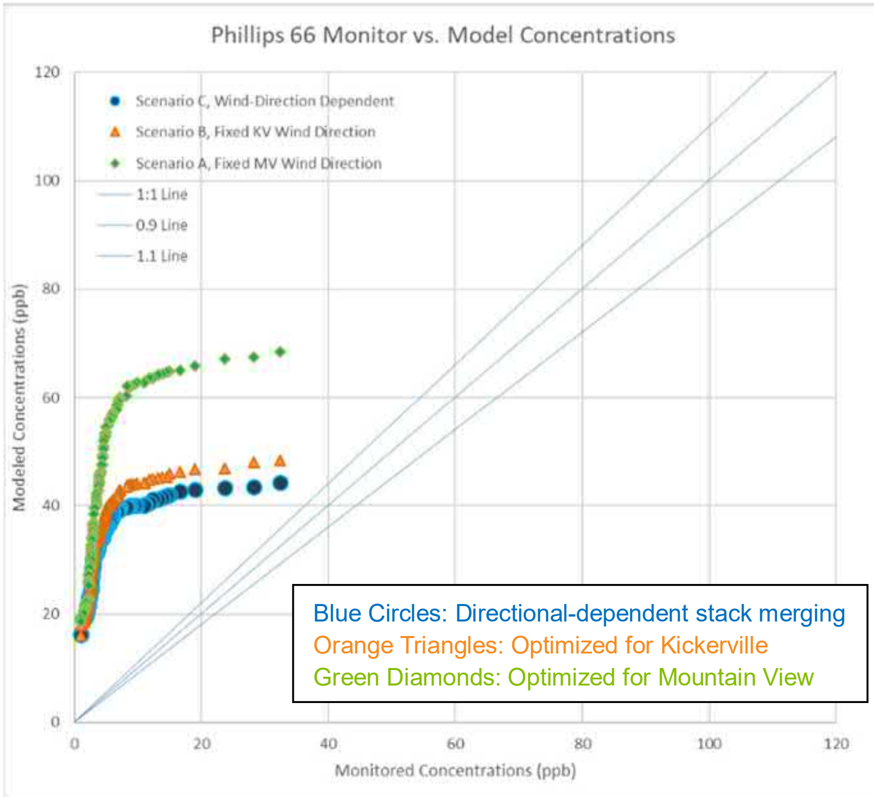

Figure E-17: Monitor-to-Model Design Value Concentrations for Each Scenario

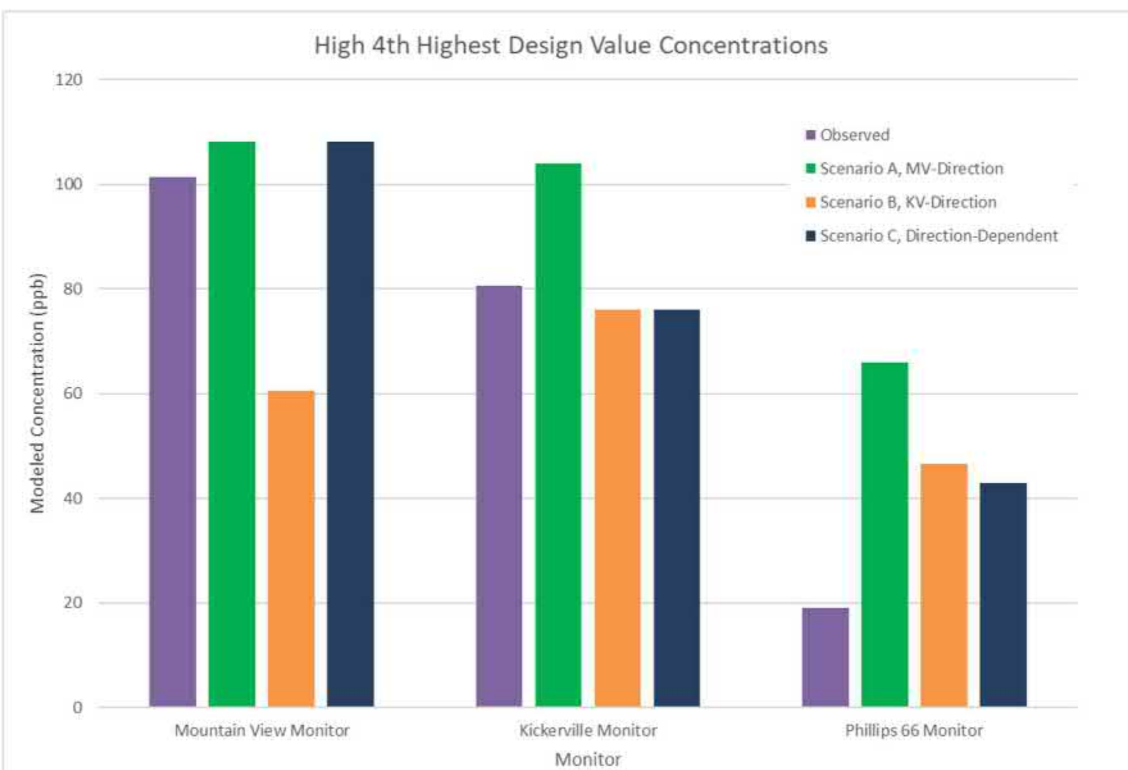

Figure E-18: Wind Direction Sectors Used for Stack Merging Approach

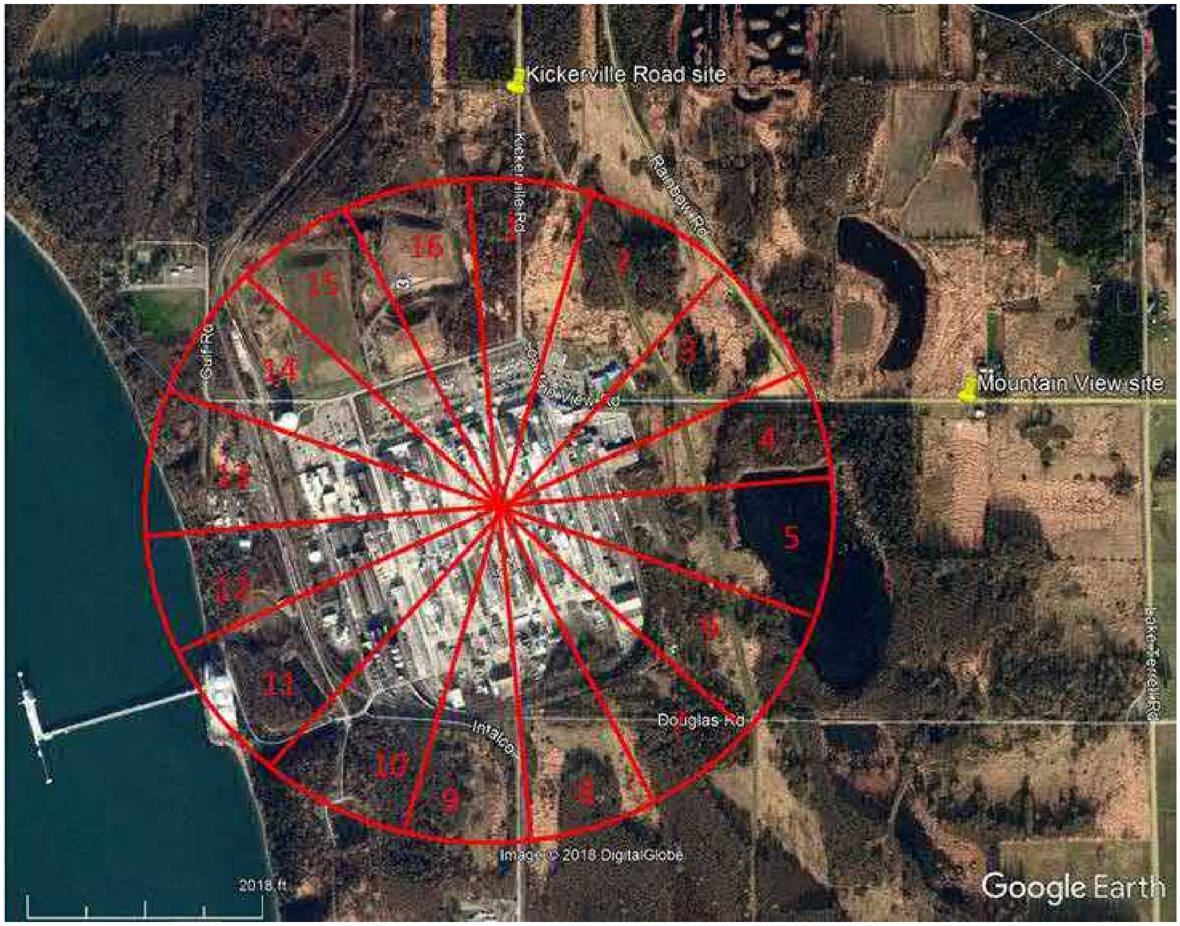

Figure E-19: Stack Merging for Wind Sectors 15, 16, and 1 (311.25° - 18.75°)

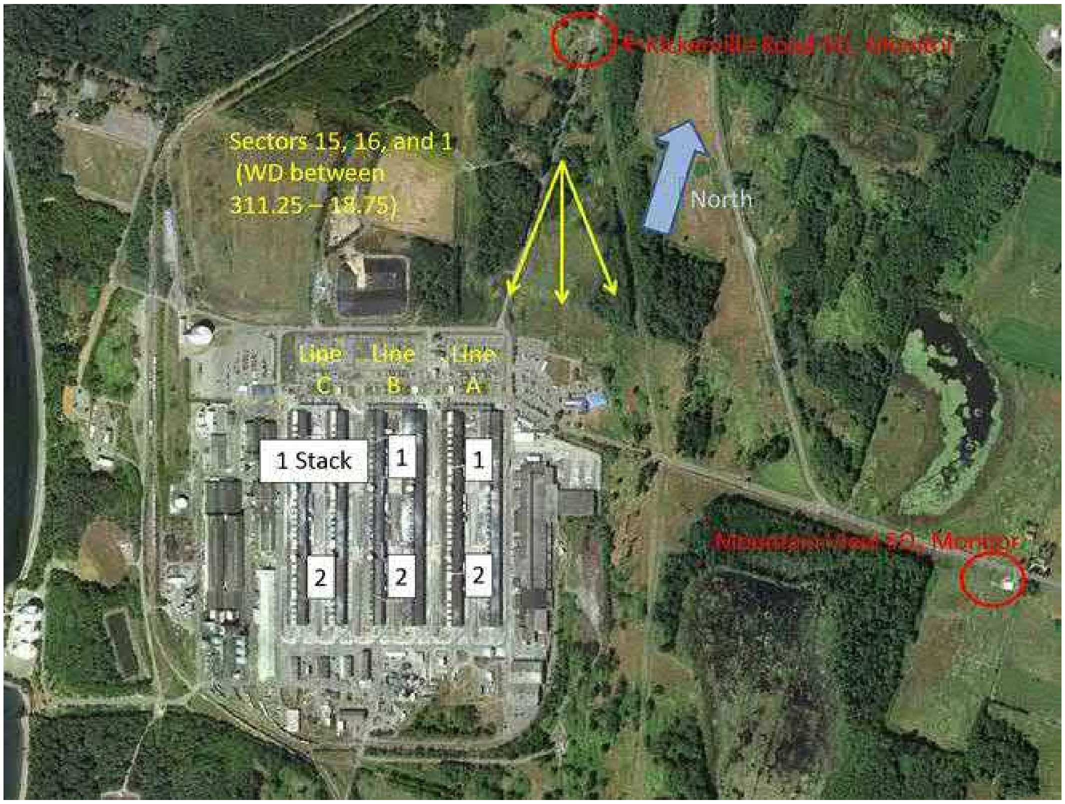

Figure E-20: Stack Merging for Wind Sector 2 (18.75° - 41.25°)

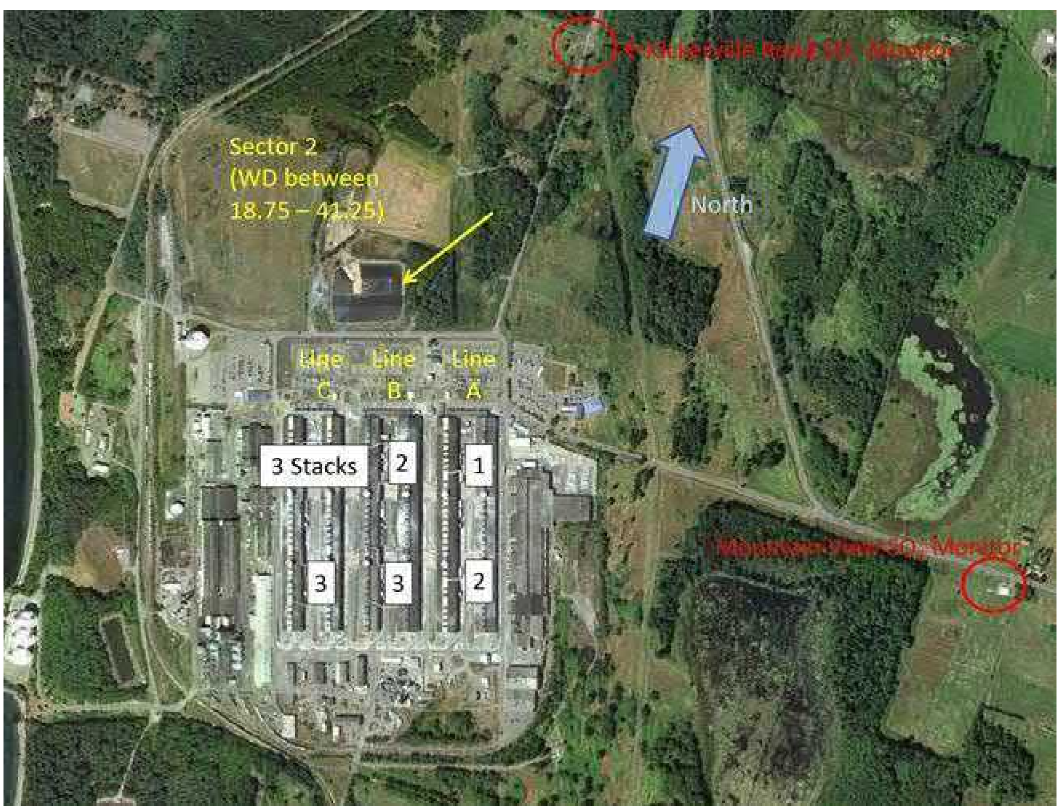

Figure E-21: Stack Merging for Wind Sector 3 (41.25° - 63.75°)

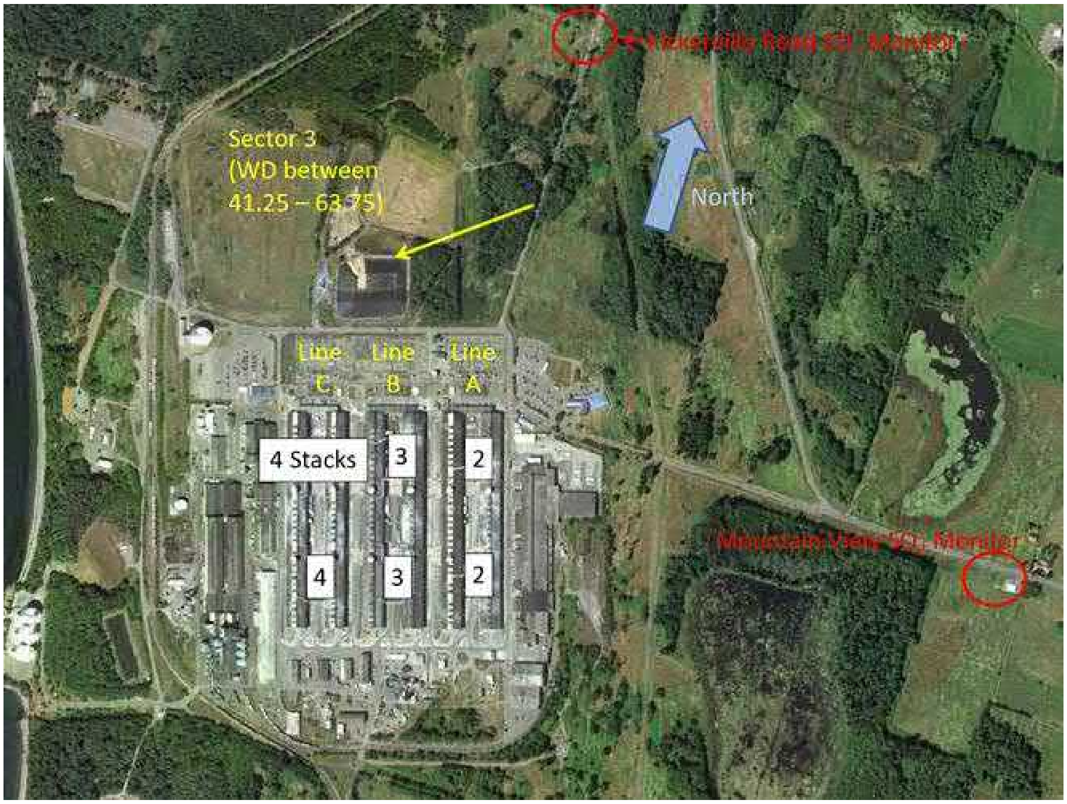

Figure E-22: Stack Merging for Wind Sector 4 (63.75° - 86.25°)

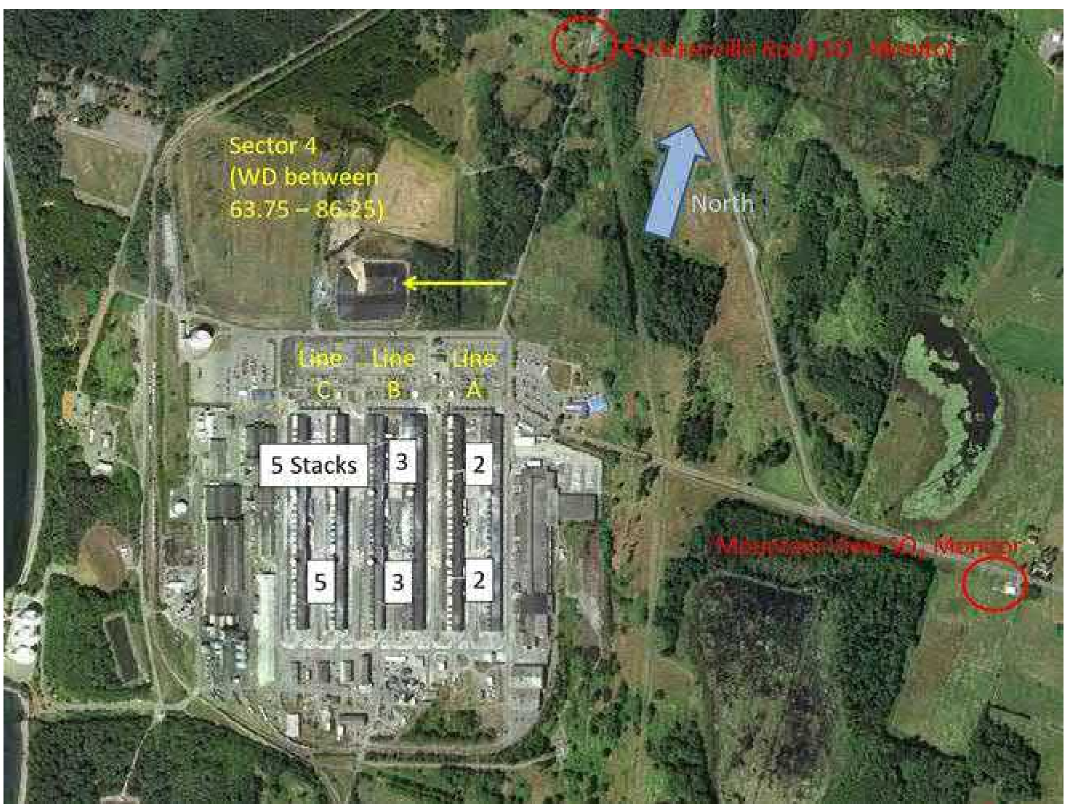

Figure E-23: Stack Merging for Wind Sector 5 (86.25° - 108.75°)

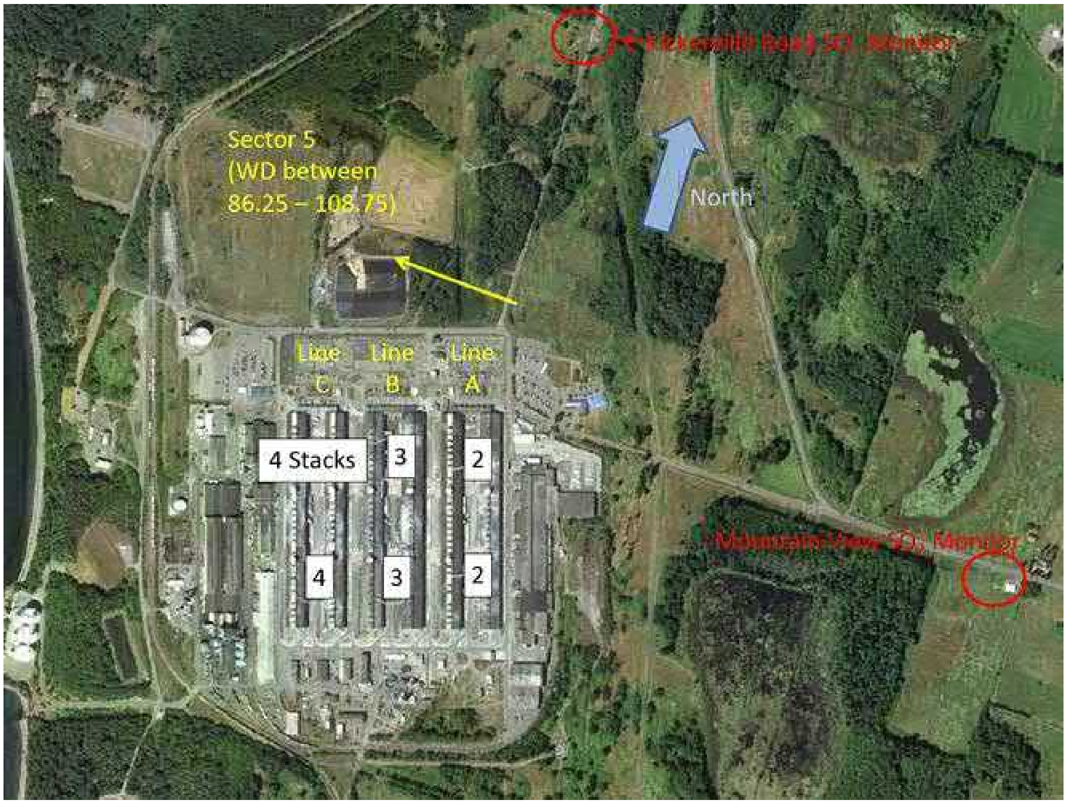

Figure E-24: Stack Merging for Wind Sector 6 (108.75° - 131.25°)

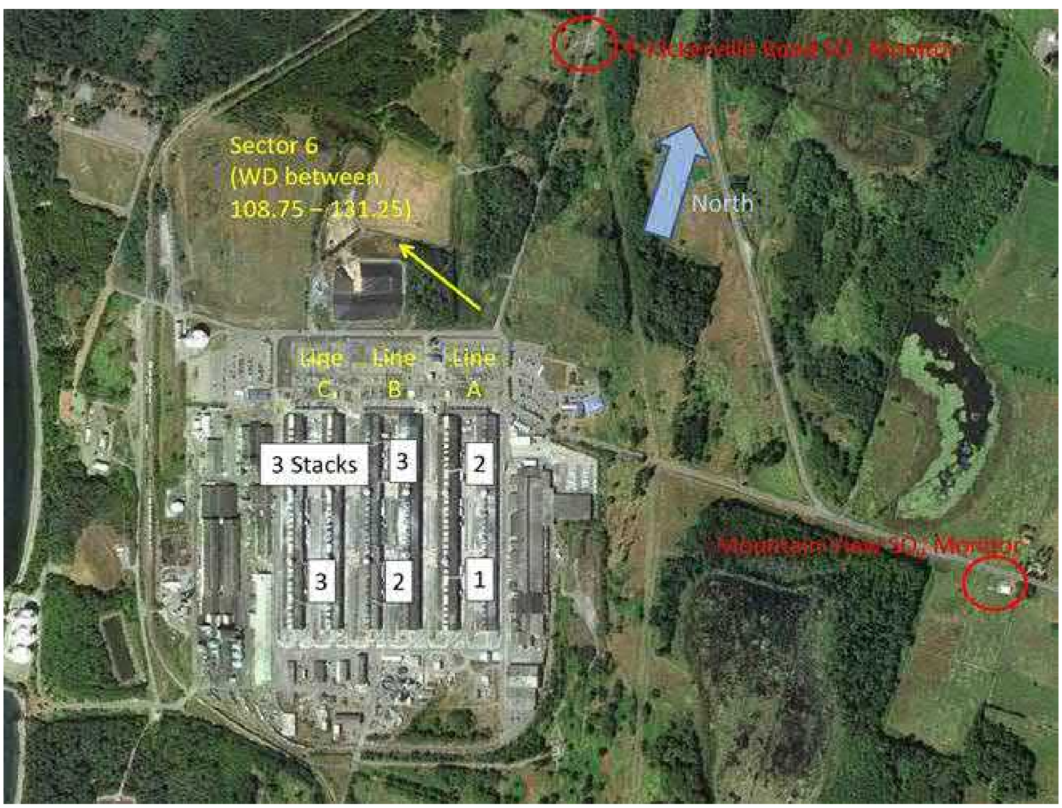

Figure E-25: Stack Merging for Wind Sectors 7-9 (131.25° - 198.75°), Consistent with Scenario B

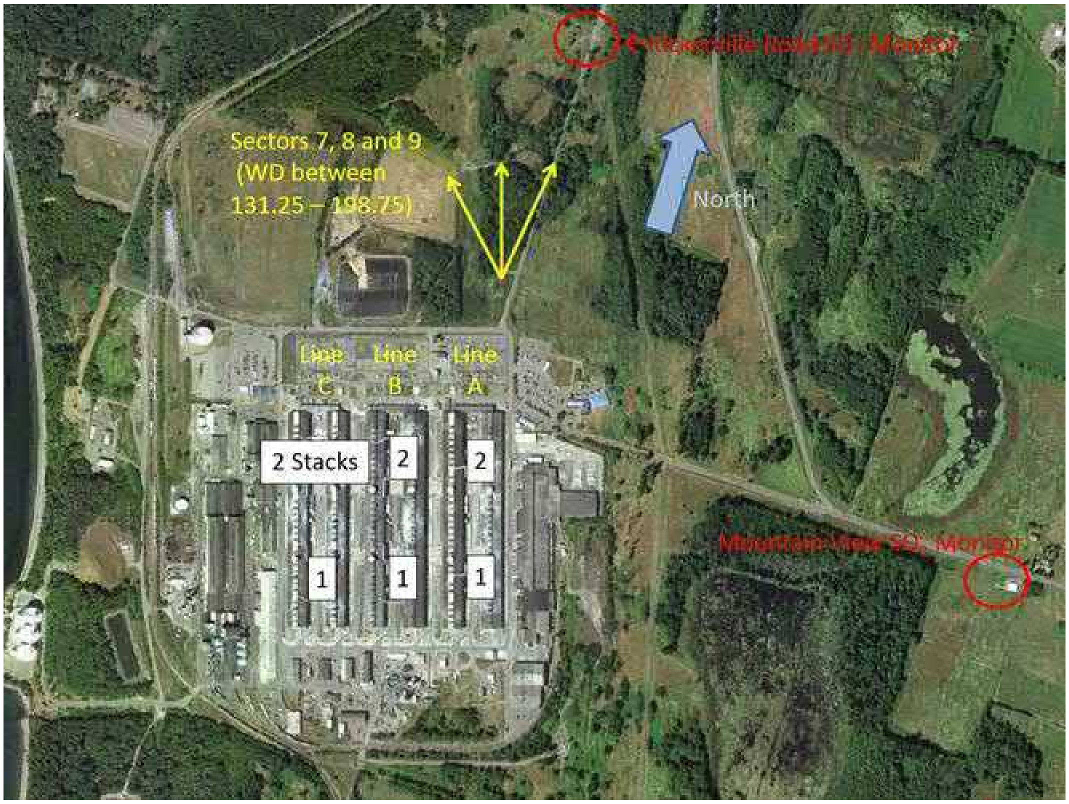

Figure E-26: Stack Merging for Wind Sector 10 (198.75° - 221.25°)

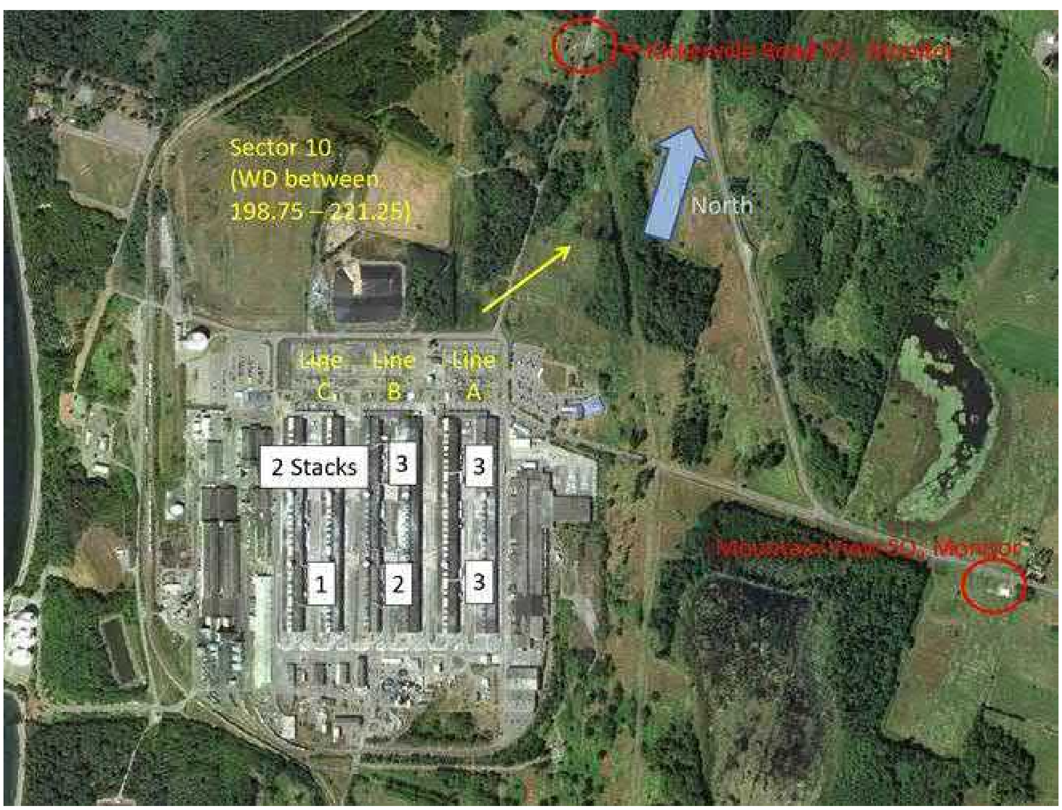

Figure E-27: Stack Merging for Wind Sector 11 (221.25° - 243.75°)

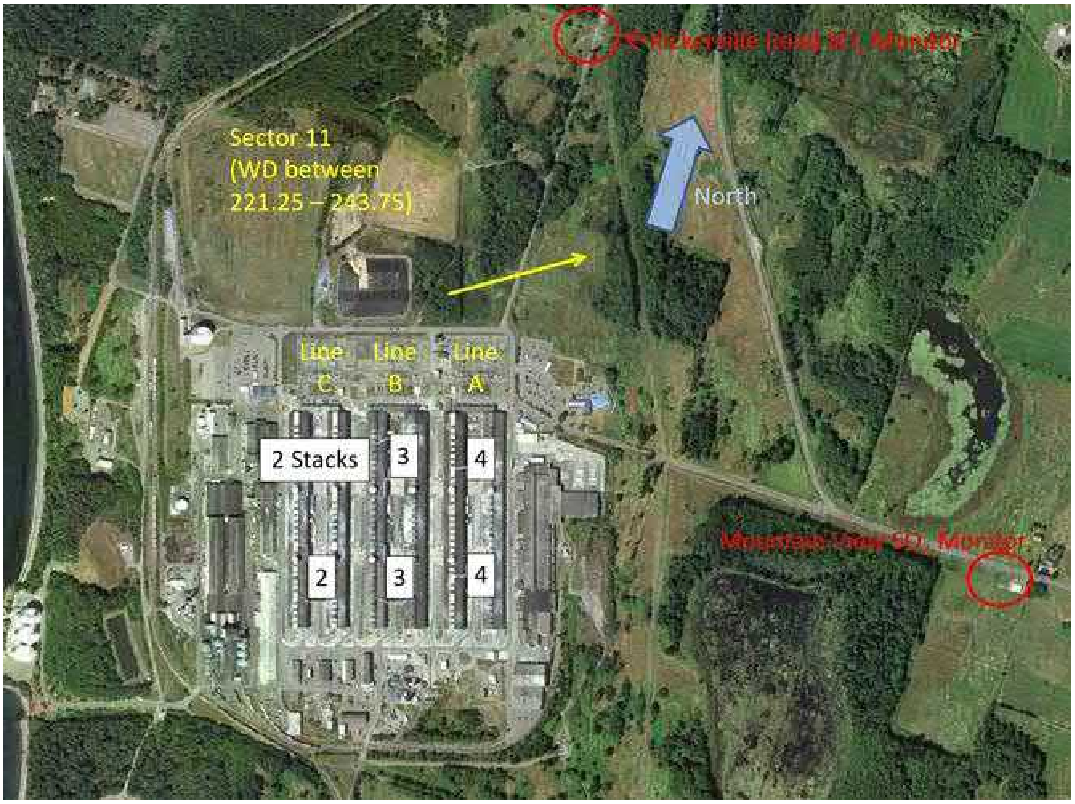

Figure E-28: Stack Merging for Wind Sector 12 (243.75° - 266.25°), Consistent with Scenario A

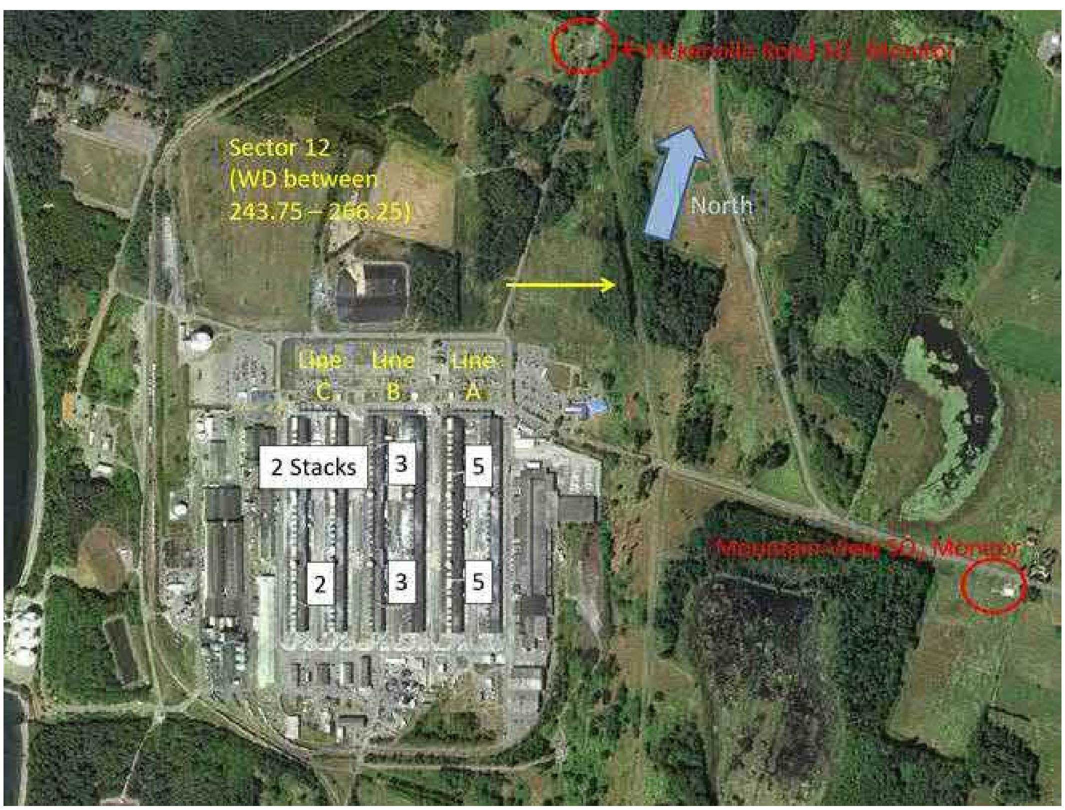

Figure E-29: Stack Merging for Wind Sector 13 (266.25° - 288.75°)

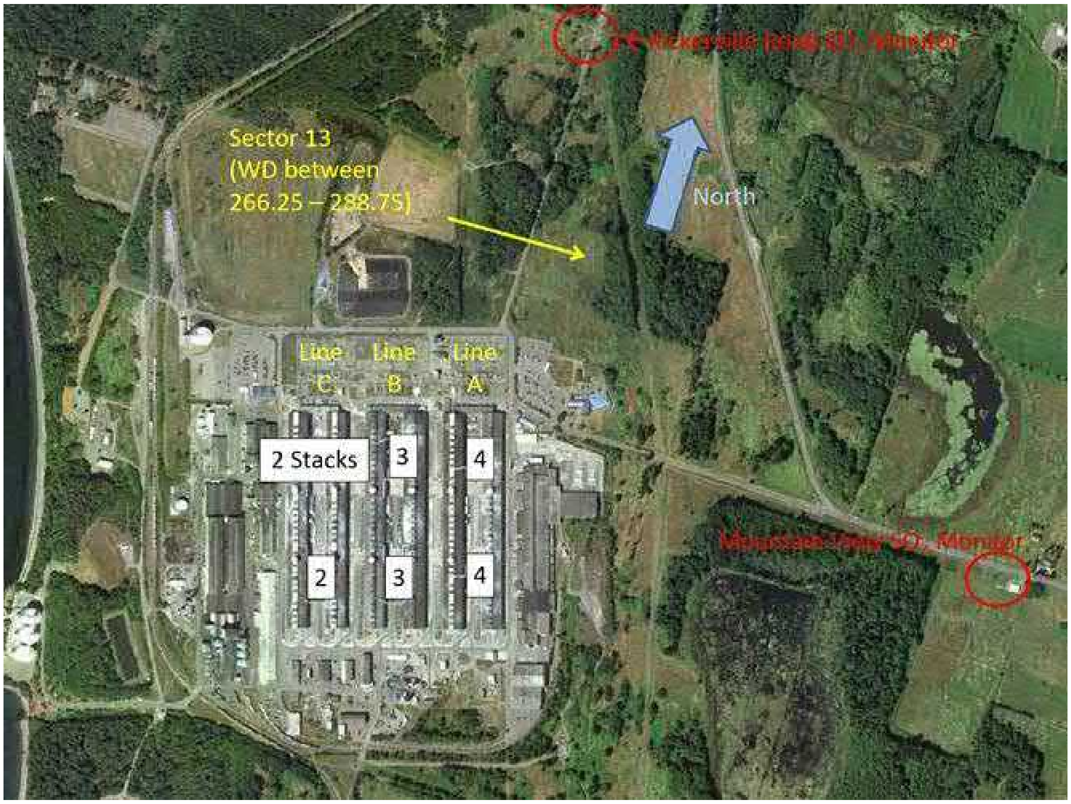

Figure E-30: Stack Merging for Wind Sector 13 (288.75° - 311.25°)

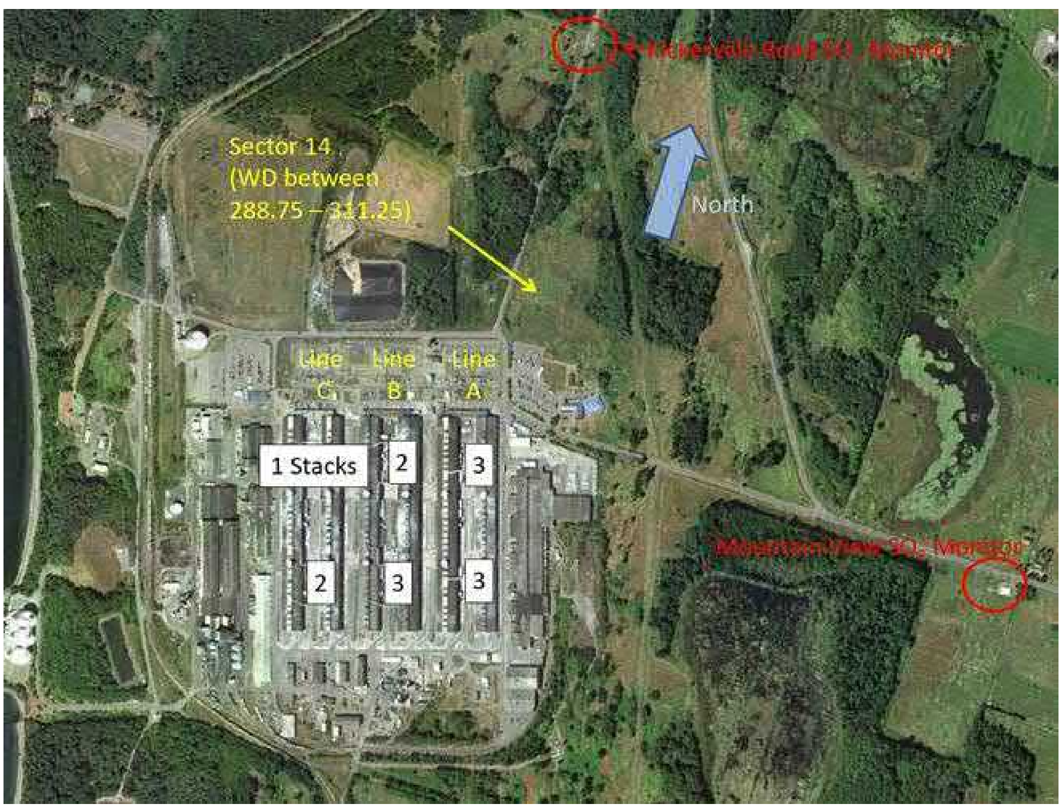

AECOM Imagine it. Delivered.

SO_2 Modeling Report for Intalco Works

Addendum: Response to Feedback

The purpose of this addendum is to address feedback received from Washington Department of Ecology (Ecology) and United States Environmental Protection Agency (EPA) Region 10 on February 26, 2020 regarding the review of the SO_2 Modeling Report for Intalco Works (February 2020). The modeling report presented the dispersion modeling approach and modeling results in anticipation of a need to characterize SO_2 concentrations in the area near Intalco in support of Ecology's area designation recommendations to EPA. The modeling approach presented in the report and in its associated modeling protocol (December 2019) were developed in coordination with Ecology and EPA Region 10 and addressed feedback received from these agencies prior to February 2020.

This addendum provides responses to feedback as organized by report sections. Each section begins with a brief summary Ecology and/or EPA's review comments, followed by a response from Intalco/AECOM. Ecology and EPA Region 10 review comments are provided as supporting information in Attachment 1 and Attachment 2.

Description of SO_2 Emission Sources

In their review, EPA has indicated that there may be a slight emissions calculation error in which emissions were too high by 3%. This potential issue is related to how the wet and dry scrubber stack emissions were added, and whether the wet scrubber stack emissions were double-counted. More explanation of the Intalco emissions is needed.

Response: The approach to estimate the wet scrubber emissions was to assume the emissions category titled "Potline SO_2 evolved from consumed of anode blocks (lbs)" referred to the dry scrubber emissions only. Therefore, the wet scrubber emissions were calculated as an additional 3% of emissions. However, it appears EPA is correct in that the potline SO_2 emissions should have been distributed among the dry scrubber and wet scrubber emission sources, where 97% of the total potline emissions are allocated to the dry scrubber and 3% allocated to the wet scrubbers. As a result, the SO_2 concentrations provided for determining the boundaries of various concentration thresholds are slightly conservative.

Dispersion Modeling Approach

EPA Region 10 found, "the proposed approach appeared to be reasonable to simulate an accurate, but still slightly conservative, SO_2 concentration distribution." However, EPA noted that the unique source characterization techniques applied in this modeling report may not be applicable for future modeling used for development of a SIP. EPA cautioned that more conservative assumptions may be required in future modeling applications.

Response: If a revised SIP needs to be developed, facility changes that may be required to address the elevated SO_2 concentrations may result in physical merging of the exhaust streams into centralized tall stacks, which would lead to a more conventional modeling approach. In any case, we believe that the modeling approach used in this application, which led to a realistic and unbiased modeling result, should be carefully considered for future modeling applications, as it is quite evident that more traditional modeling approaches have much less predictive skill for this application.

EPA Region 10 indicated that it would have been beneficial to include preliminary simplified runs to demonstrate the range of SO_2 over-estimation using a default no-stack-merging approach, but none were provided. However, that, “it is obvious, from a theoretical perspective, that no stack merging would have likely resulted in much higher concentrations due to lower average plume height and resulting additional plume entrainment in the wake of Alcoa structures.”

Response: A preliminary model evaluation was previously performed without stack merging in 2015 based on 2012-2014 emissions. The modeling results demonstrated vast over-prediction occurred with no stack merging at the nearby SO_2 monitors (see Figure 1 below). The Kickerville (labeled “Intalco”) and Phillips 66 monitoring locations exhibited consistent model over-predictions by more than a factor of 8 over a large range of values. The BP Cherry Point monitoring location, the farthest away of the three nearby monitors at the time, showed modeled over-prediction by about a factor of 2-4 over a large range of values. At the time of this analysis, the Mountain View monitor was not operational. Furthermore, it is possible Ecology has performed modeling without stack merging in preparation for siting the Mountain View monitor.[1] If this is the case, Ecology could share this information with EPA as additional justification that further demonstrates the need to characterize SO_2 concentrations in the region around Intalco with the approach that has been used in this application.

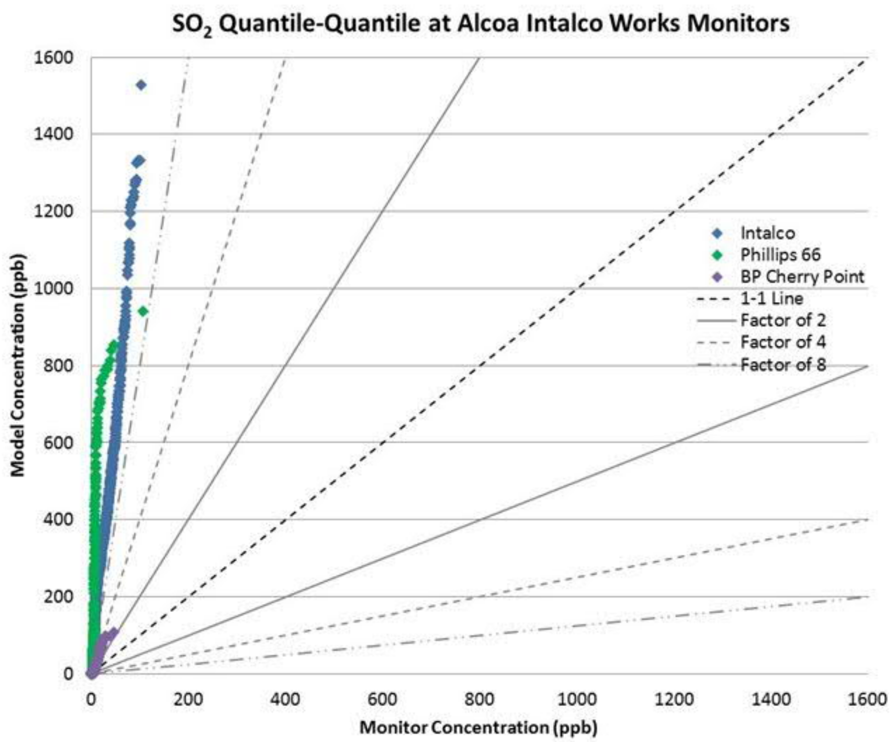

Meteorological Data Processing

Comments received from Ecology and EPA Region 10 found the meteorological data processing to have followed procedures detailed in the modeling report and modeling protocol. However, EPA noted that use of substituted precipitation data using the Bellingham 3SSW station when Bellingham airport precipitation was missing may possibly have resulted in some bias when determining wet/dry/average conditions. The substituted dataset appeared to EPA to frequently exhibit extremes values, potentially being located in a different micro-climate than Bellingham airport. However, EPA, “was not convinced any unintended bias would significantly affect the modeling results.”

Response: Because Bellingham airport precipitation data were missing from June 1996 – Sept 1998 and 4 additional months within the 30-year dataset, substitution by an alternative station was required. The Bellingham

[1] Dhammapala, Ranil and Clint Bowman, December 2015. Reconfiguring Alcoa’s Potline SO_2 Emission Points as Buoyant Line Sources in AERMOD v15181. Washington Dept. of Ecology.

3SSW station, used for substitution, was the closest available station with precipitation data during the 30-year period of interest, 1990 – 2019. A total of 32 months / 360 months were substituted, which is approximately 9% of the dataset. As a result, the majority of the precipitation data are from Bellingham airport, and therefore any potential bias with the Bellingham 3SSW station would be minor. Intalco/AECOM also agree with EPA that if a bias did indeed occur, it would not significantly affect the modeling results because it has the capability of only affecting the choice of a monthly Bowen ratio, and then only if the monthly precipitation is very close to a dry-normal-wet dividing threshold.

Receptor Processing

EPA's review of the receptor grid resulted in multiple comments on the grid density and configuration. The density of the receptors over terrain features was noted to be unnecessarily high and indicated that future modeling could be more efficient with lower density grids on these features. It was also noted that the receptor grid contained some receptors at the ground level and some at a flagpole height of 1.4 m.

Response: As stated in the modeling report and protocol, Ecology prepared a receptor grid for use with this model application with the exception of the ambient air boundary and exclusion of receptors within the ambient air boundary. The receptor grid received from Ecology included receptors at both ground level and at 1.4 m flagpole heights, depending on location. When the ambient air boundary was developed by Intalco/AECOM, the boundary's receptors were ground-level receptors. We expect very little difference in the predicted concentrations between flagpole heights at 0 and 1.4 meters, but future modeling can use 0 meters for all receptor flagpole heights to be more consistent. We agree that future modeling could be more efficient with lower density in high terrain, especially given that peak modeled concentrations have been shown to not be in the high terrain features.

EPA recommended that the National Elevation Dataset (NED) or alternative terrain dataset, could be used in future modeling to develop the receptor terrain elevations for receptors. EPA stated that SRTM data tends to provide elevations at the top of obstacles, potentially causing some receptor elevations to be biased high, especially over forested areas. However, EPA indicated that they are not recommending remodeling.

Response: Receptors provided by Ecology were processed with AERMAP using the SRTM dataset, though Ecology stated that the receptors could be reprocessed using different terrain data. Intalco/AECOM used SRTM for the ambient air boundary and monitor location receptors for consistency and so as to avoid conducting AERMAP processing for the large number of receptors that make up the modeling domain. Intalco/AECOM will consult Ecology for any future modeling on the receptor grid and the best terrain dataset to use.

Ecology expressed uncertainty as to the reasoning behind the ambient air boundary. Ecology does not believe it is reflective of parcels they understand to be Intalco-owned. The boundary also does not match a previously modeled boundary. Ecology stated that, "Exactly where public access is restricted is unclear and should be clarified." EPA has similar questions where they explain, "Additional documentation may be needed in Ecology's submission to verify the ambient air boundary. If fencing or barriers are not used in any part of the facility area not considered ambient air, a detailed description will be needed to understand the manner in which Alcoa precludes public access. An ambient air examination and determination by EPA OAQPS may be needed."

Response: The ambient air boundary used in this modeling report was based on areas of property ownership close to the facility not intersected by roads. However, this ambient air boundary does not affect the determination of a potential non-attainment area boundary because such an area would need to include the main Intalco property at a minimum. Therefore, clarification of the ambient air boundary should be undertaken for future potential modeling in development of a State Implementation Plan (SIP). Intalco will work with Ecology and EPA to document the areas owned and controlled by Intalco from which public access can be controlled for any future modeling.

Model Comparison to Monitored Data

EPA stated that the model-to-monitor evaluation, “does not contain an explanation of an objective process used to determine the case-by-case merging. It is understood the configuration chosen resulted in SO_2 concentration design values that matched those at the monitors well.”

Response: In the modeling protocol Appendix E model evaluation, three modeling demonstrations were provided. One of these modeling demonstrations, Scenario A, used an objective method of determining the number of stacks to merge. This initial modeling demonstration informed the final stack merging approach. Therefore, the modeling protocol’s Appendix E established that the wind direction dependent modeling approach ultimately used in this modeling report originated from an objective approach and was refined further using the monitors as our guide.

Cumulative Modeling Results and Conclusions

Ecology performed a comparison of monitored concentrations to modeled concentrations upon the receipt of the Intalco/AECOM modeling report archive, which included modeling input and output files and supporting data for the 2017-2019 modeling of actual emissions. Ecology determined over-predictions of modeled concentrations at the Phillips 66 and BP Cherry Point refinery monitoring locations, though both their monitored and modeled concentrations were much lower than the 1-hour SO_2 NAAQS. Ecology also indicated modeled concentrations very close to the monitored concentrations at Mountain View and Kickerville where monitored concentrations were 106 ppb and 71 ppb, respectively, and modeled concentrations were 97 ppb and 69 ppb, respectively.

Response: The modeled concentrations at Mountain View and Kickerville monitors equate to a modeled-to-monitored ratio of 0.92 (97/106 ppb = 0.92) and 0.97 (71/69 ppb = 0.97), respectively. As stated in the modeling report and protocol, ambient SO_2 monitored observations have the potential to vary from an unbiased calibration state by up to 10% and still be considered to be acceptable within the uncertainty of the measurements. This is related to the tolerance in the EPA procedures[2] associated with quality control checks and span checks of ambient measurements. Therefore, even ignoring uncertainties in model input parameters and other contributions that can also lead to modeling uncertainties, just the uncertainty in measurements indicates that modeled-to-monitored ratios between 0.9 and 1.1 are within the instrumentation tolerance and can be considered unbiased. Therefore, Ecology’s analysis provides additional documentation supporting the accuracy of the modeling approach used to characterize the Intalco area in this modeling report.

[2] Quality Assurance Handbook for Air Pollution Measurement Systems, Volume II, Ambient Air Quality Monitoring Program, 2013, available at http://www.epa.gov/ttnamti1/files/ambient/pm25/qa/QA-Handbook-Vol-II.pdf. (Table 10-3 and Appendix D, page 13).

Attachment 1:

Washington Department of Ecology Correspondence - February 26, 2020

From: Dhammapala, Ranil (ECY)
Sent: Wednesday, February 26, 2020 7:47 PM
To: Warren, Laura L
Cc: Mitchell, Kathryn M; 'Sarr, Joseph Alexander'; DeMay, James (ECY); Caudill, Anya (ECY); McAlpine, Jerrold; Paine, Bob
Subject: RE: Alcoa Intalco Draft Modeling Report

Hi Laura et al.,

Ecology, EPA and WSPA have completed their reviews of the SO2 modeling report submitted on February 6. Ecology's feedback is provided below, and EPA's and WSPA's feedback is attached.

Ecology's review of Ferndale cumulative SO2 modeling conducted by Intalco/ AECOM

- Correct 2017- 2019 meteorological data inputs have been used
  - On-site met lines up exactly with data Ecology provided. Since Ecology operates this site, we will provide documentation confirming the data's PSD quality, as per EPA request.
  - Good quality checks were performed by running AERMOD with a hypothetical source and single receptor, to check for quarterly and annual data completeness.
  - Bellingham airport data are substituted in appropriately
  - Upper air data from Quillayute are used correctly
  - Twelve land use sectors were used instead of the originally proposed five, at Ecology & EPA R10's request.

- Actual monthly emissions data from the same period are used
  - Refineries supplied data through December 2019 by ECY, are correctly represented in the model
  - Intalco's total SO2 emissions are consistent with what was previously reported to Ecology.
  - Per- stack allocation of monthly emissions is correct
  - Wind direction dependent plume merging has been implemented correctly, as described in Appendix E. Spot checks were conducted on the HOUREMIS file and found to be consistent.

- Receptors: Intalco's on- site receptors were removed from the list which Ecology provided. Excluded receptors don't cover all parcels owned by the company. See attached png map (red production area boundaries may be inaccurate). Exactly where public access is restricted is unclear and should be clarified.

- The background concentration of 3 ppb (from the Anacortes monitor, as recommended by Ecology) was added to the design values.

- As requested by EPA, the SO2 half-life was set to a very long duration, disallowing for any decay in urban environments. This is the only NON-DFAULT model option used.

- The model was setup with the three requested source groups (all Intalco sources, all refinery sources, and all sources). All electronic files were provided on a thumb drive.

- Model vs monitor comparison:

	BP	Phillips 66	Intalco-Kickerville	Intalco- Mountain View	Ferndale school (temporary)
Monitored SO2 DV, ppb	11	23	71	106	31*
Modeled SO2 DV from all sources, ppb	25	36	69	97	32

    - The over-prediction at the Phillips 66 monitor is 1.6-fold, down from the x2.3 at the time the protocol was developed. Since the direction- dependent plume merging was optimized for the Kickerville and Mountain View monitors, and the low design value at this site, this is not a big problem.
    - SO2 at BP is also over predicted by a factor of 2.3, and Intaco's plumes contribute most SO2 at this locations. But concentrations are low enough to not cause concern.
    - * NWCAA operated a temporary SO2 monitor at a school in Ferndale since July 2019; the model shows close correspondence with the pseudo- DV based on a partial year of data.

- Spatial plot of concentrations in Figures 5-1 & 5-2 are a correct depiction of model outputs.

- Using hourly POST files (9 files of 1.5GB each), stacked barcharts of SO2 contributed by each source group at the hours when the annual 4th highest concentration occurred (aka "design hour") were prepared for the location of each monitor. Intalco- only and Refineries' contributions at each receptor at their respective design hours have been mapped by Ecology. At EPA's request, we have expanded this analysis to cover all 268 NAAQS- violating receptors, and show contributions at every hour with a total modeled concentration over 75 ppb.

- Receptors exceeding 75ppb (i.e. nonattainment area) extends a few 100 meters beyond Intalco's property boundary and does not include Phillips 66 property.

- We do not anticipate the need for further modeling, refinement of existing modeling or a re-written report. An addendum addressing concerns raised in this communication will suffice.

Thanks!

~*~

Ranil Dhammapala, PhD
Atmospheric Scientist
Air Quality Program, Washington Department of Ecology
P.O Box 47600, Olympia, WA 98504-7600
Tel: 360-407-6807   Fax: 360-407-7534
Email: ranil.dhammapala@ecy.wa.gov
~*~

Attachment 2:

EPA Region 10 Correspondence - February 26, 2020

EPA Region 10	
Reviewers:	**Jay McAlpine**
Project:	**Alcoa Intalco 1-hour SO2 NAA – Feb 2020 Modeling Technical Review**
Attention:	**Ranil Dhammapala, WA Dept. Ecology**
Date:	**26 Feb 2020**

Introductory statements and summary:

- This technical review is conducted at the request of the Dept. Ecology to provide EPA Region 10 technical analysis and perspective on the submitted modeling and does not constitute an official EPA approval of the modeling. In my review, I did not consider the conclusions made in the report regarding the impacts or nearby-source contributions. It is understood the State will be using the evidence provided in the report to support a proposal for the NAA boundaries. I have reviewed only the AERMOD modeling setups and methodologies to provide my technical opinion to Ecology whether the modeling was conducted correctly and in compliance with Appendix W and the State-approved modeling protocol.
- The final NAA boundary approval is the responsibility of EPA Headquarters. Therefore, final review and approval of the modeling will be conducted by EPA Headquarters, with EPA Region 10 acting under an advisory role.
- The purpose of the submitted modeling is to provide information to help define the boundaries of the Whatcom County 1-hour SO2 Non-attainment area by:
    - a) Estimating the extent of the area where the 1-hour SO2 standard is exceeded.
    - b) Providing information on the contribution of the Cherry Point (BP) and Ferndale (Phillips 66) refineries, whose properties are adjacent to the Alcoa Intalco properties.
- The modeling at this stage is intended to provide evidence for the purposes outlined above, as part of the 5-factor analysis. Throughout the modeling protocol process, EPA Region 10 has advocated for an Appendix W approach. Unique site characterization techniques have been applied to simulate concentrations at the receptors as accurately as possible. Future modeling used for development of a SIP may require more conservative assumptions. Therefore, please take note: the site characterization techniques, meteorological inputs, and any other inputs or methodologies used in the current round of modeling may or may not be approved for future SIP modeling used for compliance and maintenance demonstrations.

#	Section	Topic	Comment
1		Emissions review	The emissions.xlsx file contains the monthly emissions of SO2 from the facility in lbs divided into four sections (pitch volatilizing, bake oven coke, anode block consumption, and natural gas consumption). For January 2017, for example, the total sum of emission results in a facility rate of 107 g/s (from 629,669 lbs/mo). However, modeled emission rates are higher than derived from the inventory (110 g/s for Jan. 2017, for example). The additional emission comes from the addition of emissions from the wet scrubber stacks. Therefore, the calculations appear to be in error, assuming the total SO2 emission from the potlines should include emissions from both the dry and wet scrubbers. If this is not a calculation error, an expanded explanation of the emissions from the potlines is needed to explain the calculations here. I recommend additional discussion be provided to describe the wet scrubbers and related emissions in more detail and provide detailed justification for including these emissions in the model dry-scrubber plumes. **Ecology should confirm the monthly SO2 emissions used in the modeling fit with their records for the 2017 – 2019 period; records may need to be submitted to confirm. **If there is an error in the emission rate calculation here, the error results in a higher emission rate than occurred 2017-2019, resulting in a conservative estimate of impacts. If there is not an error, please provide an expanded explanation of the emissions inventory and rates.

2		Emission units review	In my review of the location and source parameters of Alcoa and nearby-source units, I found no errors or discrepancies. The modeling uses a sophisticated set of hourly emissions to account for wind direction dependent stack merging. I reviewed the hourly emission files and process to create these files and found no errors in center emission rate or merging (according to the merge process proposed).
3		Stack merging	The stack merging approach used here does deviate from traditional techniques, with the purpose of accounting for enhanced thermal buoyancy from the sets of adjacent hot plumes. Much discussion and review by Ecology was conducted during the modeling protocol process regarding the stack merging. EPA Region 10 did agree with Ecology that the proposed approach appeared to be reasonable to simulate an accurate, but still slightly conservative, SO2 concentration distribution. It would have been ideal to include a set of preliminary simplified runs to demonstrate the degree of SO2 over-prediction using no stack merging, but these were not provided. Therefore, we cannot verify the amount of over-prediction the default non-merged approach would cause. However, it is obvious, from a theoretical perspective, that no stack merging would have likely resulted in much higher concentrations due to lower average plume height and resulting additional plume entrainment in the wake of Alcoa structures. The analysis included in the appendix provides a demonstration of a selected stack merging approach against the three SO2 monitors in the area of Alcoa. The analysis does not contain an explanation of an objective process used to determine the case-by-case merging. It is understood the configuration chosen resulted in SO2 concentration design values that matched those at the monitors well. **EPA Region 10 intends to complete a thorough written summary of the analysis, at a later date, to assist EPA headquarters with their review of the process.
4		Land-use / AERSURFACE	In my review I found no errors or deviations in the determination of land-use parameters. AERSURFACE was used properly, using the default 12 sector approach, using selected wet/dry/average Bowen ratio calculations per month based on the monthly precipitation versus climatic averages. The selected parameters fall into expected ranges given the observed land cover and density of friction elements in each sector. It does appear use of a substitute precipitation data (Bellingham 3SSW) may have possibly resulted in some bias in the determination of wet/dry/average conditions, because the substituted dataset did appear frequently in the extremes and the station is possibly located in a different micro-climate than KBLI. However, this was not explored in depth because I was not convinced any unintended bias would significantly affect the modeling results.
5		Meteorology / AERMET	In my review I found no errors or issues with all three stages of the 2017-2019 AERMET runs. The onsite Mt. View monitor wind data are used for the modeling. Data completeness is acceptable and minimal substitution from the KBLI ASOS was necessary. Upper air data were used appropriately. Cloud cover data from KBLI were used exclusively (no onsite temp. diff. data available, BULKRN was not used). ADJ_U* was used, as expected (no onsite turbulence data were used). **Documentation confirming the PSD-quality of the onsite meteorological dataset should be submitted with the modeling analysis.

6		Receptors	The receptor array is adequately dense and covers the areas of concern. The receptor grid extends far enough to cover nearby terrain features (the density of the receptors over terrain features is quite unnecessarily high – future modeling could be more efficient with lower density grids on these features). It was noted the receptor grid contains some receptors at the surface and some receptors at flagpole height of 1.4m. Although unusual, this should not have a significant effect on the results or conclusions. ** Additional documentation may be needed in Ecology's submission to verify the ambient air boundary. If fencing or barriers are not used in any part of the facility area not considered ambient air, a detailed description will be needed to understand the manner in which Alcoa precludes public access. An ambient air examination and determination by EPA OAQPS may be needed.
7	3.5 of report	Receptor Processing	Note: 30-meter SRTM data were used to develop the receptor terrain elevations for receptors. SRTM data tends to provide elevations at the top of obstacles, so some of the receptor elevations may be too high, especially over areas of woodland. It is best to apply USGS NED data, or alternative, that is representative of ground elevation. This is likely not a significant issue for the current modeling because: a) The area of greatest concern (exceedance) is mostly clear grassland and wetland with intermixed areas of trees. b) Plume height is significant enough to limit the amount of downwash most of the year. Higher receptor height will result in conservative concentration predictions from AERMOD. c) It should have little effect on the determination of NAA boundaries. I am not recommending remodeling, but receptor elevations should be revisited for future SIP modeling.
8		AERMOD settings	• Urban options were used, as proposed in the protocol, with a high half-life to prevent SO2 decay. • No anomalies or errors evident.
9		Outputs	• I did not review the postfile outputs or concentration field results. • It will be helpful for Ecology to report the design values at the monitor locations (model vs. monitor) for this period. • As part of the NAA boundary demonstration, I expect Ecology plans to provide a detailed summary of receptors and hours where AERMOD shows an exceedance of the NAAQS. I expect Ecology will provide a breakdown of source contribution (Alcoa, BP, Phillips 66) at the receptors for these hours, possibly concentrating on the maximum contributions. I anticipate no need to analyze impacts for periods and receptors where the 1-hour SO2 NAAQS threshold is not exceeded.